ISSN 0300 - 9254

JOURNAL OF THE NATIONAL SCIENCE COUNCIL OF SRI LANKA

Volume 15 No. 1 June 1987

Journal
of the
National
Science
Council of
Sri Lanka

PUBLICATION: One volume of two issues (June and December) is published annually by the Natural Resources, Energy and Science Authority of Sri Lanka.

Subscription

Annual subscription—Foreign $ 27.00; Local Rs. 45.00. Accepted on a calendar year basis. Rates include postage.

Single issues—Foreign $ 13.50; Local Rs. 27.50 each Rates include postage.

Payment must accompany all orders. Remittances in favour of Natural Resources, Energy and Science Authority of Sri Lanka.

Change of address notice is required 4 weeks before issue date.

Orders and all correspondence relating to them should be sent to the **Accountant**, Natural Resources, Energy and Science Authority of Sri Lanka, at the address given below.

Manuscripts

Research papers, Reviews and Short Communications in all fields of Science and Technology in Sinhala, Tamil and English may be submitted for editorial consideration. Manuscripts should conform to the style adopted in this issue. For instructions as to preparation of papers see inset at back of this issue. Separates of General Instructions and Special Instructions in Chemical, Physical and Medical Sciences may be had on application to the Secretary, Editorial Board, at the address given below.

No responsibility is assumed by the Natural Resources, Energy and Science Authority of Sri Lanka for statements and opinions expressed by the contributors to this Journal.

Manuscripts and all correspondence relating to them should be sent to the **Secretary**, Editorial Board, Journal of the National Science Council of Sri Lanka, 47/5, Maitland Place, Colombo 7, SRI LANKA.

J. Natn. Sci. Coun. Sri Lanka 1987 **15**(1): 1–10

USE OF DOLOMITE FOR FINISHING COAT IN MASONRY

H. D. GUNAWARDHANA* AND P. P. S. P. DIAS
Department of Chemistry, University of Colombo, Colombo 3.

(Date of receipt : 18 October 1985)
(Date of acceptance : 10 February 1987)

Abstract: The major drawback in the application of dolomite as a substitute for limestone is the appearance of cracks when calcined and subsequently slaked dolomitic quicklime is applied on the plaster in the form of a finishing coat. Investigations into the cause for the appearance of cracks have revealed that there are five major factors which influence the appearance of cracks. Out of the factors identified, more extensive studies were carried out on factors such as moisture content of the plaster and percentage of carbon dioxide of dolomitic quicklime. The optimum conditions for the application of dolomitic finishing coat without the appearance of cracks have been recommended. The appearance of cracks can be mitigated by achieving complete slaking of magnesium oxide component before the slaked calcium oxide is set. Pilot scale application of a dolomite under recommended conditions revealed promising results.

1. Introduction

Dolomite[3] is a carbonate of calcium and magnesium with 1 to 3% impurities such as quartz, gypsum, etc. The content and the colour of the impurities determine the colour of the rock. Dolomite or dolomitic limestone has 40 to 43% magnesium carbonate. Magnesium carbonate dissociates at 402 to 480°C, whereas the magnesium carbonate component of dolomite decomposes at higher temperatures i.e. 590°C. As a result the magnesium oxide is hard-burned in varying degrees before the calcium oxide is formed, which requires a temperature of about 898°C. It has been shown[3] that the degree of hard-burning can be mitigated by cooling the quicklime immediately after the $CaCO_3$ is calcined, and also by calcining at minimum and constant temperature for a longer duration. The traditional dolomitic limestone kilns in the Matale district of Sri Lanka seem to follow a procedure to minimize hard-burning.

$$CaCO_3 . MgCO_3 \text{ (dolomite)} + \text{heat} \rightleftharpoons CaO . MgO \text{ (dolomitic quicklime)} + 2CO_2 \quad \ldots\ldots\ldots\ldots\ldots\ldots (1)$$

Slaking of dolomitic quicklime can be represented by the following equation:[5]

**Centre for Analytical Research and Development.*

$$CaO.MgO + H_2O \rightleftharpoons Ca(OH)_2.MgO \text{ (dolomitic hydrate)} + \text{heat} \quad .. (2)$$

The calcium oxide component of dolomitic quicklime is slaked first. The hard-burned magnesium oxide component of dolomitic quicklime requires pressure for complete hydration.

$$CaO.MgO \text{ (dolomitic quicklime)} + H_2O + \text{pressure} \rightleftharpoons Ca(OH)_2.Mg(OH)_2 \text{ (dolomitic hydrate)} + \text{heat} \quad ..... (3)$$

When the dolomitic quicklime is slaked in the normal way and applied on the plaster, the appearance of cracks or fractures becomes inevitable. The appearance of cracks in cement is due to the expansion caused by the conversion of magnesium oxide to magnesium hydroxide after the setting of the hydrated components of cement.[6] Therefore, it is necessary to use limestone free of magnesium in the cement industry. When the dolomitic hydrate is applied on the plaster the hydrated calcium oxide component undergoes setting.[2] This could be attributed to the gel formation and the subsequent hardening. The slaking of magnesium oxide is slow and water penetrates into the surface pores. This exerts great internal expansive force and causes it to fracture. This paper describes an investigation on the factors which influence the appearance of cracks on dolomitic finishing coat.

2. Experimental Procedure

Analytical-grade chemicals were used wherever possible.

2.1 External rendering:

Mortar mix of 1:1:5 (cement: dolomitic hydrates: sand)[5] was used for external rendering on the brick work. The moisture content of the resulting plastered finish was determined by one of the following methods.

(i) Karl Fischer Method:[6] Karl Fischer reagent was prepared using methyl cellosolve as the solvent. Both visual and electrometric end-point detection methods were carried out.

(ii) Drying and weighing method:[7] A sample of the plaster was dried at 110°C for three hours. The difference in weight before and after drying was used to calculate the moisture content.

2.2 Determination of carbon dioxide content:[1]

Syrupy phosphoric acid was added to a weighed sample and heated gently, evolved gas was passed through a solution of syrupy phosphoric acid followed by a U-tube packed with phosphorus pentoxide and pumice stones impregnated with copper sulphate. The gas was then passed through two

U-tubes, each containing soda asbestos (carbosorb) and phosphorus pentoxide. Increase in weight of the two U-tubes containing carbosorb gives the carbon dioxide content of the sample.

2.3 Application of dolomitic finishing coat:

Dolomitic quicklime of the particle size of 60 to 100 mesh was slaked for 23 hr., the excess water was filtered off and the resulting putty was applied on the plaster maintaining the thickness of about 3.5 mm. The traditional method employed in the Matale district of Sri Lanka, involves the calcination of pieces of dolomite (about 2 cm diameter) in a kiln for about 48 hr. and slaking them in a basin with excess of water. Disintegration of the pieces occurs during this process, leading to a separation of heavier silica particles from the slaked dolomite particles. The traditional method was adapted in the laboratory by heating pieces of dolomite at about 900°C for about 90 min., in a muffle furnace and then slaking them in a beaker of water. After 23 hr. the slaked dolomitic qucklime was removed without agitating the bottom of the beaker, filtered and applied on the plaster.

2.4 Analysis of dolomite:

1.000g of sample was dissolved in perchloric acid (10 cm^3), heated to dryness on a hot plate, cooled, added a mixture of 10 cm^3 of perchloric acid and 10 cm^3 of water and filtered through a Whatman No. 40 filter paper into a 250 cm^3 volumetric flask. The filter paper was ignited quantitatively to determine the acid insoluble substances. The filtrate was made up to 250 cm^3 and used in the determination of calcium, magnesium and iron by EDTA titration.[8]

3. Results and Discussion

3.1 Possible cause for the appearance of cracks:

It has been reported[5] that magnesium oxide component of dolomitic quicklime requires pressure for complete hydration. Therefore, a sample of dolomitic quicklime (carbon dioxide content 6.03%) was slaked for 45 min. in an autoclave under a pressure of 15 lbs per sq. inch at a temperature of 121°C. When this sample was applied on a plaster having a moisture content about 2%, no cracks appeared on the resulting finishing coat. The undesirable expansive forces which are responsible for the appearance of fractures will not be created, if the magnesium oxide component is completely hydrated (slaked). However, the pressure slaking of dolomitic quicklime is not feasible in the cottage level building construction.

This necessitates the need to investigate the influence of various factors responsible for the appearance of fractures during the normal use of dolomitic quicklime for finishing coats. Our investigations revealed that application of slaked dolomitic quicklime under certain conditions gives a perfect finishing coat with no fractures. It was possible to identify that the following factors influence greatly on the appearance of fractures.

(a) The moisture content of the plaster at the time of the application of finishing coat.
(b) The carbon dioxide content of dolomitic quicklime.
(c) The particle size of dolomitic quicklime.
(d) The slaking time of dolomitic quicklime.
(e) The composition of dolomite.

It is apparent that the adjustment of these factors during the application should give a perfect finishing coat.

3.2 Effect of moisture content of the plaster at the time of the application of finishing coat

Dolomite of composition (CaO = 30.5%, MgO = 21.3% and Fe_2O_3 = 0.45%) was calcined, slaked and applied on the plaster having a moisture content of 16.8%. This application of the finishing coat and the determination of the moisture content of the plaster were continued daily. It was observed that perfect finishing coats can be obtained if the moisture content of the plaster remains at 10% or above. Cracks were observed during the application of the same dolomite under similar conditions, but keeping the moisture content of the plaster below 10%.

The continuous supply of water from a plaster possessing an adequate moisture content will prevent the early setting of the hydrated calcium oxide component of the dolomitic quicklime. This in turn gives sufficient time for the complete slaking of the magnesium oxide component. However, the tendency for the calcium oxide component to undergo an early setting, exerts a pressure on magnesium oxide. Under these conditions, with an adequate supply of water from the plaster magnesium oxide component undergoes slaking rather rapidly. This enables uniform setting of both components. Undesirable expansive forces will not be created under these circumstances.

3.3 Effect of carbon dioxide content of dolomitic quicklime on the appearance of cracks

It has been observed that 'hard-burned' dolomitic quicklime shows the appearance of cracks irrespective of the moisture content of the plaster.

The extent of 'hard-burning' can be measured in terms of the carbon dioxide content of the dolomitic quicklime.

Table 1 shows the appearance of cracks when the finishing coat is made out of dolomitic quicklime having the carbon dioxide content less than 1.0% (i.e. hard-burned). Therefore, it is essential to control the carbon dioxide content of dolomitic quicklime which is entirely dependent on the calcining temperature and duration. The calcining process expels carbon dioxide from magnesium carbonate more readily than calcium carbonate.[3] Since the proportion of magnesium carbonate to calcium carbonate differs usually from deposit to deposit, either the calcining temperature, duration or both should be varied accordingly. It is clear from Table 1, that high carbon dioxide content of dolomitic quicklime (soft-burned) is more desirable. But the finishing coat made up of soft-burned dolomitic quicklime having a carbon dioxide content greater than 10% was found to possess an undesirable texture. The finishing coat was soft and easily removable. Experiments were conducted to obtain the desirable carbon dioxide content by varying the heating time. The results are shown in Table 2. The results obtained by the application of samples of dolomite given in Table 2, as finishing coats are indicated in Table 3.

Table 1. Effect of Carbon dioxide content on the appearance of cracks.

Time taken to obtain appropriate moisture content (in Hours)	Moisture content of the plaster (%)	CO_2 Content 1.4%	0.9%	0.6%	0.4%
23	14.18	N	N	N	C
47	8.79	N	C	C	C
167	1.46	N	C	C	C
191	1.37	N	C	C	C
215	1.18	N	C	C	C
239	1.10	N	C	C	C
359	0.83	N	C	C	C
575	0.81	N	C	C	C

N = No cracks C = Cracks

Table 2. Effect of heating time at 900° C on the carbon dioxide content of dolomitic quicklime.

Heating time (min)	35	70	95	210
% CO_2	12.66	6.35	2.57	2.46

Composition of Dolomite:
Cao = 31.84%, MgO - 20.30%, Fe_2O_3 = 0.56%.

Table 3. Influence of carbon dioxide content on the appearance of cracks.

Moisture content of the plaster (%)	Carbon dioxide content			
	12.66%	6.35%	2.57%	2.40%
13.94	N	N	M	M
12.61	N	N	M	M
10.19	N	N	M	M
7.52	N	N	M	M

Composition of dolomite as in Table 2.

N = No cracks, C = Cracks, M = Mosaic grooves.

Even though any fractures did not appear on the finishing coat made up of dolomitic quicklime having the carbon dioxide content 12.66%, the texture of the finishing coat was found to be soft and unsuitable. However, the finishing coat made up of dolomitic quicklime having the carbon dioxide content 6.35% (Table 3) was found to fulfil the necessary requirements. Therefore, the carbon dioxide content of dolomitic quicklime should be maintained in the range 5 – 10% in order to achieve the requirements for a finishing coat.

Boynton[3] has reported that, at a calcining temperature of about 900° C, the magnesium oxide component undergoes hard-burning in varying degrees. The degree of hard-burning therefore should be proportional to the duration of heating. High degree of hard-burning reduces the rate of hydration of magnesium oxide resulting in an increased tendency for the appearance of cracks when applied as a finishing coat.

3.4 Effect of particle size of dolomite on the appearance of cracks

The relationship between the particle size of dolomitic quicklime and the moisture content of the plaster was observed while keeping the other factors such as carbon dioxide content, etc., constant. Nevertheless, there was a practical difficulty of obtaining an equivalent value for the carbon dioxide content of dolomitic quicklime of varying particle sizes. The carbon dioxide percentages of 300 mesh, 150 mesh, 60 mesh and 30 mesh particles of dolomitic quicklime appearing in Table 4 were 6.26%, 15.8%, 4.5% and 9.7% respectively. It is evident from the Table 4, that the smaller the particle size of dolomitic quicklime the greater is the resistance acquired by the finishing coat against the appearance of cracks. If the particles are very small, undoubtedly there is a complete hydration of both calcium oxide and magnesium oxide components during the normal slaking, thus enabling the uniform setting of both components after the application. Therefore, there is no tendency for the appearance of fractures. Table 4 shows that 300 mesh particle size is the most appropriate, however, there is a practical difficulty in obtaining such small particles especially in the cottage level. Therefore, our studies were restricted to 60 — 100 mesh particle size which could be obtained without the employment of sophisticated machinery.

Table 4. Influence of particle size of dolomitic quicklime on the appearance of cracks

Moisture content of the plaster (%)	Particle Size			
	300 mesh	150 mesh	60 mesh	30 mesh
16.8	N	N	N	N
15.4	N	N	N	N
13.5	N	N	N	N
11.2	N	N	N	N
6.1	N	N	C	C
5.5	N	N	C	C
4.8	N	N	C	C
3.8	N	N	C	C
3.6	N	N	C	C
3.4	N	N	C	C
2.9	N	N	C	C

N = No Cracks C = Cracks

3.5 Effect of slaking time of dolomitic quicklime on the appearance of cracks

Application of dolomitic quicklime possessing a carbon dioxide content 2.47%, on a plaster of moisture content 4.33% after slaking for 18, 24, 42, 96, 138 and 216 hours showed cracks irrespective of slaking time. Cracks have not been observed at any moisture content higher than 4.33%. From these results, it is evident that complete hydration of magnesium oxide component will not occur under normal conditions. The extent of hydration of magnesium oxide component is therefore independent of the time period in which dolomitic quicklime is kept in contact with water. The exposure of slaked dolomitic quicklime to atmosphere over a long period results in a recarbonation by atmospheric carbon dioxide. As a result, the standard slaking time of 23 hours was employed throughout our investigations.

3.5.1 Effect of the composition of dolomite on the appearance of cracks

Four samples of composition as shown in the Table 5 were crushed and calcined at 900°C for 90 minutes. The results of the application of these dolomitic and high calcium limestone samples are shown in Table 6.

Table 5. Composition of dolomite and high calcium limestone used.

Sample Number	% CaO	%MgO	% Fe_2O_3	% Acid Insoluble matter
1	53.65	1.14	0.36	0.62
2	30.80	21.69	0.36	0.40
3	31.09	21.59	0.15	1.89
4	54.82	1.04	0.34	4.38

Table 6. Effect of using different dolomitic and high calcium limestone on the appearance of cracks
Sample Nos. 1, 2, 3 and 4 are as in Table 5.

Moisture content of the plaster (%)	Powdered Samples				Traditionally Slaked Granules			
	1	2	3	4	1	2	3	4
11.59	N	N	N	N	N	N	N	N
11.48	N	N	N	N	N	N	N	N
11.23	N	N	N	C	N	N	N	N
10.02	M	N	N	C	N	N	N	M
4.25	C	C	C	C	C	C	C	C

N = No Cracks, C = Cracks, M = Mosaic grooves.

A method similar to the traditional way was adapted in the laboratory by crushing dolomite into granules of about 1.5 cm diameter and calcining under the same conditions. The slaking of these dolomitic quicklime granules gave a powder which was applied on the plaster in a similar manner. The results are also shown in Table 6.

It is apparent from Table 6, that the appearance of cracks is independent of the composition of dolomite. However, the early appearance of cracks in high calcium limestone (sample No. 4) could be attributed to the presence of a high percentage of acid insoluble matter such as silica. Independent employment of traditional slaking methods gave identical results. It is evident from Table 6, that superior results could be achieved by the employment of the traditional method. This could be attributed to the fact that a certain amount of acid insoluble matter is removed during the traditional slaking process as a result of the settlement of the acid insoluble matter at the bottom of the vessel used for slaking.

4. Conclusion

Out of the factors which govern the appearance of cracks on dolomitic finishing coats, the moisture content of the plaster at the time of the application of finishing coat and the carbon dioxide percentage of dolomitic quicklime are considered to be two major important factors. In conclusion, it is apparent that one can obtain a perfect finishing coat without any fractures if one applies slaked dolomitic quicklime of carbon dioxide content in the range 5 – 10%. Therefore, dolomitic finishing coat can be successfully applied without the appearance of cracks under the above conditions irrespective of the composition of dolomite. Moreover, under the use of any other conditions which provide adequate measures to prevent the differential hydration and setting of magnesium oxide and calcium oxide components of slaked dolomitic quicklime, it is possible to obtain dolomitic finishing coats without any fractures.

Acknowledgements

The authors are grateful to the Industrial Development Board of Sri Lanka for providing a research studentship to one of us (PPSPD). They also gratefully acknowledge the Natural Resources, Energy & Science Authority of Sri Lanka for providing a research grant and a studentship (PPSPD) to complete the project.

References

1. ALEXEYEV, V. (1969) *Humidity and Moisture,* Vol. 3 and 4, Reinhold, New York.

2 BIRCHALL, J. D. & HOWARD, A. J. (1978) *New Sci.* 78: 228.

3. BOYNTON, ROBERT, S. (1966) *Chemistry and Technology of lime and limestone,* Interscience, New York.

4. MICHELL JUR. J. & SMITH, D. (1948) *Aquametry,* Interscience, New York.

5. STOWELL, E. P. (1963) *Limestone as raw material in industry,* Imperial Chemical Industries Ltd., Oxford University Press.

6. TAYLOR, H. F. W. (1964) *Chemistry of Cements,* Academic Press, London.

7. WEXLER, ARNOLD, (1965) *Humidity and Moisture,* Vol. 3 and 4, Reinhold, New York.

8. WELCHER, FRANK, J. (1957) *The analytical uses of ethylenediaminetetra acetic acid,* Van Nostrand, Princeton.

9. THE LIMESTONE FEDERATION, (1959) *The Use of Lime in Building,* The British Lime Manufacturers, London.

J. Natn. Sci. Coun. Sri Lanka 1987 15 *(1) : 11–16*

SPONTANEOUS BREAKING OF L – D SYMMETRY IN BIOCHEMICAL EVOLUTION

K. TENNAKONE
Institute of Fundamental Studies, Sri Lanka

and

Department of Physics, University of Ruhuna, Matara, Sri Lanka

(Date of receipt : 9 February 1986)
(Date of acceptance : 17 February 1987)

Abstract : A simple mathematical model is constructed to show that a minute difference Δ E in the activation energies of L and D isomers of biomolecules is sufficient to achieve optical stereoselection in biochemical evolution. Rate equations describing the competition between self-replicating molecules of two types are shown to exhibit spontaneous breaking of right-left symmetry.

1. Introduction

The richness and diversity of the universe depends on lack of perfect symmetry. The most symmetric universe would be a time reversible homogeneous gravitating system of Photons[10]. 'Physics' would become meaningless in such a situation as intelligent beings cannot evolve in this world where there is no 'Chemistry'. In fact if matter is CP invariant a homogeneous photon universe is probably the only possible realization.

The major macroscopic asymmetries in the universe are (1) the arrow of time, ie, the general irreversibility of all natural processes, (2) the inhomogeneity of space, ie, the matter in the universe are lumped into galaxies placed far apart, (3) the chemical asymmetry, ie, nearly symmetric forms of matter allowed by microscopic laws of nature do not exist with equal abundance, either locally or globally.

Although, the macroscopic world is largely asymmetric, the fundamental interactions among elementary particles respect it to a much higher degree of accuracy, parity and time reversal invariance are only slightly violated. Recent developments in nonequilibrium thermodynamics[6-8] indicate that in a system far from thermal equilibrium the minute asymmetries could get amplified to generate large scale macroscopic asymmetries. Thus it is possible that macroscopic asymmetries in the universe are direct consequences of microscopic asymmetries. Current developments in elementary particle physics suggest that the observed baryon-antibaryon asymmetry in the universe is a result of small violations in CP and the baryon number conservation[1, 11]Several authors have proposed

that biochemical L – D stereoselection is caused by parity violations in weak interactions.[9, 12] After the discovery of weak neutral currents much attention is given to this idea,[2,4] as the neutral currents could give rise to minute but nonzero difference in the activation energies of the two enantiomers of the same compound. In this work we present a simple exactly soluble model which clearly shows biochemical L – D stereoselection could result as a spontaneous breaking of symmetry in an nonequilibrium process.

1.1 Model

It is generally believed that life originated in primeval oceans containing dissolved organic compounds formed by the action of solar ultraviolet radiation or electrical discharges on the primitive atmosphere.[5,7] As there are no significant right-left distinguishing factors in the chemical or geophysical environment, we assume that the prebiotic medium was a racemic mixture of 'basic chemical building blocks of life' (eg, amino acids) and stereoselection occurred after the development of self-replicating molecules. At the initial stages both L and D isomers of primitive self-replicating molecules would have existed in comparable concentrations. These molecules use compounds in the prebiotic medium of the correct type (L or D) as food and regenerate molecules of the same type. However, because of the difference in activation energies resulting from neutral currents, the rate constants of replication K_L and K_D for the two types of molecules will not be exactly equal. Again the self-replicating molecules of one type could interact with the other type inhibiting growth mutually. Perhaps the mixed polymers formed with L and D molecules cannot undergo replication. If N_L and N_D are the concentrations of the two types of self-replicating molecules, the rate equations governing their evolution can be written in the form,

$$\frac{dN_L}{dt} = K_L N_L - aN_L N_D$$

$$\frac{dN_D}{dt} = K_D N_D - aN_D N_L \qquad (1)$$

where, a = constant and K_L, K_D are the replication constants of the two types of molecules. In the presence of neutral currents K_L is not exactly equal to K_D and before considering the asymmetric equations with $K_L \neq K_D$ we consider the symmetric equations with $K_L = K_D = K$. If we impose the symmetric initial condition $N_L = N_D$, $t \to \infty$, the equation (1) with $K_L = K_D = K$ has a symmetric solution,

$$N_L = N_D = K(a + abe^{-Kt}) \qquad (2)$$

and two asymmetric solutions, where b is a constant.

$$N_L = Ae^{kt}[1 - e^{-(aA/K)e^{Kt}}]^{-1}$$

$$N_D = Ae^{kt}\ e^{-(aA/K)e^{kt}}\ [1 - e^{-(aA/K)e^{Kt}}]^{-1} \qquad (3)$$

or

$$N^D = Ae^{kt}[1 - e^{-(aA/K)e^{-Kt}}]^{-1}$$

$$N_L = Ae^{kt}\ e^{-(aA/K)e^{kt}}\ [1 - e^{-(aA/K)e^{Kt}}]^{-1} \qquad (4)$$

The symmetric solution and the two asymmetric solutions are plotted in Figure 1 and the phase trajectories are shown in Figure 2. In the first asymmetric solution $N_L \to \infty$, $N_D \to 0$ as $t \to \infty$, the reverse happens in the second asymmetric solution. Stability analysis shows that the symmetric solution become unstable once the equilibrium concentration $N_L = N_D = K/a$ is reached and bifurcate into one of the stable solution. Clearly the model exhibits spontaneous breaking of L – D symmetry. However, this is ineffective in generating the required stereoselection. Points in the medium, where the symmetry is broken in one sense would occur with equal probability as the places where the symmetry is broken in the opposite sense. Nevertheless a difference in K_L and K_D however small is sufficient to ensure the survival of the two isomers. If $K_L > K_D$ the appropriate solution of (1) is,

$$N_L = N_o e^{K_L t}$$

$$N_D = N_o e^{K_D t}\ e^{-aN_o/ke^{Kt}} \qquad (5)$$

The solution (5) is sketched in Figure 3. It is seen that once the concentration of L and D isomers reach a value comparable to the equilibrium concentration an unstability develops and

$N_L \to \infty$, $N_D \to 0$ as $t \to \infty$.

We have ignrored the diffusion of interacting molecules. In the actual situation, diffusion plays an important role in determining the spatio-temporal distribution of the reaction products. When diffusion is included into (1) we obtain the equations

$$\frac{\partial N_L}{\partial t} = KN_L - aN_L N_D + b\nabla^2 N_L$$

$$\frac{\partial N_D}{\partial t} = KN_D - aN_D N_L + b\nabla^2 N_D \qquad (6)$$

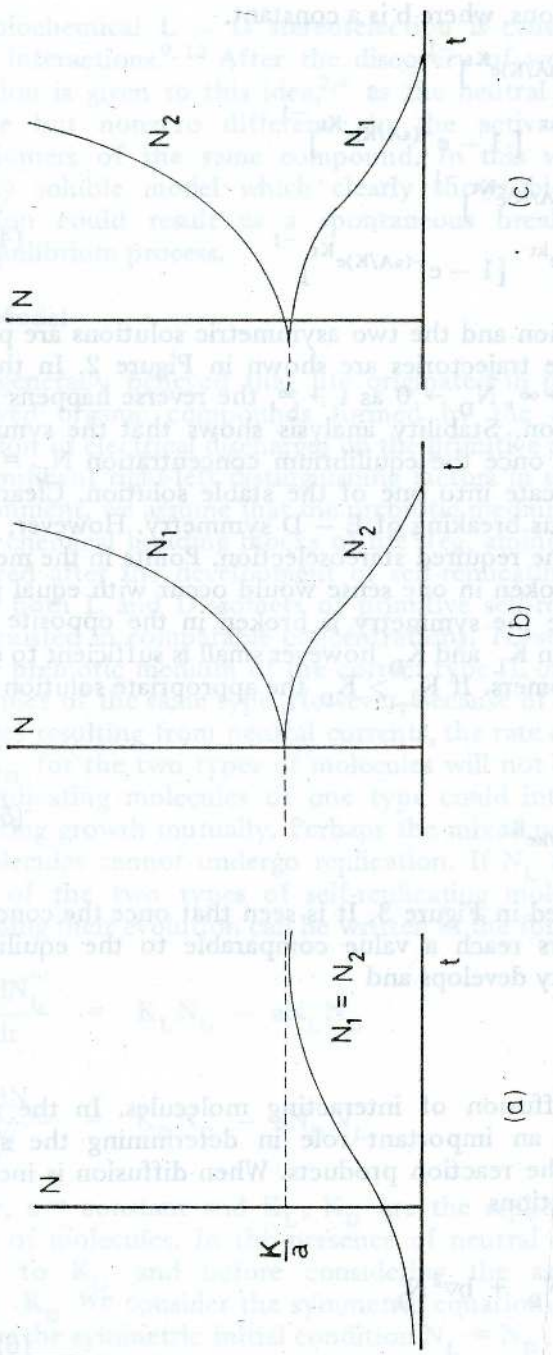

Figure 1 : The plot of $N_1 = N_L$ or $N_2 = N_D$) vs t
(a) the symmetric solution where $N_L = N_D$
(b) the asymmetric solution where $N_D \to 0$, $N_L \to \infty$ as $t \to \infty$
(c) the asymmetric solution where $N_L \to 0$, $N_D \to \infty$ as $t \to \infty$

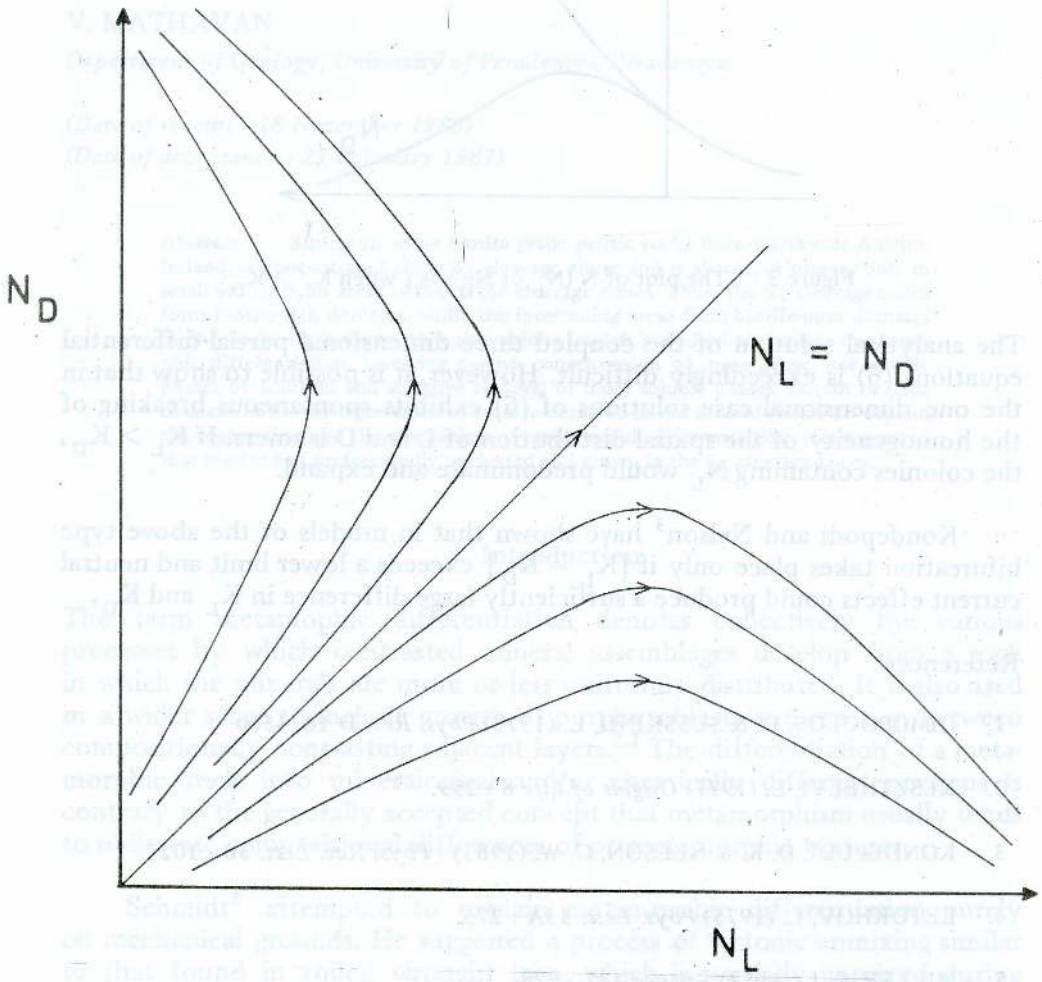

Figure 2 : Phase trajectories showing the unstability of the symmetric solution.

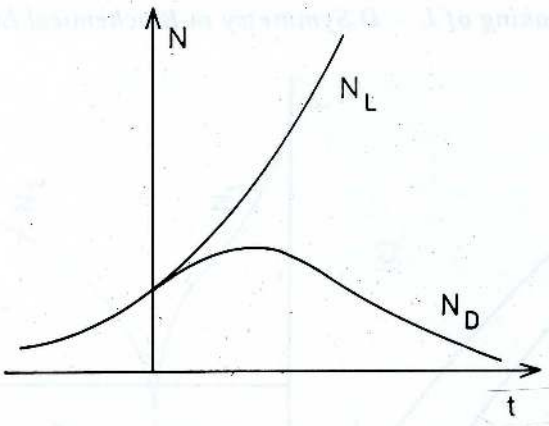

Figure 3 : The plot of N (N_L or N_D) vs t when $K_L > K_D$

The analytical solution of the coupled three dimensional partial differential equations (6) is exceedingly difficult. However, it is possible to show that in the one dimensional case solutions of (6) exhibits spontaneous breaking of the homogeneity of the spatial distribution of L and D isomers. If $K_L > K_D$, the colonies containing N_L would predominate and expand.

Kondepodi and Nelson[3] have shown that in models of the above type bifurcation takes place only if $[K_L - K_D]$ exceeds a lower limit and neutral current effects could produce a sufficiently large difference in K_L and K_D.

References

1. DIMOPOULOS, D. & SUSSKIND, L. (1978) *Phys. Rev.* **D 18,** 4500.

2. KESZTHELYI, L. (1977) *Origins of Life* **8** : 299.

3. KONDEPUDI, D. K. & NELSON, G. W. (1983) : *Phys. Rev. Lett.* **50** : 1023.

4. LETOKHOV, L. (1975) *Phys. Lett.* **53A** : 275.

5. MILLER, S. L. (1953) *Science* **117** : 528.

6. NIOLIS, G. & PRIGOGINE, I. (1977) *Self-Organization in Nonequilibrium Systems.* Wiley, New York.

7. OPARIN, A. I. (1953) *The Origins of Life* Dover Publications, London.

8. PRIGONINE, I. (1979). From Being to Becoming, Freeman, San Francisco.

9. VESTER, F., ULBRICHT, T. L. V. & KRAUCH, H. (1959). *Naturwis* **46** : 68.

10. WEINBERG, S. (1972) *Gravitation and Cosmology* Wiley, New York.

11. WEINBERG, S. (1979) *Phys. Rev. Lett.* **42** : 850.

12. YAMAGATE, Y., THEOR. J. (1975) *Biol.* **11** : 299.

J. Natn. Sci. Coun. Sri Lanka 1987 **15**(1): 17–23

METAMORPHIC DIFFERENTIATION IN SOME BIOTITE SCHISTS FROM NORTH-EAST ANTRIM, IRELAND

V. MATHAVAN

Department of Geology, University of Peradeniya, Peradeniya.

(Date of receipt : 18 November 1986)
(Date of acceptance : 23 February 1987)

Abstract : Biotite in some biotite grade pelitic rocks from north-east Antrim, Ireland, is concentrated along S_2 cleavage zones and is absent, or present only in small amounts, in areas between the cleavage zones. Thus, the S_2 cleavage zones form biotite-rich domains, while the intervening areas form biotite-poor domains in the rocks. It is shown that the various models proposed to explain metamorphic differentiation, involving passive concentration of more dense, less soluble phases by solution and selective removal of more soluble phases, cannot be used to account for the differentiated feature observed in the studied rocks. To explain the segregation and the mechanism of metamorphic differentiation, it is suggested that biotite had preferentially nucleated and grown in the S_2 cleavage zones.

1. Introduction

The term metamophic differentiation denotes collectively the various processes by which contrasted mineral assemblages develop from a rock in which the minerals are more or less uniformly distributed. It is also used in a wider sense to include growth of porphyroblasts and reaction between compositionally contrasting adjacent layers.[2,7] The differentiation of a metamorphic rock into mineralogical and/or chemically different portions is contrary to the generally accepted concept that metamorphism usually tends to obliterate compositional differences of premetamorphic textures.

Schmidt[8] attempted to explain metamorphic differentiation purely on mechanical grounds. He suggested a process of tectonic unmixing similar to that found in rolled wrought iron, which is partially unmixed during deformation into layers of relatively pure iron alternating with carbon-rich iron. According to him, shearing of rocks causes more ductile minerals (eg. micas and amphiboles) to concentrate in layers of intense shear, whereas less ductile minerals (eg. quartz and feldspars) tend to remain in less sheared portions of the rock.

Nicholson[6] described metamorphic differentiation associated with crenulation cleavages in quartz-mica schists which showed concentrations of quartz at the crests of crenulations and development of mica-rich zones at the limbs of the crenulations. He suggested that migration of silica from areas of high strain and recrystallization of quartz at sites of minimum strain

develop this type of metamorphic differentiation. Talbot and Hobbs[9] and Gray[3] also described metamorphic differentiation associated with discrete crenulation cleavages. Gray produced analytical data to support his conclusion that the discrete crenulation cleavages were solution planes and he suggested that the differentiated nature was caused by passive concentration of relatively insoluble materials, such as micas and chlorite, due to solution and removal of quartz along the cleavages.

Hyndman[4] discussed the formation of quartzo-feldspathic layers parallel to schiotosity and axial surfaces of folds in a series of silt and shale beds. He proposed that the metamorphic differentiation process involves migration of some compounds (eg. to form quartz and feldspars) to lower pressure surfaces parallel to schistosity and migration of other components less of this tendency to the higher pressure sites (eg. to form mafic minerals) during metamorphism and deformation.

In this paper, metamorphic differentiation associated with crenulation cleavages in some biotite schists is described and on the basis of petrographic data, it is proposed that biotite may have nucleated and grown preferentially in S_2 cleavage zones.[5] It is also shown that the above described processes such as solution, recrystallization and tectonic unmixing cannot explain this differentiated feature.

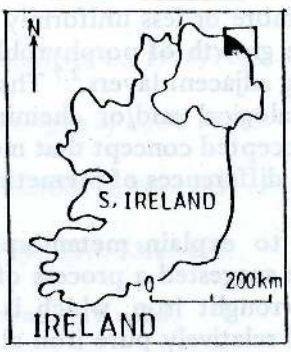

Figure 1 : Location of the study area

2. Geological setting of the study area

The samples examined in the present study were collected from the Dalradian rocks of north-east Antrim, Ireland (Figure 1). These rocks represent biotite grade metamorphism and have been affected by three phases of deformation. The first deformation phase (D_1) produced a slaty cleavage (S_1) and the second phase deformed these rocks intensively and produced the regional schistosity which is a discrete crenulation cleavage (S_2). The third deformation phase D_3 produced small-scale folding and crenulation of S_2 to form S_3.

3. Petrography

The examined samples are dark grey, fine grained rocks with abundant white/grey albite porphyroblasts which gave a spotted appearance to these rocks. S_2 crenulation cleavage is well developed but S_3 is weak or may be absent.

The petrographic microscope reveals that the rocks are composed of albite, muscovite, biotite, quartz, chlorite, apatite, tourmaline and ore minerals and the modal percentages of the minerals indicate that they belong to the category of pelites.

Albite : albite porphyroblasts (best seen under a microscope) are abundant in the studied rocks. A characteristic feature of the albite porphyroblast is that they contain numerous trails of inclusions which define various microstructures including S_2 and S_3 crenulations. In some specimens, albite porphyroblasts are reversely zoned at the rim. A much larger area which included north-east Antrim was studied and the age relationships of albite porphyroblast growth established. The albite porphyroblast grew during two static periods following D_2 and D_3 phases of deformation.[5]

Biotite : Two types of biotite crystals occur: fabric-forming type and slightly larger crystals (microporphyroblasts). The fabric-forming type crystals are dimensionally oriented parallel to S_1 and S_2 cleavages but they are

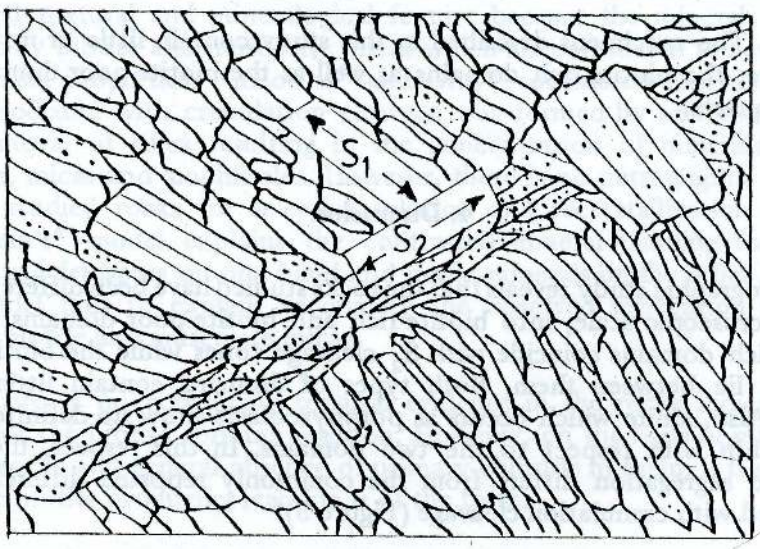

Figure 2 : Concentration of biotite crystals (stippled) along S_2 cleavage zone and predominance of muscovite crystals (unshaded) outside S_2 cleavage zone. Diagramatically redrawn from a microphotograph.

characteristically concentrated along S_2 cleavage zones and define biotite-rich domains in the rock. The areas between S_2 cleavage zones are composed mainly of muscovite and they form the biotite-poor domains (Figure 2). Fabric-forming biotite crystals are highly strained and they are curved at the junction between S_1 and S_2 cleavages indicating either rotation of the crystals during the development of S_2 or Syn D_2 formation of biotite crystals. Some microporphyroblasts are dimensionally aligned parallel to S_1 and S_2 but others are randomly oriented across S_2 cleavage. Biotite microporphyroblasts are strain free or only slightly strained. On the basis of texture and optical character it is inferred that biotite has grown mainly during syn D_2 to post D_2 period although an extended pre-D_2 age cannot be ruled out.

Muscovite : muscovite crystals also occur in two forms and they are mainly confined to biotite-poor domains. Fabric-forming crystals and most microporphyroblasts are dimensionally aligned parallel to S_1. Some microporphyroblasts are dimensionally oriented across S_1. Both types of crystals may be intergrown with biotite. Textural study reveals that muscovite continued to crystallize from earliest to late stage development of the rocks.

Chlorite : primary chlorite is generally absent in the rocks studied. However, when primary chlorite is present, it occurs as dimensionally aligned crystals or the crystals may be clustered together.

Quartz : The specimens described in this study contain little or no quartz. Therefore, the biotite-rich domains as well as the biotite-poor domains are poor in quartz.

4. Discussion

The petrographic study reveals that the rocks studied have been differentiated, on a microscopic scale, into biotite-rich and biotite-poor domains and the biotite-rich domains coincide with S_2 cleavage zones while the biotite-poor domains lie between them. Both types of domains contain little or no quartz. Also, albite which occurs as porphyroblasts show no definite spatial relationship with respect to the two domains. In this respect, the above described segregation differs from the commonly reported differentiation associated with crenulation cleavage (Figure 3).

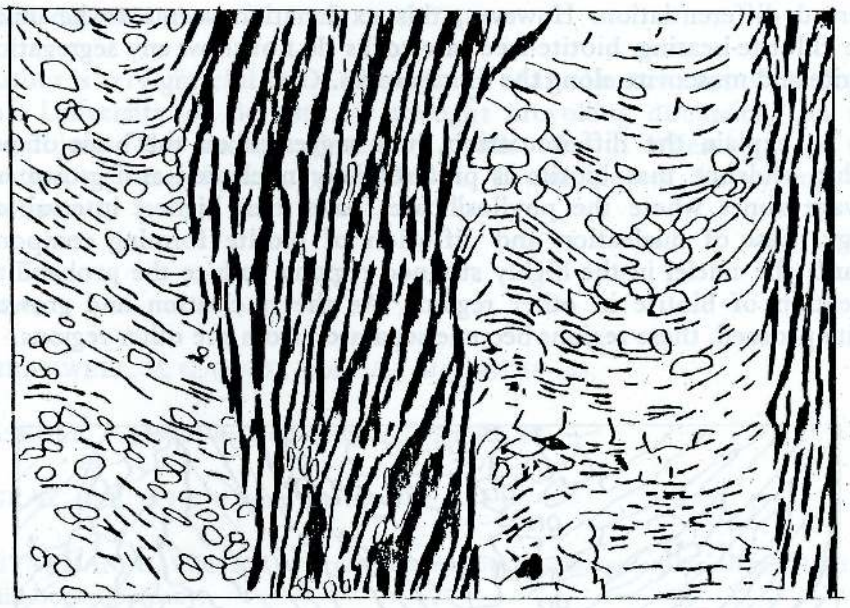

Figure 3 : Differentiation associated with crenulation cleavage. Note the dominance of quartz and feldspar (subrounded to polygonal grains) in the biotite-poor domains. Biotite-black, muscovite – blank (After De Sitter, L. U.(1964). Structural geology, McGraw Hill).

Schmidt's[8] tectonic unmixing model cannot be used to account for the observed textural and mineralogical feature because the minerals involved are mainly biotite and muscovite micas which are considered to have similar mechanical properties. Nicholson[6] and Gray[3] considered that the segregation associated with crenulation cleavage was formed by selective solution and removal of silica resulting in the concentration of minerals such as chlorite, micas and amphiboles. However, there is no petrographic evidence in the studied rocks for selective solution and recrystallization of silica. Hyndman's[4] model explains the contrasted mineral banding formed by quartz and feldspars on one hand and mafic minerals on the other hand but the model fails to explain adequately the observed segregation involving mainly biotite and muscovite micas.

There is no convincing textural evidence in the rocks indicating the nature of the biotite forming reaction. However, on the basis of mineralogy of the rocks and general absence of primary chloride in them, it is suggested that the biotite producing reaction is of the form,

$$\text{muscovite}_1 + \text{chlorite} \rightarrow \text{biotite} + \text{muscovite}_2 + \text{quartz} + H_2O$$

Therefore, if the biotite producing phases were segregated along the S_2 cleavage zones due to any one or more of the above discussed mechanical or chemical processes, then the growth of biotite would have produced the

observed differentiation. However, this explanation seems to be unlikely since chlorite-bearing, biotite-free rare rocks do not show any segregation of chlorite and muscovite along the S_2 cleavages.

To explain the differentiation, it is suggested on the basis of petrographic evidence that biotite is preferentially nucleated and grown in S_2 cleavage zones where the phyllosilicates have their highest interval strain energy. Ease of nucleation and diffusion of biotite forming components towards the nuclei in the highly strained regions, reduce the probability of nucleation of biotite in other regions. As the nucleation and growth of biotite proceed, these regions become separated from the other regions.

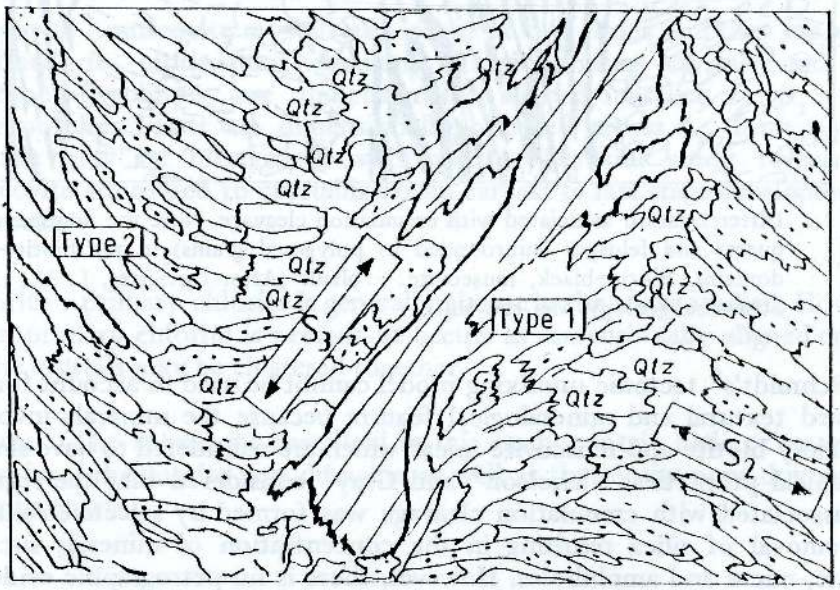

Figure 4 : Large kyanite crystals (Type 1) formed along S_3 cleavage zone and smaller (Type 2) kyanite crystals formed outside S_3 cleavage zone. Biotite stippled, muscovite-unshaded, quartz marked as qtz. (Redrawn from Fig. 2 of Bramwell, 1985).

Recently, Bramwell[1] has described concentration of kyanite crystals in S_3 cleavage zones in some pelitic rocks from Switzerland (Figure 4). The kyanite crystals in the S_3 zones are compositionally zoned with respect to Fe_2O_3. He has used textural and analytical data to show that kyanite first nucleated in the S_3 zones and later in the regions outside these zones. Bramwell suggested that the differentiation was produced by preferred nucleation and growth of kyanite crystals in the S_3 zones. Thus preferred nucleation and growth of minerals in highly strained regions may be an important process causing differentiation.

Acknowledgements

The author is very grateful to Dr. K. A. Jones of the Department of Geology, Queen's University of Belfast, for thought provoking discussions on the above subject. The author wishes to thank Mrs. J. Wijesekera for the preparation of the figures, and Mr. K. Dunuhappawa for typing the manuscript.

References

1. BRAMWELL, M. G. (1985). *Mineralog. Mag.* **49**: 59–64.

2. ESKOLA, P. (1932) *Bull. Comm. Geol. Finl.* **97**: 68.

3. GRAY, D. R. (1977) *Lithos*, **10**: 89–101.

4. HYNDMAN, D. W. (1972) *Petrology of igneous and metamorphic rocks.*, McGraw-Hill Book Company.

5. MATHAVAN, V. (1984). A textural and chemical study of some Dalradian albite schists. Thesis. Queen's University of Belfast.

6. NICHOLSON, R. (1966) Metamorphic differentiation in crenulated schists, *Nature* **209** : 68–69.

7. RAMBERG, H. (1952) Origin of metamorphic and metasomatic rocks, Univ. Chicago Press.

8. SCHMIDT, W. (1932) Tektonik und Verformungslehre. Barnstraeger, Berlin.

9. TALBOT, J. L. and HOBBS, B. E. (1968). *J. Geol.* **76**: 581–587.

J. Natn. Sci. Coun. Sri Lanka 1987 **15** *(1): 25–36*

STUDIES ON RICE HULL ASH CEMENT

D. R. K. LOKULIYANA, M. G. M. U. ISMAIL
Minerals Technology Section, Ceylon Institute of Scientific and Industrial Research, P. O. Box 787, Colombo 7, Sri Lanka.

and

R. P. GUNAWARDANE
Department of Chemistry, University of Peradeniya, Peradeniya, Sri Lanka.

(Date of receipt : 17 July 1986)
(Date of acceptance : 24 February 1987)

Abstract : Rice hull ash cement has been produced by grinding a mixture of rice hull ash and hydrated lime. The most suitable conditions for its production and the important properties of the product such as compressive strength, setting times and hydration have been investigated. The compressive strength of the cement is found to be in between the values for portland and masonry cements. Major hydration products have been identified as tobermorite gel, dicalcium silicate hydrate, xonolite and tobermorite type of calcium silicate hydrate. The binding property of cement can be mainly attributed to the formation of tobermorite gel and dicalcium silicate hydrate. Observed variation of compressive strength of rice hull ash cement with composition, water content, curing time and fineness has been discussed.

1. Introduction

Rice hull is one of the major agricultural by-products in rice growing countries. Recently several Asian countries have found[1] that rice hull ash obtained by burning rice hull possesses pozzolanic properties and hence a cheap pozzolanic type of hydraulic cement can be prepared by mixing with a calcareous material such as quick lime or hydrated lime. For the development of the quality of cement and to determine optimum conditions for production, it is essential to study the effect of lime/rice hull ash ratio, water/cement ratio, fineness, etc., on the strength and other physical properties of cement. It is also necessary to investigate the nature of hydration products.

This paper reports the results of investigation on the hydration process of rice hull ash cement and the nature of hydration products.

2. Experimental

Cement samples for this study were prepared by grinding a mixture of rice hull ash and hydrated lime in a ball mill. Since quick lime is highly reactive and difficult to handle hydrated lime has been used in the present study.

The rice hull ash was obtained by burning two different varieties of rice hull BG 11-11 and BG 34-8 under different laboratory conditions. Physical properties such as compressive strength, standard consistency, setting times, fineness, specific gravity, bulk density and loss on ignition have been investigated. The standard consistency and setting times were determined by using Vicat apparatus, compressive strength and fineness by using universal compression testing machine and Blaine air permeability apparatus, model EL 38-100, respectively. These determinations have been carried out according to the methods described in the British Standard.[2]

Cement samples were hydrated by mixing 1 g of cement with 0.66 ml of distilled water in a petri dish for 24 h., 7, 28, 60 and 90 days. Area of the paste was made to about one square inch and kept at room temperature (25°C) and under atmospheric pressure. A mixture of rice hull ash (0.73 g) and hydrated lime (0.27 g) was hydrated with the same amount of water and kept under the same conditions. The hydrated samples were examined by differential thermal analysis (DTA) and X-ray powder diffraction. Instruments used for this study were MOM, Q-Derivatograph and JDX-8SD with K_{α} radiation, respectively.

3. Results and Discussion

3.1 Preliminary Studies on Cement

Figure 1 shows the variation of compressive strength of cement with rice hull ash to hydrated lime ratio. The most suitable ratio of rice hull ash and hydrated lime for production of cement was found to be 8:3. The compressive strength of cement increases with increase of water/cement ratio upto 0.6 and decreases, as shown in Figure 2. This indicates that the water requirement of cement is high when compared with ordinary portland cement. The relationship between development of strength of cement and duration of curing of mortar cubes is given in Figure 3.

It has been found that the compressive strength increases rapidly upto 7 days and then increases very slowly with time. This indicates that the concentration of hydrated compounds which are responsible for binding property increases rapidly upto 7 days. Figure 4 shows the relationship between the compressive strength of cement and grinding time. It was found that the strength increases with increase of grinding time. This indicates that the compressive strength of this kind of pozzolana cement is proportional to the fineness of cement.

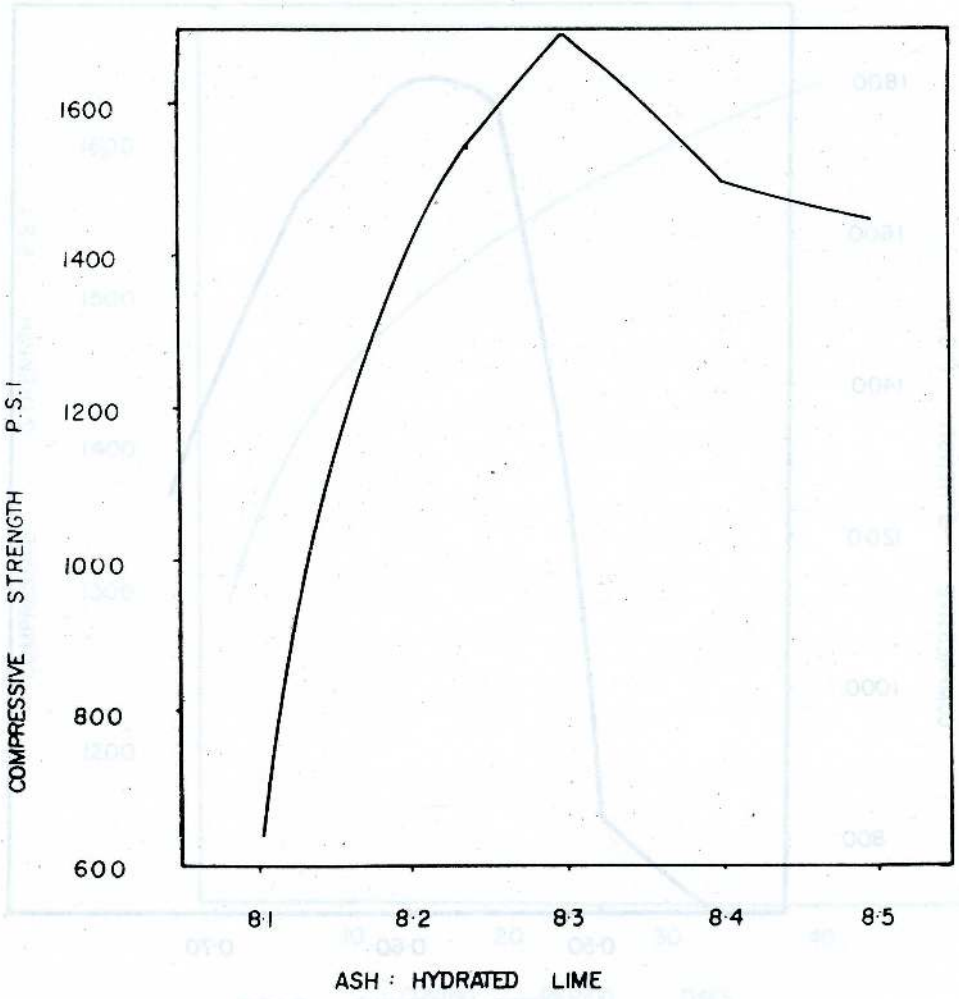

Figure 1. Effect of composition of mixture on compressive strength

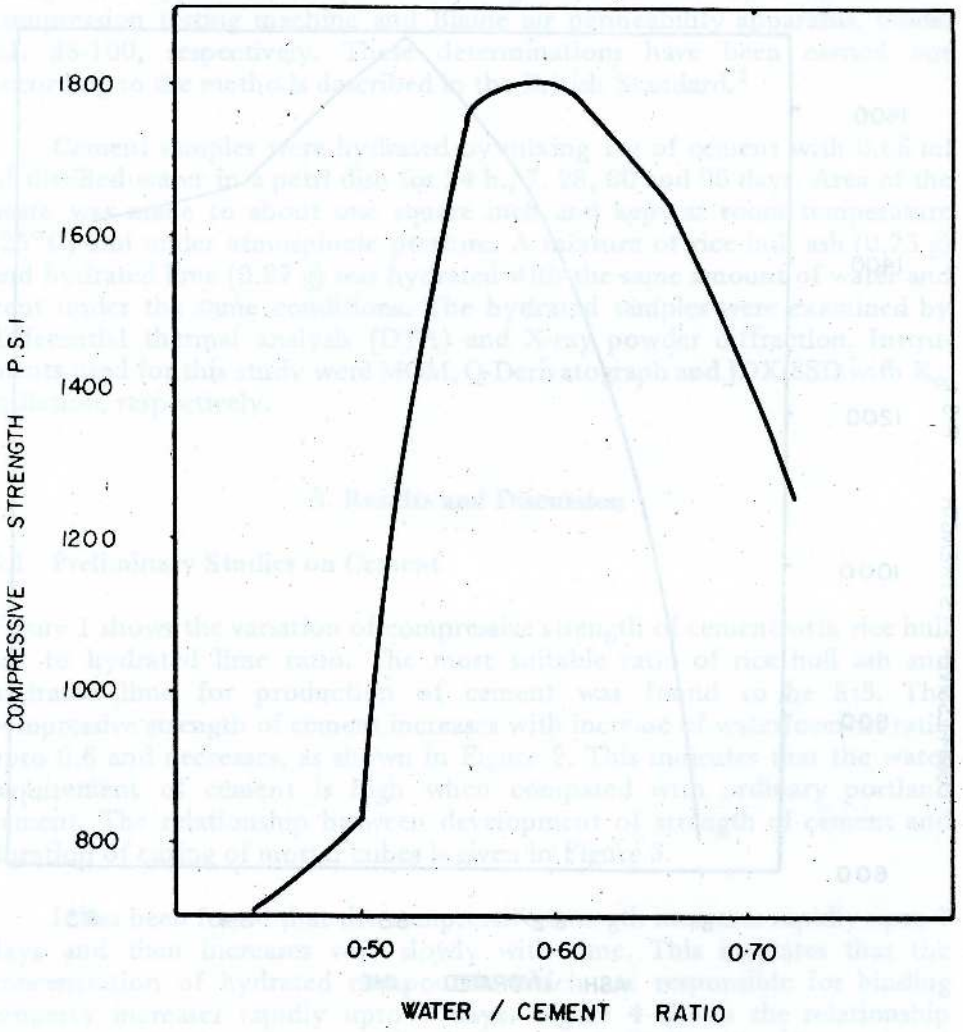

Figure 2. Effect of water/cement ratio on compressive strength

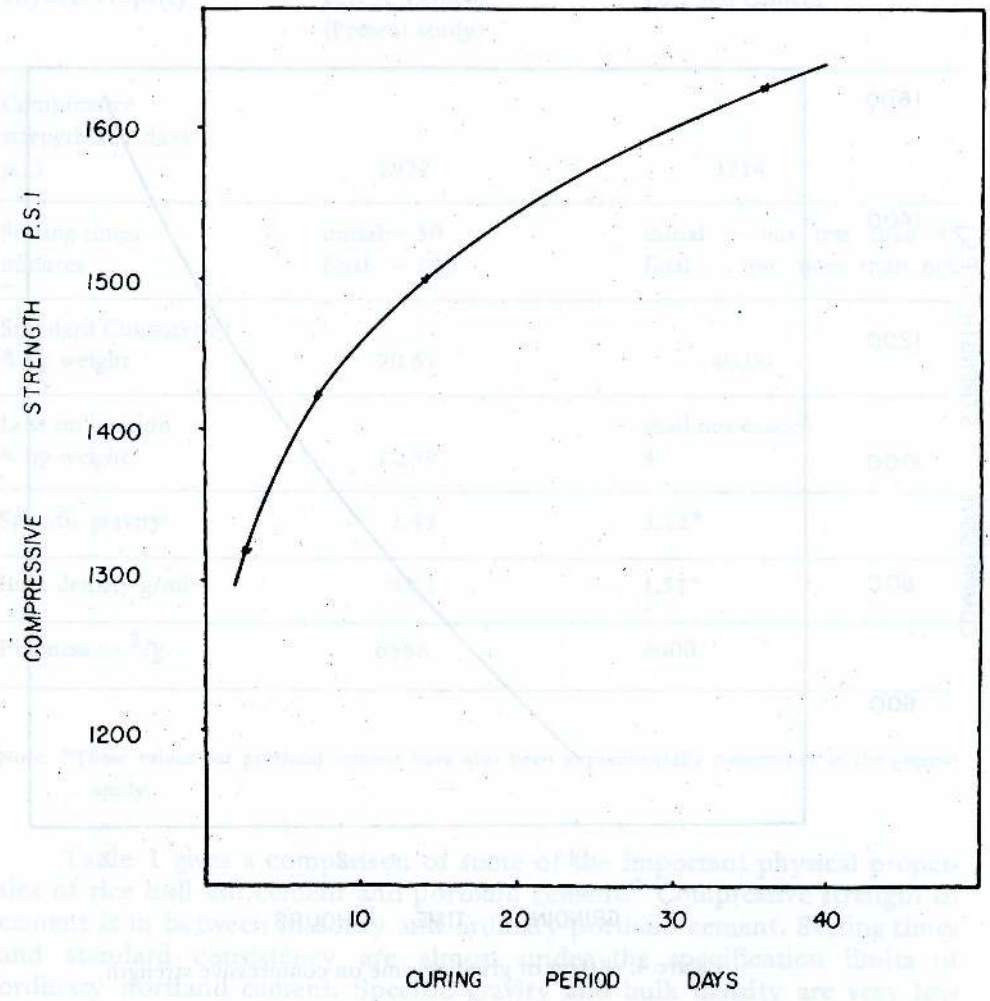

Figure 3. Effect of curing period on compressive strength

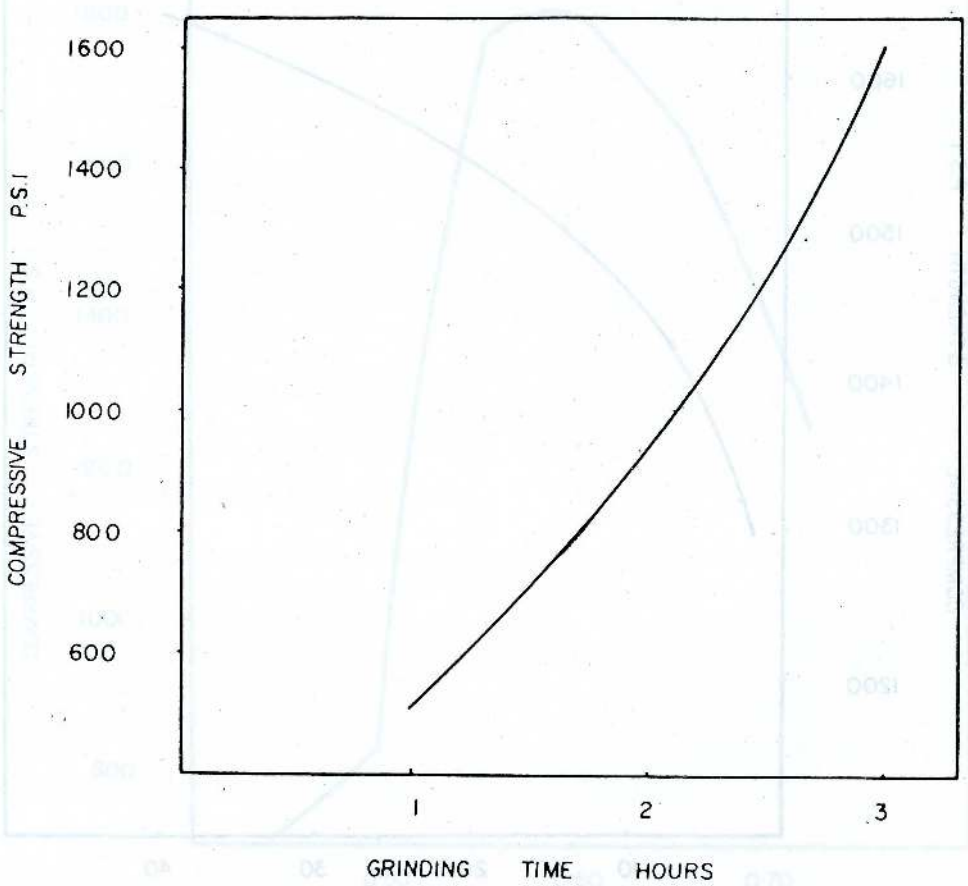

Figure 4. Effect of grinding time on compressive strength

3.2 Physical Properties of Cement

Table 1. Physical properties of rice hull ash cement and portland cement

Physical Property	R.H.A. Cement (Present study)	Portland Cement
Compressive strength at 7 days p.s.i	1922	4714
Setting times minutes	initial – 50 final – 140	initial – not less than 45 final – not more than 600
Standard Consistency % by weight	70.67	40.00
Loss on ignition % by weight	12.59	shall not exceed 4
Specific gravity	2.43	3.12*
Bulk density g/ml	0.61	1.51*
Fineness cm^2/g	6986	4000

Note: *These values for portland cement have also been experimentally determined in the present study.

Table 1 gives a comparison of some of the important physical properties of rice hull ash cement and portland cement.[2] Compressive strength of cement is in between masonry and ordinary portland cement. Setting times and standard consistency are almost under the specification limits of ordinary portland cement. Specific gravity and bulk density are very low when compared with portland cement. This is mainly due to the presence of a large amount of organic matter in rice hull ash and also due to the presence of amorphous silica and hydrated lime as unreacted forms in cement. High loss on ignition is due to the oxidation of organic matter in rice hull ash and the decomposition of hydrated lime.

3.3 Hydration Studies

DTA and X-ray diffraction pattern of hydrated samples are shown in Figures

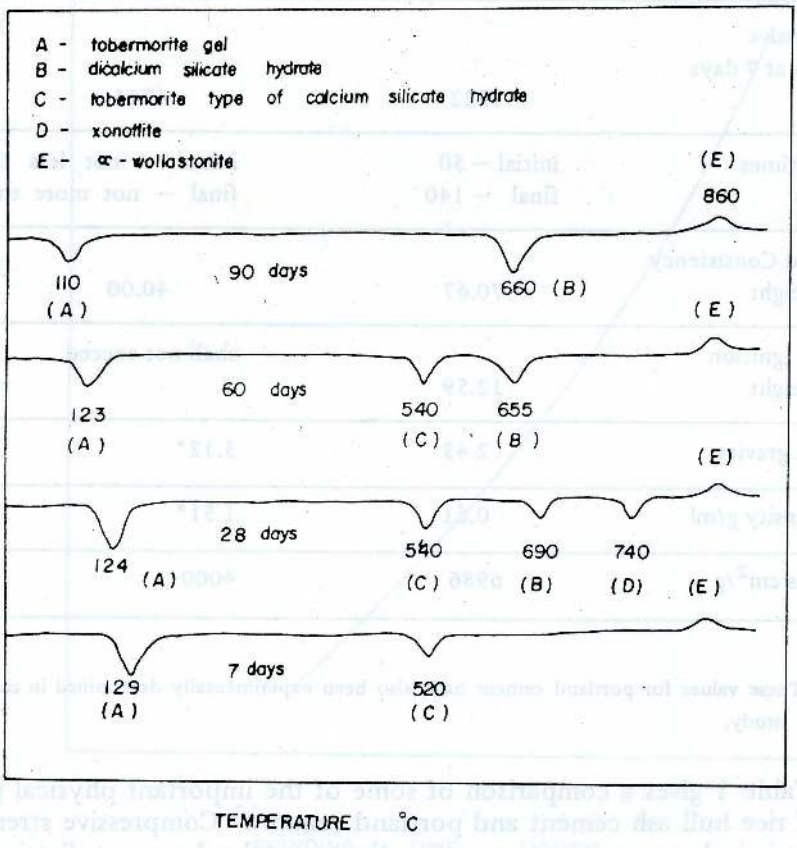

Figure 5. DTA of hydrated cement

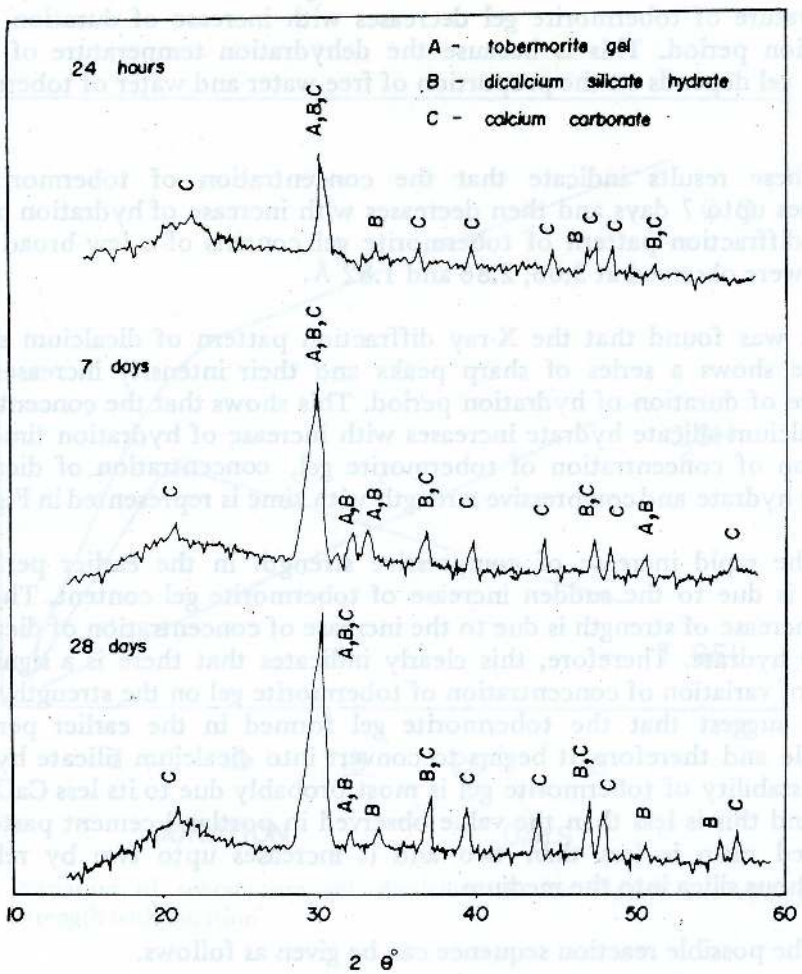

Figure 6. XRD pattern of hydrated cement

5 and 6. Hydrated compounds such as tobermorite gel, dicalcium silicate hydrate, tobermorite type of calcium silicate hydrate and xonolite have been detected. DTA also showed an exothermic reaction at 860°C due to formation of α-wollastonite from CaO and amorphous silica.

This kind of dehydration reactions were observed by thermal treatment of artificial and natural minerals.[3, 4] It is significant that the dehydration temperature of tobermorite gel decreases with increase of duration of the hydration period. This is because the dehydration temperature of tobermorite gel depends on the proportion of free water and water of tobermorite gel.

These results indicate that the concentration of tobermorite gel increases upto 7 days and then decreases with increase of hydration period. X-ray diffraction pattern of tobermorite gel consists of a few broad peaks which were observed at 3.06, 2.86 and 1.82 Å.

It was found that the X-ray diffraction pattern of dicalcium silicate hydrate shows a series of sharp peaks and their intensity increases with increase of duration of hydration period. This shows that the concentration of dicalcium silicate hydrate increases with increase of hydration time. The variation of concentration of tobermorite gel, concentration of dicalcium silicate hydrate and compressive strength with time is represented in Figure 7.

The rapid increase of compressive strength in the earlier period of curing is due to the sudden increase of tobermorite gel content. Then the slow increase of strength is due to the increase of concentration of dicalcium silicate hydrate. Therefore, this clearly indicates that there is a significant effect of variation of concentration of tobermorite gel on the strength. These results suggest that the tobermorite gel formed in the earlier period is unstable and therefore, it begins to convert into dicalcium silicate hydrate. The instability of tobermorite gel is most probably due to its less CaO/SiO_2 ratio and this is less than the value observed in portland cement paste. The observed ratio is less than two and it increases upto two by releasing amorphous silica into the medium.

The possible reaction sequence can be given as follows.

$$x\,CaO.\,y\,SiO_2.\,H_2O \longrightarrow 2CaO.\,SiO_2.\,H_2O + z\,SiO_2$$

tobermorite gel	dicalcium silicate hydrate	amorphous silica

$(x/y < 2)$

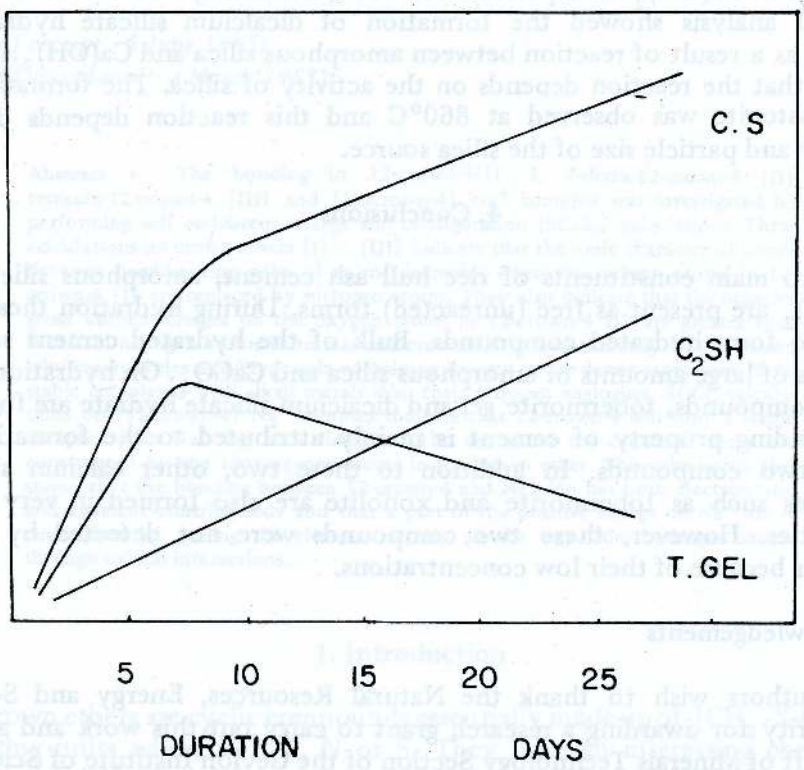

Figure 7. Variation of tobermorite gel, dicalcium silicate hydrate and compressive strength with duration

The hydrated mixture of rice hull ash and hydrated lime after 28 days showed the presence of organic matter, $CaCO_3$, amorphous silica, tobermorite type of calcium silicate hydrate and xonolite. This indicates that the fineness of the rice hull ash particles is not sufficient to produce tobermorite gel.

3.4 Studies on Unhydrated Cement

It has been found that the two major constituents of cement, amorphous silica and $Ca(OH)_2$ are present as free (unreacted) forms. Differential thermal analysis showed the formation of dicalcium silicate hydrate at 480°C as a result of reaction between amorphous silica and $Ca(OH)_2$. It was found that the reaction depends on the activity of silica. The formation of α-wollastonite was observed at 860°C and this reaction depends on the activity and particle size of the silica source.

4. Conclusions

The two main constituents of rice hull ash cement, amorphous silica and $Ca(OH)_2$ are present as free (unreacted) forms. During hydration these two react to form hydrated compounds. Bulk of the hydrated cement sample consists of large amounts of amorphous silica and $CaCO_3$. On hydration, two main compounds, tobermorite gel and dicalcium silicate hydrate are formed. The binding property of cement is mainly attributed to the formation of these two compounds. In addition to these two, other calcium silicate hydrates such as tobermorite and xonolite are also formed in very small quantities. However, these two compounds were not detected by XRD analysis because of their low concentrations.

Acknowledgements

The authors wish to thank the Natural Resources, Energy and Science Authority for awarding a research grant to carry out this work and also to the staff of Minerals Technology Section of the Ceylon Institute of Scientific and Industrial Research for their assistance.

References

1. Rice husk ash cement : Proceedings of a joint workshop, (1979); Bangalore 560052, India : Regional Centre for Technology Transfer.

2. British Standard BS 12, (1978), Specification for ordinary and rapid hardening Portland Cement, British Standard Institution.

3. HELLER, L., TAYLOR, H. F. W., (1951), Hydrated calcium silicates, Part II, *J. Chem. Soc.*, 2397–2401.

4. HELLER, L., TAYLOR, H. F. W., (1956), Crystallographic data for the calcium silicates, Her Majesty's Stationary Office, London.

J. Natn. Sci. Coun. Sri Lanka 1987 **15** *(1): 37–45*

SELF-CONSISTENT CHARGE AND CONFIGURATION (SCCC) CALCULATIONS ON CROWN ETHERS

RAJESWARY MAGESWARAN
Department of Chemistry, University of Jaffna, Jaffna, Sri Lanka

AND

N. J. FITZPATRICK
Department of Chemistry, University College Dublin, Belfield, Dublin 4, Ireland.

(Date of receipt : 5 June 1985)
(Date of acceptance : 2 March 1987)

Abstract : The bonding in 12-crown-4[I], 1, 7-diaza-12-crown-4 [II] tetraaza-12-crown-4 [III] and [12-crown-4] Na^+ complex was investigated by performing self consistent charge and configuration [SCCC] calculations. These calculations on crown ethers [I] – [III] indicate that the ionic character of bonds between neighbouring pairs of atoms decreases when the oxygen atoms in 12-crown-4 [I] are replaced by nitrogen atoms. They also indicate that the negative gross atomic charges on the oxygen atoms in 12-crown-4 [I] are greater than those on nitrogen atoms in tetraaza-12-crown-4[III] and this may be the reason why macrocycles and cryptands containing oxygen as the donor atom form more stable complexes with alkali metals than their nitrogen analogues. SCCC calculations on [12-crown-4] Na^+ complex indicate that 12-crown-4 will form a stable complex with Na^+ ion at a distance 0.150 nm above the centre of the plane constructed by the four oxygen atoms in the crown ether. This calculation also shows that the bonding between 12-crown-4 and Na^+ ion has both electro-static and covalent contributions and that a part of the positive charge on Na^+ ion is neutralised by pulling the electron density all the way from hydrogen atoms through orbital interactions.

1. Introduction

The crown ethers are cyclic compounds essentially made up of-$[CH_2$ -X-$CH_2]$- repeating units where X = 0, N or S. They have an interesting chemistry and one of their important properties is their ability to selectively take metal cations into their cavities to form stable complexes. They are also important with respect to metal ion transport. Hence the synthesis and characterisation of crown ethers and the study of their interaction with metal ions and ammonium guest molecules have been of interest to many chemists. Crown ethers are also of great interest to the theoretical chemists because they represent the simplest model system which might contain some of the features of enzyme specificity. The crown ethers can usually adopt more than one conformation. The actual conformation adopted depends on the nature of the guest molecule and this conformation may be different from the stable conformation of the uncomplexed crown ether. For example, 1, 4, 7, 10-tetraoxacyclododecane [12-crown-4] [I] can adopt[4,7,16,17,20] three different conformations. Out of these, the $ag^+g^+ag^+g^+ag^+g^+ag^+g^+$ confor-

mation [IV] of C_4 symmetry is observed[3,4,5] in alkali metal complexes whereas the more stable conformation of uncomplexed 12-crown-4 is[7] $ag^-g^+ag^+g^+ag^+g^-ag^-g^-$ conformation [V]. We present our results on the self-consistent charge and configuration [SCCC] calculations performed[1] on 12-crown-4 [I] 1,7-diaza-12-crown-4 [II] tetraza-12-crown-4[III] and [12-crown-4] Na^+ complex [VI] in order to study the bonding in these molecules. The $ag^+g^+ag^+g^+ag^+g^+ag^+g^+$ conformation of 12-crown-4 was taken as the model for our calculations.

2. Computational Method

The method used was the FORTICON[8] programme of Hoffmann and co-workers.[1,2,3,5,8] This is an all valence electron calculation [3s and 3p atomic orbitals of sodium atom, 2s and 2p orbitals on second row atoms and 1s on hydrogen atom are used] and was used in its charge iteration mode. Iterations were continued until successive ones produced a change less than 10^{-4}e [e = electronic charge] in the charge on any atom. The geometry of 12-crown-4 used was taken from reported X-ray crystallographic data.[16] The same geometry was used for diaza-12-crown-4 [IV], tetraaza-12-crown-4[V] and [12-crown-4] Na^+ complex. C—H, C—C, C—O, C—N and N—H bond lengths of 0.1091, 0.1536, 0.1430, 0.1472 and 0.1008 nm respectively were used.

3. Results and Discussion

Self-consistent charge and configuration calculation provides four pieces of information, namely the gross atomic charges, the overlap populations, the molecular orbital energy levels and the LCAO expansion of molecular orbitals which could be used to compare the electronic structures of crown ethers and their complexes.

3.1 Gross Atomic Charges

The gross atomic charges are given in Table 1. The negative charges on oxygen atoms and positive charges on carbon atoms in 12-crown-4 and 1,7-diaza-12-crown-4 are in agreement with the more electronegative character of oxygen compared with carbon. The hydrogen atoms attached to carbon are also positively charged. Thus the oxygen atoms withdraw electrons not only from carbon but also from hydrogen through the orbital interaction. Table 1 also shows that the negative charges on oxygen atoms in 12-crown-4 [−0.305e] and 1,7-diaza-12-crown-4 [−0.318e] are very much greater than those on nitrogen atoms in 1,7-diaza-12-crown-4 [−0.144e] and tetraaza-12-crown-4 [−0.155e] and this difference in gross atomic charges is also in

Table 1. Gross Atomic Charges in Molecule I – IV

Atom	Gross Atomic Charges (in electron unit)			
	12-crown-4	Diaza-12-crown-4	Tetraaza-12-crown-4	(12-crown-4) Na^+ complex
O	−0.305	−0.318	–	−0.375
^1C	0.110	0.074	0.062	0.118
^2C	0.110	0.097	0.062	0.118
H	–	−0.144	−0.155	–
H(^1C)	0.021	0.007	0.003	0.077
H(^2C)	0.021	0.016	0.003	0.077
H(N)	–	0.026	0.022	–
Na^+	–	–	–	0.328

agreement with the electronegativities of oxygen and nitrogen atoms. For the same reason the positive charges on carbon atoms of 1,7-diaza-12-crown-4 and tetraaza-12-crown-4 (Table 1). The positive charges on hydrogen atoms attached to carbon are also very small [almost negligible] in the case of tetraaza-12-crown-4. In other words, overall charge separation in tetraaza-12-crown-4 is very much less when compared with those in 12-crown-4. This explains the observed[12,13,15,18] marked decrease in stability of the alkali cation complexes with macrocyles and cryptands when oxygen binding sites are replaced by nitrogens.

3.2 The overlap population

Table 2. Overlap populations in molecules I – IV

Bond	12-crown-4	Diaza-12-crown-4	Tetraaza-12-crown-4	(12-crown-4) Na^+ complex
C–O	0.675	0.680	–	0.669
C–H	0.818	0.822	0.824	0.803
C–C	0.831	0.825	0.816	0.823
N–H	–	0.790	0.790	–
C–N	–	0.730	0.739	–
C–Na^+	–	–	–	0.124

Further insight into the bonding is obtained from the overlap populations. The overlap populations between neighbouring pairs of atoms are given in Table 2. It shows that the overlap populations between carbon atoms and nitrogen atoms in diaza-12-crown-4 [0.730] and tetraaza-12-crown-4 [0.739]

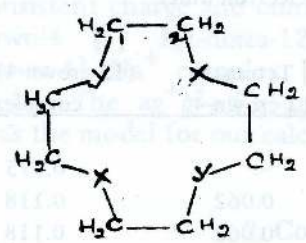

(I) X = Y = O

(II) X = O; Y = NH

(III) X = Y = NH

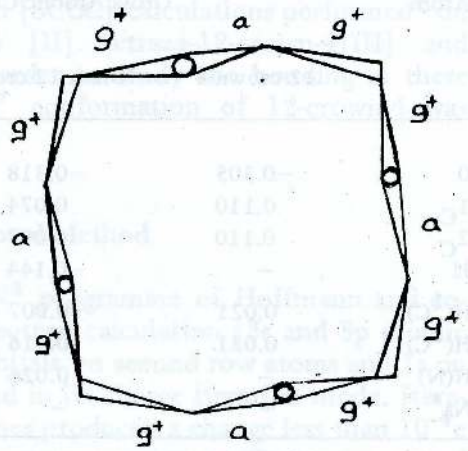

(IV)

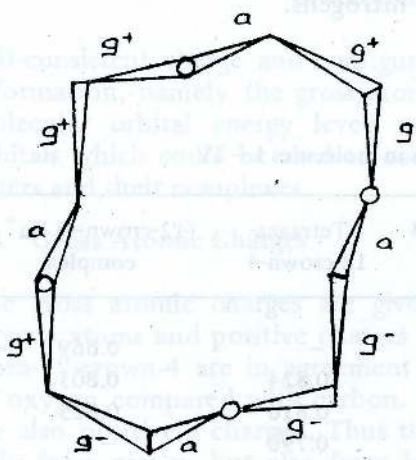

(V)

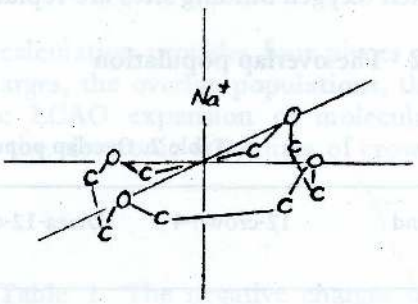

(VI)

are greater than those between carbon atoms and oxygen atoms in 12-crown-4 [0.675] and diaza-12-crown-4 [0.680]. This again reflects the more covalent character of C–N bond when compared with C–O bond. Table 2 also shows that the overlap populations between carbon atoms and hydrogen atoms increase when the heteroatoms in 12-crown-4 are changed from oxygen to nitrogen and this is in agreement with the observed decrease in positive charges on carbon and hydrogen atoms.

Table 3. Total Energy of Valence Electrons and Energies of first ten HOMO's and LUMO

Orbital	Energy/eV		
	12-crown-4	Diazo-12-crown-4	Tetraaza-12-crown-4
HOMO	−10.10 (9e)	− 9.90 (5e)	− 9.74($5b_2$)
	−10.12($7b_1$)	−10.40 (4e)	−10.25(12e)
	−10.15($6a_1$)	−10.80(14b)	−10.90($5a_1$)
	−10.81($6b_1$)	−10.95(12a)	−12.40(11e)
	−10.98 (8e)	−12.24(11a)	−12.58(10e)
	−11.19($5a_1$)	−12.43(13b)	−13.59($4b_2$)
	−12.53($5b_2$)	−12.63(12b)	−13.73 (9e)
	−12.58($4b_2$)	−12.92(11b)	−
LUMO	−0.504($8b_1$)	0.675(13a)	2.04(13e)
Total Energy of Valence Electrons	−1260.13	−1247.8	−1237.6

3.3 Molecular Orbitals and the Energies of Valence Electrons

The calculated molecular orbital energies of the first ten highest occupied molecular orbitals (HOMO.s) and the total energy of valence electrons of 12-crown-4, diaza-12-crown-4 and tetraaza-12-crown-4 are given in Table 3. It is interesting to note that these calculated molecular orbital energies of 12-crown-4 agrees well with the reported[9] binding energy values by photoelectron spectra. The LCAO expansion of these molecular orbitals show that, in 12-crown-4, the first eight HOMO.s have contributions from oxygen atoms only and hence could be considered as lone pair molecular orbitals. The ninth and tenth molecular orbitals [E = −12.53eV and −12–58eV] have contributions from all oxygen atoms and carbon atoms and could be assigned to σ molecular orbitals. Similarly, in diaza-12-crown-4, the first six HOMO.s are found to have the lone pair nature [contributions from oxygen and nitrogen atoms only] whereas in tetraaza-12-crown-4, the first four HOMO.s have the lone pair nature[contributions from nitrogen atoms only]. Table 3 also gives the molecular orbital energies of LUMO of crown ethers.

The LCAO expansion of LUMO.s of crown ethers have contributions from the heteroatoms [oxygen atoms and/or nitrogen atoms] and carbon atoms. Table 3 further shows that the replacement of oxygen atoms by nitrogen atoms in crown ethers decreases the binding energies of valence electrons and increases the molecular orbital energy of LUMO slightly. In other words, the energy difference between HOMO and LUMO increases slightly from 12-crown-4 to tetraaza-12-crown-4.

3.4 [12-crown-4] Na^+ Complex

SCCC calculations on [12-crown-4]Na^+ complex were performed by changing the distance of Na^+ from the centre of the plane constructed by the four oxygen atoms in 12-crown-4 in a direction perpendicular to the plane away from the carbon atoms. The plot of total energy of valence electrons vs the distance is shown in Figure 1. From this plot it is evident that Na^+ ion is too large an ion to be at the centre of the cavity of 12-crown-4 and that the stable complex is formed when the Na^+ ion is at a distance 0.150 nm out of plane. This is in agreement with the reported[16] X-ray crystallographic data for bis[12-crown-4]Na^+ complex. The bonding between the crown ether and Na^+ ion could be considered to have both electrostatic and covalent contributions. The electrostatic contribution is mainly from the ion-dipole interaction between Na^+ ion and negatively charged oxygen atoms. The gross atomic charges (Table 1) and the overlap populations (Table 2) of [12-crown-4] Na^+ complex indicate that there is a reasonable amount of covalent contribution to bonding between Na^+ ion and 12-crown-4. This is mainly due to charge transfer interaction. Table 1 shows that in [12-crown-4] Na^+ complex, the negative charges on all oxygen atoms have been increased by 0.070e, the positive charges on carbon atoms have been increased only by a small amount [0.010e] and the positive charges on hydrogen atoms have been increased by 0.056e. This indicates that a part of the positive charge on Na^+ ion is neutralised by pulling the electron density all the way from hydrogen atoms through orbital interaction. This is also indicated by reduction in the overlap populations between carbon and hydrogen atoms and carbon and oxygen atoms (Table 2).

4. Conclusion

SCCC calculations on crown ethers I – III indicate that the negative gross atomic charges on the heteroatoms decrease when the oxygen atoms in 12-crown-4 [I] are replaced by nitrogen atoms. This explains the observed[12,13,15,18] marked decrease in stability constants of the alkali cation complexes of crown ethers and cryptands when oxygen binding sites are replaced by nitrogen atoms as the metal ion-oxygen bond in alkali metal complexes could be predominantly ionic. SCCC calculations on [12-crown-4] Na^+ complex indicate that the arrangement for a stable complex is that with Na^+ ion at a distance 0.150 nm above the centre of the plane

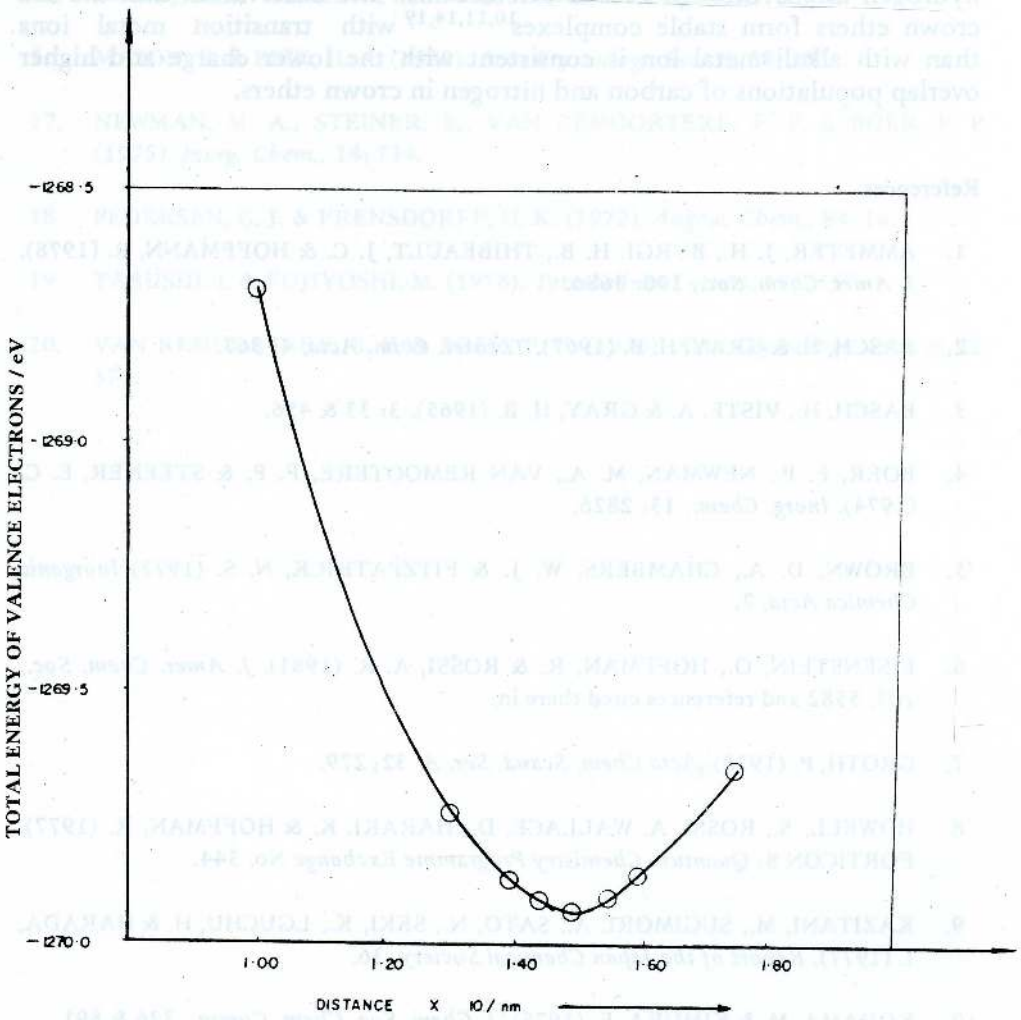

Figure 1. The plot of total energy of valence electrons of (12-crown-4) Na^+ complex vs the distance of Na^+ from the centre of the plane constructed by the four oxygen atoms in 12-crown-4.

constructed by the four oxygen atoms in the crown ether. This calculation also shows that the bonding between 12-crown-4 and Na^+ ion has both electrostatic and covalent contributions and a part of the positive charge on Na^+ ion is neutralised by pulling the electron density all the way from hydrogen atoms through orbital interactions. The observation that the aza crown ethers form stable complexes[10,11,14,19] with transition metal ions than with alkali metal ion is consistent with the lower charge and higher overlap populations of carbon and nitrogen in crown ethers.

References

1. AMMETER, J. H., BURGI, H. B., THIBEAULT, J. C. & HOFFMANN, R. (1978). *J. Amer. Chem. Soc.*, **100**: 3686.

2. BASCH, H. & GRAY, H. B. (1967). *Theoret. Chim. Acta*, **4**: 367.

3. BASCH, H., VISTE, A. & GRAY, H. B. (1965). **3**: 33 & 456.

4. BOER, F. P., NEWMAN, M. A., VAN REMOOTERE, F. P. & STEENER, E. C. (1974). *Inorg. Chem.*, **13**: 2826.

5. BROWN, D. A., CHAMBERS, W. J. & FITZPATRICK, N. S. (1972) *Inorganic Chemica Acta*, **7**.

6. EISENSTEIN, O., HOFFMAN, R. & ROSSI, A. R. (1981). *J. Amer. Chem. Soc., 103;* 5582 and references cited there in.

7. GROTH, P. (1978). *Acta Chem. Scand. Ser. A*, **32**; 279.

8. HOWELL, S., ROSSI, A. WALLACE, D., HARAKI, K. & HOFFMAN, R. (1977). FORTICON 8: *Quantum Chemistry Programme Exchange* No. 344.

9. KAZITANI, M., SUGIMORI, A., SATO, N., SEKI, K., LGUCHU, H. & HARADA, I. (1977). *Report of the Japan Chemical Society*, 36.

10. KODAMA, M. & KIMURA, E. (1975). *J. Chem. Soc. Chem. Comm.*, 326 & 891.

11. LEHN, J. M. (1978). *Acc. Chem. Research*, **11**; 49 & 392.

12. LAHN, J. M. & MONTAVON, F. (1978). *Helv. Chim. Acta*, 61; 67.

13. LEHN, J. M. & SAUVAGE, J. P. (1975). *J. Amer. Chem. Soc.*, **97**; 5022.

14. LEHN, J. M. & SIMON. J. (1977). *Helv. Chim. Acta*, **60**; 141.

15. LEHN J. M. & VIERLING, P. (1980). *Tetrahedron Letters*, **21**; 1323.

16. MASON, E. & EICK, H. A. (1982). *Acta Crystallogr. Sect B*, **38**; 1821.

17. NEWMAN, M. A., STEINER, E., VAN REMOORTERE, F. P. & BOER, F. P. (1975). *Inorg. Chem.*, **14**; 734.

18. PEDERSEN, C. J. & FRENSDORFF, H. K. (1972). *Angew. Chem.*, **84**; 16.

19. TABUSHI, I. & FUJIYOSHI, M. (1978). *Tetrahedron Letters*, **19**; 2157.

20. VAN REMOORTERE, E. P. & BOER, F. P. (1976). *Acta Crystallogr. Sect. B*, **32**; 370.

J. Natn. Sci. Coun. Sri Lanka 1987 **15** *(1): 47–59*

SELF-CONSISTENT CHARGE AND CONFIGURATION (SCCC) CALCULATIONS ON 1,6-DICARBA-CLOSO-HEXABORANE (6), 2,4-DICARBA-CLOSO-HEPTABORANE (7) AND THEIR METALLO-DERIVATIVES

RAJESWARY MAGESWARAN
Department of Chemistry, University of Jaffna, Jaffna.

and

N. J. FITZPATRICK
Department of Chemistry, University College, Dublin, Dublin 4, Ireland

(Date of receipt : 14 May 1985)
(Date or acceptance : 2 March 1987)

Abstract : The bonding in 1, 6-dicarba-closo-hexaborane [6] [I], $[C_2B_3H_5\{Fe(CO)_3\}]$ [II]. 2,4-dicarba-closo-heptaborane[7] [III], $[C_2B_4H_6\{Fe(CO)_3\}]$ [IV], and $[C_2B_3H_5\{Fe(CO)_3\}_2]$ [V] was investigated by carrying out self consistent and configuration [SCCC] calculations. These investigations show that an apical boron atom uses $2p_x$, $2p_y$ atomic orbitals and a $[2s, 2p_z]$ hybrid orbital for bonding with rest of the cluster. In cluster compounds containing $Fe(CO)_3$ units, the iron atom uses predominantly $[3d_{xz}, 4p_x]$ and $[3d_{yz}, 4p_y]$ combinations for bonding with the rest of the cluster and there is no evidence for the involvement of a $[4s, 4p_z, 3d_{z^2}]$ hybrid orbital similar to the $[2s, 2p_z]$ hybrid observed in the boron analogue. Analysis of the total overlap population associated with metallo-group and the rest of the cluster shows that the $Fe(CO)_3$ group is weakly bonded into the cluster when compared with BH group of compounds in which $Fe(CO)_3$ is replaced by BH. This analysis also indicates that $Fe(CO)_3$ group uses less than two electrons for cluster bonding.

1. Introduction

Understanding of the electronic structure and bonding of metal carbonyl clusters is of present interest. The number of orbitals involved in bonding [> 100 atomic orbitals] makes it difficult to perform detailed molecular orbital calculations on metal carbonyl clusters. But it is believed that certain metallo groups such as $Fe(CO)_3$ and $Co(CO)_3$ are isolobal and isoelectronic with the BH and CH groups respectively. In terms of Wade's approach[19] a BH or a $Fe(CO)_3$ group formally supplies two electrons for cluster bonding whereas CH and $Co(CO)_3$ groups supply three each. In addition, many boranes, carboranes, metalloboranes, metallocarboranes, and metal carbonyl clusters have similar geometries.[13,19] Thus the study of the electronic structure and bonding of boranes, carboranes, metallo-boranes and metallo-carboranes could be used to compare the bonding capabilities of transition metal carbonyl fragments, $M(CO)_3$ with those of the BH or CH Units in cluster compounds. In our study, self-consistent charge and configuration (SCCC) calculations were used to investigate the bonding in 1,6-dicarba-

closo-hexaborane[6] [I], $[C_2B_3H_5\{Fe(CO)_3\}]$ [II], 2,4-dicarba-closo-heptaborane [7] [III], $[C_2B_4H_6\{Fe(CO)_3\}]$ [IV] and $[C_2B_3H_5\{Fe(CO)_3\}_2]$ [V].

2. Computational Method

The method used was the FORTICON[8] programme of Hoffman and co-workers.[15] This calculation is an all valence electron, extended Huckel calculation [3d, 4s and 4p atomic orbitals on transition metal atoms, 2s and 2p on second row atoms and on hydrogen atom are used] and was used in its charge iteration mode according to $H_{ii} = VSIE[Q]$ where H_{ii} is the diagonal Hamiltonian matrix element and VSIE[Q] is the valence state ionisation energy of orbital i when the atom has total charge Q. The off diagonal Hamiltonian matrix elements are calculated in the normal manner[9] using the expression,

$$H_{ii} = k\frac{S_{ii}}{2}[H_{ii} + H_{jj}]$$

where ki is a constant.

The VSIE[Q] functions are assumed to be of the form,

$$VSIE[Q] = AQ^2 + BQ + C$$

where A,B and C are parameters,[16,20] which depend on the atom and the orbital. Iterations are continued until successive ones produced $< 10^{-4}$e change in the charge on any atom [e = electronic charge]. The well known problem of obtaining convergence with such self-consistent charge calculations was eased by an improved damping scheme and by the use of a Madelung correction. The orbital occupations are summed separately over the p and d orbitals on each atom. The resulting p and d occupations, along with s occupations, are damped according to the equation

$$\rho_r^{\text{input } k+1} = \rho_r^{\text{input } k} + \lambda\left(\rho_r^{\text{output } k} - \rho^{\text{input } k}\right)$$

where ρ is the summed orbital occupation of a given type, s,p or d, indexed by r on the k^{th} cycle and λ is a damping parameter.

The geometries of carboranes used were taken from reported,[17,18] electron diffraction data. The same geometries were used for metallocarboranes. The geometry of the $Fe(CO)_3$ unit was taken from that of $[Fe(CO)_3\ \eta^4\text{-}C_4H_4]$[10]. Fe – C and C–O bond lengths of 0.182 nm and 0.115 nm respectively were used. Changing the position of the metallo-units by $\pm$ 10% with respect to the carborane base produced no significant change in the results.

Table 1. Gross atomic charges in molecules [I] – [V]

Molecules	Atom sites as shown in diagrams [I] to [V]										
	1	2	3	4	5	6	7	Carbonyl group			
								Carbon		Oxygen	
								d	e	d	e
[I]	−0.014	0.094	0.094	0.094	0.094	−0.014	–	–	–	–	–
[II]	−0.055	0.057	0.074	0.057	0.733	−0.055	–	0.041	–	−0.200	–
[III]	0.124	−0.022	0.105	−0.022	0.070	0.070	0.124	–	–	–	–
[IVa]	0.824	−0.062	0.066	−0.062	0.043	0.043	0.095	0.043	–	−0.202	–
[IVb]	0.078	−0.037	0.077	−0.044	0.780	0.057	0.078	–	0.028	–	−0.216
[Va]	0.723	−0.074	0.038	−0.074	0.026	0.026	0.723	0.040	–	−0.200	–
[Vb]	−0.848	0.010	0.096	−0.065	2.615	0.054	0.054	0.102	−0.080	−0.220	−0.312

d – Charge on the carbon/oxygen atom of carbonyl group when the $Fe(CO)_3$ unit is apical.
e – Charge on the carbon/oxygen atom of carbonyl group when the $Fe(CO)_3$ unit is basal.
Note: 1,2,3 etc. corresponds to the atom positions labelled 1,2,3 etc. in the diagrams [I] to [V].

Table 2. Charges localised on BH_2 Ch and $Fe(CO)_3$ units in molecules [I] – [V]

Molecule	Atom sites as shown in diagrams [I] – [IV]						
	1	2	3	4	5	6	7
[I]	−0.045	0.022	0.022	0.022	0.022	−0.045	–
[II]	−0.013	−0.034	0.002	−0.034	0.271	−0.103	–
[III]	0.055	−0.051	0.034	−0.051	−0.021	−0.021	0.055
[IVa]	0.344	−0.111	−0.026	−0.111	−0.063	−0.063	0.027
[IVb]	−0.001	−0.069	−0.003	−0.081	0.217	−0.042	−0.021
[Va]	0.250	−0.127	−0.069	−0.127	−0.086	−0.086	0.250
[Vb]	−1.204	−0.033	0.007	−0.118	1.447	−0.060	−0.038

Table 3. Overlap population in molecules [I] and [II]

Bond	I	II
$C^{1[6]}-B2$	0.579	0.740
$C^{1[6]}-B^3$	0.579	0.672
$C^{1[6]}-B^5$	0.579	–
$C^{1[6]}-Fe^5$	–	0.340
B^2-B^3	0.519	0.570
B^2-Fe^5	–	0.285
$C^{1[2]}-H$	0.841	0.877
$B^{2[4]}-H$	0.816	0.839
B^3-H	0.816	0.806

3. Results and Discussion

The details of the cluster bonding in carboranes and metallocarboranes can be considered from three pieces of information provided by the SCCC calculation. They are [i] the gross atomic charges [ii] the overlap populations and [iii] the molecular orbital energy levels and their LCAO expansions.

3.1 1,6-$C_2B_4H_6$ [I] and 2,4-$C_2B_5H_7$ [III]

The gross atomic charges (Table 1) and the overlap populations (Table 3) indicate that the four BH units in 1,6-$C_2B_4H_6$ are equivalent and so are the two CH units. This is in agreement with the predicted[17] D_{4h} symmetry of the molecule. The presence of three distinct type of BH units in 2,4-

$C_2B_5H_7$ is shown by the localised charges [Tables 1 and 2], the boron atom in apical position being more positively charged. The overlap populations [Table 4] bonding these BH units into the cluster [in 2,4-$C_2B_5H_7$] are slightly different and reflect the positive charges on boron atoms. Thus the two apical BH units are less strongly bonded into the cluster when compared with the three basal BH units. The gross atomic charges on carbons and borons agree with the more electronegative character of carbon compared with boron. Our values for located charges on C–H and B–H moieties [−0.045 and 0.022 respectively] of 1,6-$C_2B_4H_6$ are comparable with the values [−0.05 and 0.03 respectively] reported[12] earlier by a different SCF

Table 4. Overlap populations in Molecules [III] – [V]

Bond	[III]	[IVa]	[IVb]	[Va]	[Vb]
$B^{1[7]} - H$	0.836	0.828	0.862	–	0.856
$C^2 - H$	0.827	0.861	0.830	0.881	0.852
$B^3 - H$	0.836	0.858	0.838	0.871	0.848
$C^4 - H$	0.827	0.861	0.856	0.881	0.891
$B^{6[5]} - H$	0.839	0.860	9.860	0.871	0.881
$B^7 - H$	0.836	0.828	0.860	–	0.856
$B^{7[1]} - C^2$	0.469	0.536	0.518	–	0.558
$B^3 - C^2$	0.776	0.865	0.823	0.985	0.879
$B^3 - B^{7[1]}$	0.355	0.414	0.394	–	0.427
$B^{6[5]} - B^{7[1]}$	0.447	0.538	0.584	–	0.657
$B^6 - C^2$	0.726	0.878	0.785	0.994	0.908
$[B^5 - C^4]$					
$B^6 - B^5$	0.693	0.751	–	0.842	
$B^7 - C^4$	0.469	0.536	0.651	–	0.712
$Fe^1 - C^2$	–	0.359	–	0.245	0.183
$Fe^1 - B^3$	–	0.294	–	0.235	0.147
$Fe^1 - C^4$	–	0.359	–	0.245	0.141
$Fe^1 - B^{6[5]}$	–	0.290	–	0.212	0.115
$Fe^5 - B^{7[1]}$	–	–	0.315	–	0.293
$Fe^5 - C^2$	–	–	0.340	–	0.299
$Fe^5 - B^6$	–	–	0.285	–	0.217
$Fe^1 - Fe^5$	–	–	–	–	0.777

calculation. Three cluster bonding molecular orbitals are found in 1,6-$C_2B_4H_6$. The HOMO[$2b_{2g}$] is a B_4 combination [E = −11.75eV] followed by a degenerate pair [$3e_u$] [E = −12.38eV] which has C_2B_4 combination. In 2,4-$C_2B_5H_7$, two cluster bonding molecular orbitals [E = − 25.95 and −12.81eV] of C_2B_5 combination have been found in addition to the HOMO [E = −11.2eV] which is a combination of mainly the planar carbon and boron atoms. Our results [Table 4] also show that in 2,4-$C_2B_5H_7$, the site to site $[BH]_{basal} - [BH]_{basal}$ overlap population is

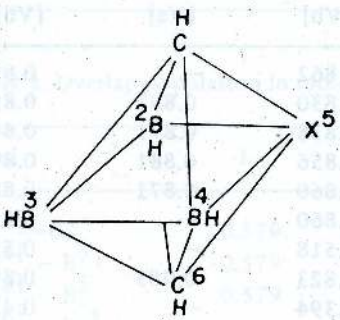

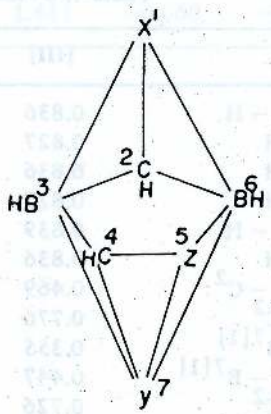

(I) X = BH
(II) X = $Fe(CO)_3$

(III) X = Y = Z = BH
(IVa) X = $Fe(CO)_3$; Y = Z = BH
(IVb) X = Y = BH; Z = $Fe(CO)_3$
(Va) X = Y = $Fe(CO)_3$; Z = BH
(Vb) X = Z = $Fe(CO)_3$; Y = BH

SCHEME – [I]

greater than that of $[BH]_{basal}$ – $[BH]_{apical}$ population and this is in agreement with the difference in observed[18] bond lengths $[BH]_{basal}$ – $[BH]_{basal}$ = 0.1659nm, $[B^1H] - [B^5H]$ = 0.1772nm and $[B^1H] - [B^3H]$ = 0.1852mm].

Let us commence the discussion of metallocarboranes by comparing the orbitals available on BH and $Fe(CO)_3$ units for cluster bonding. In terms of Wade's approach[19] both the BH and the $Fe(CO)_3$ units use two electrons and three orbitals for cluster bonding. Iron in the $Fe(CO)_3$ unit has nine valence shell orbitals [c.f. boron which has four valence shell orbitals], three of these are used to form M–C δ-bonds, three more as well as three electron pairs are used to form π-bonds to the carbonyl groups. This leaves the Fe atom with three valence shell orbitals and two electrons.

SCCC calculations show that in BH the HOMO is a δ-level composed of 2s and 2p while LUMOs[e] [$2p_x$ and $2p_y$] are the π-levels. In the case of $Fe(CO)_3$, the HOMO is a hybrid [a_1] orbital having 4s, $4p_z$ and $3d_z2$ components and the LUMOs[e] orbitals are formed from [$4p_x$, $3d_{xz}$] and [$4p_y$, $3d_{yz}$] combination as has been reported.[11] This is in agreement with Wade's skeletal electron counting technique. Thus the orbitals* available for cluster bonding on BH and $Fe(CO)_3$ units, as shown in Figure 1, are similar in symmetry as reported[11] earlier. [*The 2D projections of the HOMO and LUMO orbitals of BH and $Fe(CO)_3$ units obtained by z plot programme[1-4,9,16,20] also had similar shapes].

3.2 $[C_2B_3H_5\{Fe(CO)_3\}]$ [II]

Replacement of the BH unit is 1,6-$C_2B_4H_6$ by the $Fe(CO)_3$ unit, as in [II], increases [Table 1] the net negative charge on carbons by 0.041 and decreases the positive charge on boron by values in the range 0.020–0.037. Table 3 shows that the overlap population bonding the metallo-unit to the $C_2B_2H_4$ base is about 57% of that bonding the BH in 1,6-$C_2B_4H_6$. In other words the replacement of a BH unit by a $Fe(CO)_3$ group makes the resulting compound even more electron-deficient than the parent carborane. A similar result has been observed in borane clusters.[7] Table [I] shows that the iron atom of ferracarborane [II] carries a positive charge [0.733] and this may be the reason for the reduction in overlap population betwen the metallo-unit and carborane base. The positive charge on iron atom may be due to the valence electrons in iron atom being largely delocalised over the carbonyl ligands. Replacement of a BH unit in 1,6-$C_2B_4H_6$ by a $Fe(CO)_3$ unit did not change the energy of the cluster orbitals appreciably. The comparison of the cluster bonding molecular orbitals shows that the roles of the boron $2p_x$ and $2p_y$ atomic orbitals in carboranes are taken up by the iron $3d_{xz}$ and $3d_{yz}$ with some admixture of $4p_x$ and $4p_y$. According to the isolobal principle the $3d_z2$, 4s and $4p_z$ metal atomic orbitals should combine to form a hybrid orbital which takes on the role of the boron 2s and $2p_z$ orbitals. In $Fe(CO)_3$, the $3d_z2$ atomic orbital is involved in bonding but plays no

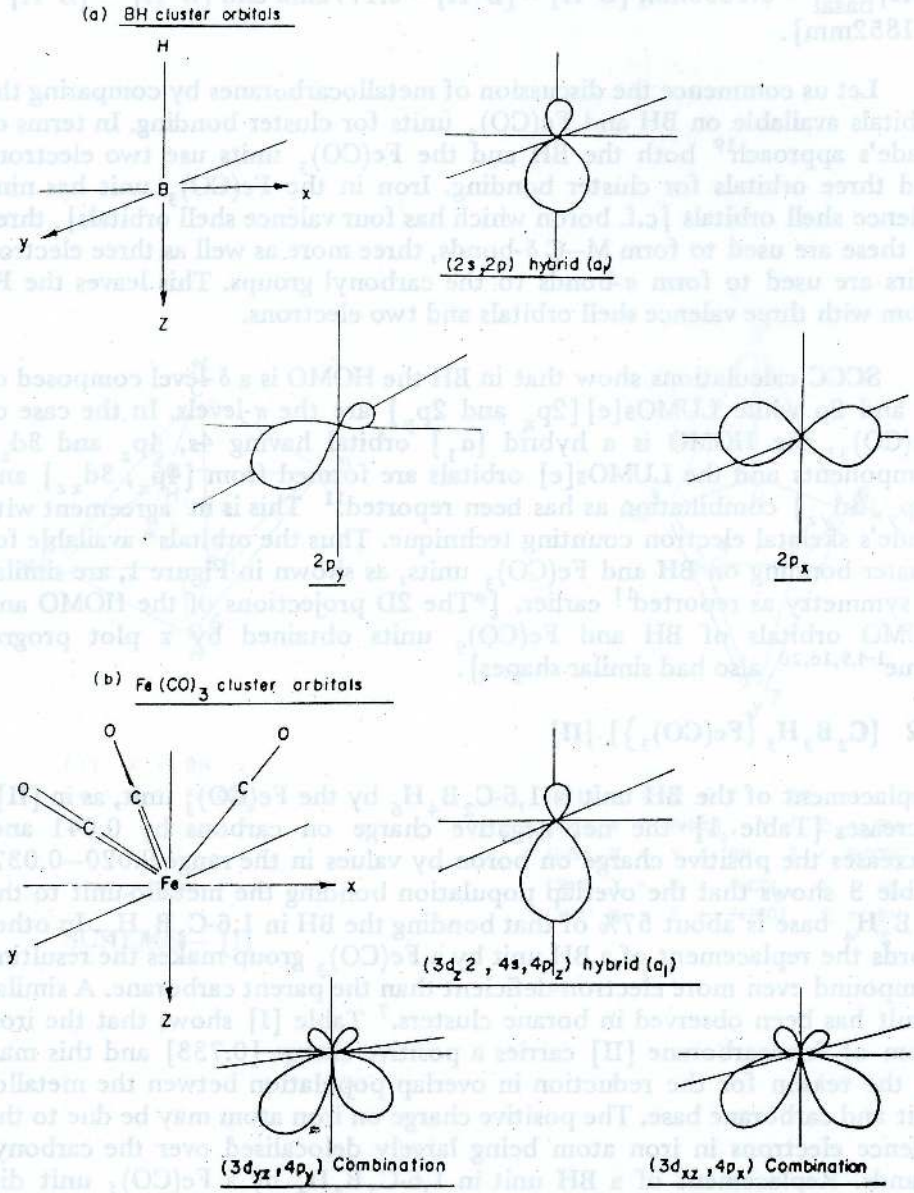

Figure 1. The orbitals available for cluster bonding on BH and $Fe(CO)_3$ units.

significant part in cluster bonding, whereas, the a_1 cluster molecular orbital of BH unit [which is equivalent to 2s, $2p_z$ hybrid of boron atom] plays a significant part in cluster bonding. A similar result has been reported[8] in metalloboranes. LCAO expansion of HOMO of [II] shows that it has a small contribution from the $3d_{x^2-y^2}$ of Fe and carbonyl carbon and oxygen atomic orbitals.

Table 5. Total energy of Valence Electrons

Molecule	Energy/eV
[I]	−403.8
[II]	−940.0
[III]	−462.3
[IVa]	−992.4
[IVb]	−987.9
[Va]	−1538.1
[Vb]	−1521.5

3.3 $[C_2B_4H_6\{Fe(CO)_3\}]$ [IV]

The replacement of an apical BH unit in 2,4-$C_2B_5H_7$ as in [IVa], [i] increases the net negative charge on carbon atoms by 0.040 [ii] decreases the positive charges on boron atoms [Table 1] and [iii] decreases the overlap population bonding the replaced site $Fe(CO)_3$, c.f.BH, to the $C_2B_3H_5$ base by about 27%. The replacement of a basal BH unit by a $Fe(CO)_3$ unit in 2,4-$C_2B_5H_7$ as in [IVb], also increases the net negative charges on carbon atoms but the increase is low [0.015 on C^2 and 0.022 on C^4] and decrease the positive charges on boron atoms [again the decrease is low, Table 1]. The total overlap population associated with the metallo-group in [IVb] is markedly less than that in [IVa] and is much smaller than that of the BH replaced [Ca 54%]. There is a corresponding increase in overlap population between adjacent boron and carbon atoms in [IVa] and [IVb] [Table 4] compared with those in 2,4 $C_2B_5H_7$. The total overlap population associated with the metallo-group and the total energy of valence electrons [Table 5] indicate that the 1-isomer [IVa] is more stable than the 5-isomer [IVb]. As mentioned earlier, the 2,4-$C_2B_5H_7$ has three cluster bonding molecular orbitals. two of C_2B_5 combinations and the third [HOMO] of basal carbon and boron atoms combination. The replacement of either the apical B^1H or basal B^5H by a $Fe(CO)_3$ unit did not change the energy of any of these orbitals appreciably. The comparison of the LCAO expansion of these orbitals shows that there is no significant contribution from the metal $3d_z2$, 4s and $4p_z$ atomic orbitals to these cluster bonding molecular orbitals and the roles of $2p_x$ and $2p_y$ atomic orbitals of boron are taken up by iron $3d_{xz}$ and $3d_{yz}$ atomic orbitals with small contributions

from $4p_x$ and $4p_y$. LCAO expansion of HOMOs of both the ferracarboranes [IVa] and [IVb] show that they have a small contribution from the $3d_{x^2-y^2}$ atomic orbital of iron and carbonyl carbon and oxygen atomic orbitals.

3.4 $[C_2B_3H_5\{Fe(CO)_3\}_2]$ [V]

The replacement of the second apical BH unit by a $Fe(CO)_3$ unit as in [Va], increases the negative charge on carbon atoms further but the increase is low [0.012 compared with 0.040 in IVa] and decreases the positive charge on basal boron atoms by similar ratios [Table 1]. The total overlap population associated with bonding of $Fe(CO)_3$ unit with $C_2B_3H_5$ base had also been decreased further by about the same ratio [Ca 27%]. The replacement of the basal B^5H unit by the $Fe(CO)_3$ unit, as in [Vb], changes the charge on C^2 from −0.062 to +0.010 [but the charge on C^4 has changed only slightly from −0.062 to 0.065] and increases the positive charges on boron atoms [Table 1]. Also, it should be noted in [Vb], Fe^1 atom has a negative net charge whereas Fe^5 atom has a high positive net charge [Table 1]. The total overlap populations associated with the bonding of metallo-groups with the rest of the cluster units in [Vb] are markedly less than those in [Va] and shows that the basal $Fe^5(CO)_3$ unit is weakly bonded into the cluster unit when compared with the apical $Fe(CO)_3$ unit. The total overlap population associated with the bonding of metallo-groups with the rest of the cluster unit and the total energy of valence electrons [Table 5] suggest that the compound [Va] is more stable than compound [Vb].

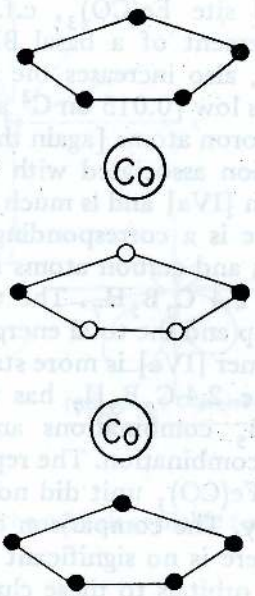

SCHEME [2]

It is interesting to note that the compound 1,7,2,4-[(η5-C_5H_5)$_2$ $Co_2C_2B_3H_5$] [VI] which is analogous to [Va] had been synthesised[6] and is stable. Our calculations also show that the replacement of either B^1H or B^7H or B^1H and B^5H by $Fe(CO)_3$ units did not change the energy of cluster bonding molecular orbitals appreciably. Analysis of LCAO expansion of molecular orbitals for [Va] and [Vb] is too complex because of the two $Fe(CO)_3$ units present in these molecules. But LCAO expansion of HOMOs of [Va] and [Vb] show that there are contributions from $3d_{x^2-y^2}$ atomic orbitals of iron atoms and atomic orbitals of the carbonyl carbon and oxygen.

3.5 Comparison of bonding by BH and $Fe(CO)_3$ units

As mentioned earlier in terms of Wade's approach the BH and the $Fe(CO)_3$ units use two electrons each and the CH unit uses 3 electrons for cluster bonding. The overlap population and the atomic orbital contributions in cluster molecular orbitals in carboranes and metallocarboranes studied show that the BH and the CH units use approximately two electrons each and that the $Fe(CO)_3$ unit uses less than two electrons [varies with the position and the number of BH units replaced by $Fe(CO)_3$ units] for cluster bonding. Our results [Tables 3 and 4] also show that the CH unit uses only one electron from carbon for the C—H bond. Hence the fourth electron from carbon must have become delocalised into the cluster bonding. The total overlap populations associated with the bonding of $Fe(CO)_3$ groups into the cluster in all ferracarboranes studied are much smaller than those of the BH replaced. Table 1 shows that in ferracarboranes [except the Fe^1 of (Vb)] the iron atoms carry net gross positive atomic charges and these positive charges on iron atoms may be the reason for the reduction in total overlap population between the $Fe(CO)_3$ unit and the rest of the cluster unit. The analysis of localised charges on the $Fe(CO)_3$ units [Table 2] and the gross atomic charges on the carbonyl carbon and the oxygen atoms [Table 1] suggest that the high positive charges on iron atoms may be due to the valence electrons in iron atom being largely delocalised over the carbonyl ligands and this may be the reason for weak bonding between the $Fe(CO)_3$ unit and the rest of the cluster unit.

As discussed earlier, the analysis of LCAO of the cluster bonding molecular orbitals shows that only $3d_{xz}$, $3d_{yz}$, $4p_x$ and $4p_y$ atomic orbitals of iron atom are used in cluster bonding but all 2s, $2p_x$, $2p_y$ and $2p_z$ orbitals of both boron and carbon atoms are used.

4. Conclusion

SCCC calculations on carbones [I] and [III] and ferracarboranes [II] [IVa], [IVb], [V] and [Vb] show that even though in terms of Wade's approach, the BH and the $Fe(CO)_3$ units are considered to be isolobal and isoelectronic,

the $Fe(CO)_3$ unit is weakly bonded into the cluster when compared with the BH unit replaced and this may be due to the valence electrons in iron atom being largely delocalised over the carbonyl ligands in ferracarboranes. Our calculations also show that even though the CH unit appears to use only two electrons for cluster bonding the third electron may be delocalised into the cluster. The comparison of the LCAO of the cluster bonding molecular orbitals shows that even though the roles of $2p_x$ and $2p_y$ atomic orbitals of boron are taken up by the iron $3d_{xz}$ and $3d_{yz}$ orbitals with some admixture of $4p_x$ and $4p_y$ atomic orbitals there is no evidence for the involvement of $[4s, 4p_z, 3d_z2]$ hybrid orbital which is analogous to boron $[2s, 2p_z]$ hybrid.

References

1. BALLHAUSEN, C. J. & GRAY, H. B. (1964). *Molecular Orbital Theory*, W. A. Benjamin Inc. New York, 120.
2. BASCH, H. & GRAY, H. B. (1967). *Theoret. Chem. Acta*, 4 : 367
3. BASCH, H., VISTE, A. & GRAY, H. B. (1960) *J. Chem. Phys*, 44 : 10.
4. BASCH, H., VISTE, A. & GRAY, H. B. (1965). *Theoret. Chem. Acta*, 3 : 33.
5. BEER, D. C., GRIMES, R. N., SNEDDON, L. G., MILLER, V. R. & WEISS, R. (1974). *Inorg. Chem.*, 13 : 1138.
6. BEER, D. C. MILLER, V. R., SNEDDON, L. G., GRIMES, R. N., MATHEW, M. & BALENIK, G. J. (1973), *J. Amer. Chem. Soc.* 95 : 3046.
7. BRINT, P. & SPALDING, T. R. (1979). *Inorg. Nuclear Chem. Letters*, 15 : 355.
8. BRINT, P. & SPALDING, T. R. (1980). *J. Chem. Soc. Dalton Trans.*, 1236.
9. BROWN, D. A., CHAMBERS, W. J. & FITZPATRICK, N. J. (1972). *Inorganic Chemica Acta*, 7 and references cited there in.
10. DAVIS, N. T. & SPEED, C. S. (1970). *J. Organometal, Chem.* 21 : 401.
11. ELIAN, M., CHEN, M. M. L., MINGOS, D. M. P. & HOFFMAN, R. (1976), *Inorg. Chem.*, 15 : 1148.
12. EPSTEIN, I. R., KOETZE, T. F., STEVENS, R. M. & LIPSCOMB, W. N. (1970). *J. Amer. Chem. Soc.*, 92 : 7019.
13. GRIMES, R. N. (1978). *Acc. of Chem. Res.*, 11 : 420.
14. GRIMES, R. N. & WEISS, R. (1976). *J. Organometal. Chem.* 27 : 113.

15. HOWELL, J., ROSSI, A., WALLACE, D., HARAKI, K. & HOFFMAN, R. (1977). FORTICON8: *Quantum Chemistry Programme Exchange No. 334.*

16. McGLYNN, S. P., VANQUIKENBORNE, L. G., KINOSHITA, M. & CARROLL, D. G. *Introduction to Applied Quantum Chemistry* Edited by Holt, Rinehart & Winston, Inc., New York, 423—431.

17. McNEILL, E. A., GALLABER, K. L., SCHOLER, F. R. & BAUER, S. H. (1973). *Inorg. Chem.*, **12** : 2108.

18. McNEILL, E. A. & SCHOLER, F. R. (1975). *J. Mol. Struct.*, **27** : 151.

19. WADE, K. (1976). *Adv. Inorg. Chem. Radiochem.*, **18** : 1.

20. WHITHEAD, M. A. (1970). *Semi-empirical All-valence-electron SCF-CNDO Theory*, edited by Sinanoglu, O. & Wiberg, K. Yale Press, 50.

J. Natn. Sci. Coun. Sri Lanka 1987 **15**(1): 61 – 69

ZINC AND COPPER CONTENT OF SOME COMMON FOODS

T. M. S. ATUKORALA
Department of Biochemistry, Faculty of Medicine, University of Colombo, Colombo 3.

and

U. S. de S. WAIDYANATHA
Department of Chemistry, Faculty of Science, University of Colombo, Colombo 3.

(Date of receipt : 08 October 1985)
(Date of acceptance : 23 March 1987)

Abstract : The zinc and copper contents of some plant and animal foods commonly available in Sri Lanka were determined. The bio-availability of zinc in plant foods was assessed by determining their phytate content. The food samples in their raw, uncooked state were subjected to wet digestion and the respective concentrations of zinc and copper were measured by atomic absorption spectroscopy. The phytate phosphorus content of plant foods was determined by the method of Oberleas. The zinc content of foods was higher than that of copper. Fish and Ox liver were the richest sources of zinc and copper. All animal foods studied could make a significant contribution to the supply of zinc in the diet. Of the plant foods analysed, pulses were good sources of both nutrients, while cereals and starchy roots contained moderate amounts. However, both pulses and cereals had phytate to zinc molar ratios exceeding 12, thus decreasing the bio-availability of zinc in these foods. Green leafy vegetables and legumes had higher amounts of copper and bio-available-zinc compared to other vegetables and fruits.

1. Introduction

Zinc and copper are two of the most metabolically active and intensively investigated trace metal nutrients. The established biochemical role of zinc is as a component of many metalloenzyme systems, including some enzymes which play a central role in nucleic acid metabolism. In addition, zinc is now known to be a membrane stabiliser and a stimulator of the immune response.[5] Deficiency of zinc leads to many clinical manifestations including impaired growth and sexual maturation.[10] Copper is also a component of many important enzyme systems, such as cytochrome oxidase, lysyl oxidase and ceruloplasmin, an iron-oxidising enzyme in blood.[6] The observation of anaemia in copper deficiency may probably be related to its role in facilitating iron absorption and in the incorporation of iron into haemoglobin.[3]

Deficiency of these two elements may arise either as a result of decreased dietary intake or as a result of decreased availability from foods, especially in zinc, where the bio-availability may be decreased by the presence of a large amount of phytate.[11] Therefore, it is important to identify good dietary sources of zinc and copper.

Knowledge of the trace element content of foods is very limited. The data available at present is based on analysis carried out on Indian foods[7] and a preliminary study by Atukorala *et. al.*[2]

In the present study, the zinc and copper content of some common foods has been determined and the bio-availability of zinc in foods assessed by determining phytate content.

2. Materials and Methods

2.1 Materials

Plant and animal foods (as purchased) in their raw, uncooked state were used. The food samples were purchased in Colombo and four different samples of each item of food were collected at random and analysed and the mean ± SEM taken. The food samples were washed thoroughly with glass distilled water and dried well with filter paper. The specimens for replicate estimations were taken from different parts of each food. Each food sample was analysed in quadruplicate, for the estimation of zinc and copper and in duplicate for the determination of phytate.

The variation of zinc and copper content of plants with environmental conditions, specially, soil conditions, was evaluated by determining the content of these elements in 2 varieties of green leafy vegetables *(Centella asiatica* — "Gotukola" and *Alternanthera sessilis* — "Mukunuwenna") collected from 5 different areas of Sri Lanka. There was no statistically significant difference in the values obtained from the 5 areas.

All glassware used was soaked overnight in dilute hydrochloric acid, washed thoroughly with glass distilled water and dried prior to use. Analytical grade reagents (BDH) were used in all experiments.

2.2 Methods

2.2.1 Estimation of zinc and copper

The organic matrix of foods was destroyed by wet digestion.[9] A weighed amount (0.2 — 0.5 g) of food was digested by heating with a mixture of conc. nitric acid and 65% perchloric acid. The residue obtained was dissolved in 2M hydrochloric acid and the concentration of zinc and copper was determined by atomic absorption spectrometry.

Zinc acetate dihydrate and copper sulphate pentahydrate were used to prepare standard solutions. The absorbance of working standard solutions was checked with standard solutions for atomic absorption spectroscopy (Sigma). The standards and blanks were processed in the same manner as the

samples. The mean percentage recoveries for zinc and copper were found to be 98.20 ± 0.67 and 97.51 ± 0.87 respectively. The absorption was measured using a Varian AA 75 Atomic absorption spectrophotometer. The following conditions were used in measurement.

	Copper	Zinc
Lamp current (mA)	4	5
Wave length (nm)	324.7	213.9
Spectral band pass (nm)	0.5	1.0

2.2.2 Estimation of phytate

The phytate content was determined by a direct phosphate method.[8] Hydrochloric acid (1.2%) containing 10% sodium sulphate was used for the extraction of phytic acid. Phytate phosphorus was hydrolysed by digesting with a mixture of concentrated sulphuric acid and perchloric acid (3:1). The digest was diluted and the phosphate content determined by the method of Gomeri.[4]

2.2.3 The moisture content of foods was determined using an Infra Red moisture meter.

3. Results and Discussion

The zinc and copper contents of some foods commonly available in Sri Lanka were determined and expressed on a wet weight basis. In general, the zinc content of almost all foods tended to be higher than that observed for copper.

Of the animal foods analysed (Table 1), fish liver was the richest source of zinc, while ox liver was the richest source of copper. Beef muscle had a higher zinc content compared to chicken or different varieties of fish, while chicken muscle and prawns had higher amounts of copper compared to other types of meat or fish. Eggs contained large amounts of both zinc and copper, while milk was a good source of zinc.

Table 1. Zinc and copper content of animal foods

Commodity	zinc (mg/100g wet weight)	Copper (mg/100g wet weight)	Moisture (g/100g)
Liver			
Ox Liver	3.786 ± 0.289	2.515 ± 0.203	76.0
Fish liver ("Para")	6.134 ± 0.673	1.969 ± 0.164	N.D.
Meat			
Beef, muscle	2.340 ± 0.338	0.211 ± 0.025	78.0
Chicken, muscle	1.370 ± 0.176	0.436 ± 0.060	N.D.
Fish			
Seer *(Scomber sp.)**	1.470 ± 0.169	0.148 ± 0.033	73.0
"Para" *(Carangids sp.)**	1.678 ± 0.155	0.085 ± 0.014	N.D.
"Kelawalla" *(Euthynnus sp.)**	1.128 ± 0.100	0.133 ± 0.013	71.0
"Hurulla" *(Sardinella sirus)*	0.930 ± 0.087	0.155 ± 0.048	76.4
"Salaya" *(Sardinella Jussieu)*	1.023 ± 0.198	0.137 ± 0.019	78.3
Prawns *(Penaeus sp.)**	1.349 ± 0.270	0.414 ± 0.108	77.4
Eggs			
Hen (whole)	1.185 ± 0.119	0.295 ± 0.037	73.5
Milk			
(Pasteurised, bottled)	0.900 ± 0.017	trace	100

Each value is the mean ± SEM of 4 samples.
* The edible portion without skin or shell was used for analysis.
N.D. – not determined.

All animal foods studied could make a significant contribution to the supply of zinc in the diet. Moreover, the zinc in animal foods is more bio-available than in plant foods owing to absence of phytate in animal foods. Most animal foods were moderate sources of copper, except for milk, which contained only traces of this nutrient.

Table 2. Zinc and copper content of cereals, pulses and starchy roots

Commodity	Zinc (mg/100g wet weight)	Copper (mg/100g wet weight)	Moisture (g/100g)
Rice			
Raw, milled ("kekulu")	0.980 ± 0.109	0.260 ± 0.023	15.0
Parboiled, milled ("Samba")	1.110 ± 0.030	0.220 ± 0.090	15.0
Parboiled, lightly milled ("Samba")	1.460 ± 0.110	0.327 ± 0.033	15.0
Flour			
Wheat (white, 70% extraction)	1.193 ± 0.189	0.240 ± 0.041	15.0
Rice	1.870 ± 0.030	0.490 ± 0.060	15.0
Soya *(Glycine max)*	3.940 ± 0.160	2.473 ± 0.180	–
Pulses			
Cowpea *(Vigna unguiculata)*	2.835 ± 0.060	0.609 ± 0.043	–
Mysoor-dhal *(Cajanus cajan)*	2.683 ± 0.110	1.070 ± 0.010	19.0
"Mung" *(Phaseolus aureus)*	2.620 ± 0.020	1.071 ± 0.100	16.5
Mung-dhal *(Phaseolus aureus)*	2.350 ± 0.080	1.035 ± 0.030	–
Starchy roots*			
Potato *(Solanum tuberosum)*	1.133 ± 0.230	0.328 ± 0.061	80.0
Sweet Potato *(Ipomea batatas)*	0.595 ± 0.170	0.172 ± 0.023	70.0
Manioc *(Manihot esculenta)*	1.103 ± 0.091	0.590 ± 0.081	–
"Kiriala" *(Colacasia esculenta)*	0.860 ± 0.013	0.631 ± 0.030	–

Each value is the mean ± SEM of 4 samples.
* Edible portion without skin was used for analysis.

All varieties of rice were moderate sources of zinc and copper, with a noticeable decrease due to milling and polishing. (Table 2). Parboiling seemed to reduce the loss of nutrients during milling and polishing. A decrease in zinc content of rice with increase in degree of polishing has also been reported in studies carried out in India.[7] Rice flour had a higher content of zinc and copper compared to 70% extraction wheat flour. Pulses were good sources of both zinc and copper (Table 2) and soya flour had higher amounts of both nutrients. In pulses too, the trace element content decreased with increase in milling and polishing. This is evident from studies on Mung and Mung dhal. Starchy roots had moderate amounts of both zinc and copper (Table 2).

Table 3. Zinc and copper content of vegetables

Commodity	Zinc (mg/100g wet weight)	Copper mg/100g wet weight)	Moisture (g/100g)
Dark green leafy vegetables:			
"Gotukola" *(Centella asiatica)*	3.930 ± 0.810	0.555 ± 0.041	95.0
"Mukunuwenna" *(Alternanthera sessilis)*	2.545 ± 0.625	0.363 ± 0.024	85.0
"Kathurumurunga" *(Sesbania grandiflora)*	2.473 ± 0.483	0.145 ± 0.015	N.D.
"Kankun" *(Ipomea aquatica)*	1.270 ± 0.108	0.221 ± 0.023	90.0
Spinach *(Basella alba)*	0.783 ± 0.230	0.440 ± 0.120	95.0
"Sarana" *(Trianthema decandra)*	1.077 ± 0.188	0.416 ± 0.057	N.D.
Other vegetables			
Brinjals *(Solanum melongena)*	1.300 ± 0.529	0.236 ± 0.104	N.D.
Carrots *(Daucus carota)*	0.901 ± 0.190	0.243 ± 0.026	89.5
"Kekiri" *(Cucumis melo var. agrestis)*	0.434 ± 0.052	0.105 ± 0.063	98.0
Ladies fingers *(Hibiscus esculentus)*	1.406 ± 0.392	0.129 ± 0.001	N.D.
Bitter-gourd *(Momordica charantia)*	0.743 ± 0.010	0.105 ± 0.007	91.0
Jak *(Artocarpus heterophyllus)*	0.660 ± 0.080	0.300 ± 0.044	N.D.
Ash plantain *(Musa sapientum var.)*	0.931 ± 0.280	0.130 ± 0.021	N.D.
Cabbage *(Brassica oleracea)*	0.603 ± 0.030	0.043 ± 0.010	95.0
Legumes			
Green bean *(Phaseolus vulgaris)*	2.150 ± 0.072	0.226 ± 0.046	90.6
String bean *(Vigna cylindrica)*	1.646 ± 0.304	0.232 ± 0.026	90.0
Winged bean *(Psophocarpus tetragonolobus)*	1.346 ± 0.254	0.230 ± 0.038	N.D.

Each value is the mean ± SEM of 4 samples.
N.D. – not determined

Dark green leafy vegetables were good sources of both zinc and copper with "Gotukola" *(Centella asiatica)* having the highest amount of both nutrients (Table 3). There was considerable variation in zinc and copper content among the other vegetables studied. Legumes had a higher content of zinc composed to the other vegetables. The lowest copper content was seen in cabbage.

These results are similar to the values reported on Indian foods.[7]

Table 4. Zinc and copper content of fruits and nuts

Commodity	Zinc (mg/100g wet weight)	Copper (mg/100g wet weight)	Moisture (g/100g)
Fruits			
Plantains *(Musa sapientum)* "Ambul" variety	*0.473* ± 0.170	0.166 ± 0.052	80.0
Plantains *(Musa sapientum)* "Ambun" variety	0.510 ± 0.110	0.190 ± 0.021	80.0
Plantains *(Musa sapientum)* "Kolikuttu" variety	0.183 ± 0.003	0.320 ± 0.040	77.1
Pineapple *(Ananas comosus)*	0.587 ± 0.089	0.299 ± 0.041	87.3
Mango *(Mangifera indica)* "Karthakolumban" variety	0.618 ± 0.065	0.274 ± 0.030	N.D.
Papaw *(Carica papaya)*	0.749 ± 0.075	0.292 ± 0.040	87.0
Avocado *(Persea grattissima)*	1.015 ± 0.200	0.351 ± 0.091	N.D.
"Veralu" *(Eleocarpus obovatus)*	0.783 ± 0.130	0.315 ± 0.144	N.D.
Orange *(Citrus auranteum)* (Sweet variety)	0.754 ± 0.213	0.170 ± 0.084	77.2
Ripe Jak *(Artocarpus beterophyllus)*	0.610 ± 0.160	0.251 ± 0.013	N.D.
Coconut *(Cocos nucifera)*	1.666 ± 0.405	0.946 ± 0.083	N.D.

Each value is the mean ± SEM of 4 samples.
N.D. – not determined.

Fruits studied contained relatively small amounts of both zinc and copper (Table 4), except for Avocado which had a moderately high zinc content. Coconut had a moderately high content of both zinc and copper.

It has been shown that the bio-availability of zinc in plant foods may be decreased by the presence of a large amount of phytate.

Table 5. Phytate P content and the molar ratio of phytate to zinc in some plant foods

Commodity	Phytate P[a] (mg/100g)	Phytate/zinc molar ratio
Cereals		
Rice, raw milled	43.65	15.60
Rice, par boiled	38.12	9.32
Flour		
Rice flour	88.80	17.05
Wheat flour (white, 70% extraction)	38.44	11.44
Soya flour	236.00	20.79
Pulses		
Cowpea *(Vigna unguiculata)*	144.00	19.37
"Mung" *(Phaseolus aureus)*	112.80	15.03
Mysoor dhal *(Cajanus cajan)*	62.44	15.01
Legumes		
Green bean *(Phaseolus vulgaris)*	37.20	6.06
Winged bean *(Psophocarpus tetragonolobus)*	11.70	9.30
String bean *(Vigna cylindrica)*	5.84	4.96
Leafy vegetables		
"Kankun" *(Ipomea aquatica)*	23.40	6.41
"Kathurumurunga" *(Sesbania grandiflora)*	19.40	2.75
"Gotukola" *(Centella asiatica)*	19.36	3.09
"Mukunuwenna' *(Alternanthera sessilis)*	4.03	4.01
Starchy roots*		
Potato *(Solanum tuberosum)*	3.72	1.17
Sweet potato *(Ipomea batatas)*	2.48	1.12
Manioc *(Manihot esculenta)*	6.20	1.97

[a] Each value is the mean of 2 samples.

*Analyses were made on the edible portion without skin.

The phytate phosphorus content of cereals and pulses was higher than that of the vegetables (Table 5). Soya flour and cowpea had a higher content of phytin phosphorus compared to cereals and other pulses.

The possible importance of a given food as a source of zinc is determined by the molar ratio of phytate to zinc rather than by its absolute content of zinc. It has been suggested that molar ratios of phytate to zinc of 12 and above would decrease the bio-availability of zinc.[1]

Our studies show that although zinc is present in significant amounts in pulses and cereals, it may be less bio-available because of phytate to zinc molar ratios exceeding 12. Soya flour was the richest source of zinc among the plant foods analysed, but its bio-availability may be decreased by the high phytate to zinc molar ratio of 20.8. In contrast, green leafy vegetables and legumes which contained moderately high amount of zinc also had lower phytate to zinc molar ratios and therefore represent an important source of zinc in a Sri Lankan diet.

Acknowledgements

This work was supported by a Research Grant from the University of Colombo. We thank Dr. N. R. de Silva for his help in trace element analysis. Our thanks also go out to Professor R. S. Ramakrishna for permitting the use of the facilities at the Department of Chemistry. The technical assistance of Mr. and Mrs. M. Balasubramaniam of the Department of Chemistry is gratefully acknowledged.

References

1. ANON (1983) *Nutr. Rev.* **41** (2) : 64 – 66.
2. ATUKORALA, T. M. S., SILVA, G. K. J. & DE SILVA, N. R. (1983) *Proc. Sri lanka Ass. Advmt. Sci.* (abstracts) **39**(1) : 69.
3. FAO/WHO (1974) *Hand book on human nutritional requirements FAO Nutritional studies* No. **28** p. 63 – 64.
4. GOMERI, G. (1942) *J. Lab. Clin. Med.* **27** : 955.
5. HAMBIDGE, K. M. (1978) *J. Hum. Nutr.* **32** : 99 – 100.
6. MILLS, C. F. (1981) Symposia from the XII International Congress of Nutrition Ed. A. E. Harper and G. K. Davis, *Prog. Clin. Biol. Res.* **77** : 165 – 77.
7. National Institute of Nutrition, *Annual Report* (1982) Hyderabad, India p. 1 – 7.
8. OBERLEAS, D. (1971) Methods of Biochemical Analysis **20** : 87 – 100.
9. PEARSON, D. (1981) *Chemical analysis of foods* Ed. Egan, H., Kirk, R. S. and Sawyer, R., Pub. Churchill, Livingstone p. 591.
10. PRASAD, A. S. (1981) Symposia from the XII International Congress of Nutrition Ed. A. E. Harper and G. K. Davis *Prog. Clin. Biol. Res.* **77** : 165 – 77.
11. W.H.O. (1973) *World Health Organisation Technical Report Series* No. 532 p. 9 – 19.

J. Natn. Sci. Coun. Sri Lanka 1987 **15(1)**: 71–81

ON ORDINARY LIMITABILITY FACTORS FOR CESARO MEANS

C. YOGACHANDRAN
Department of Mathematics and Statistics, University of Maiduguri, Nigeria.

(Date of receipt : 23 December 1985)
(Date of acceptance : 24 March 1987)

Abstract : This paper deals with the problem of finding necessary and sufficient conditions in order that, for some l', $f(x)g(x) \sim l'x^{p+q}$ (C, μ) whenever $f(x) \sim l\,x^p$ (C, λ) for some l, where $\mu \geqslant \lambda \geqslant 1$, $p > -1$, $p + q > -1$ and $f \in L_{loc}$. This problem is a generalization of a problem considered earlier,* in which μ, λ were replaced by positive integers r, k, $r \geqslant k$ and l and l' were zero.

1. Introduction

Let f be a real function with domain $\leqslant [1, \infty)$. If $f \in L_{loc}$ (i.e. f is locally Lebesgue integrable) and $\lambda > 0$, we define

$$f_\lambda(x) = I_\lambda f(x) = \frac{1}{\Gamma(\lambda)}\int_1^x (x-t)^{\lambda-1} f(t)dt, \text{ and set } f_0(x) = f(x).$$

we say that f(x) is Cesaro limitable of order λ in the ordinary sense to l, written $f(x) \to l(C, \lambda)$ if $\Gamma(\lambda+1)x^{-\lambda}f_\lambda(x) \to l$ as $x \to \infty$. More generally, if $p > -1$. $l \neq 0$, we write $f(x) \sim lx^p$ (C, λ) if

$$\frac{\Gamma(\lambda+p+1)}{\Gamma(P+1)}x^{-p-\lambda}f_\lambda(x) \to 1 \text{ as } x \to \infty.$$

If p is real, we write $f(x) = 0(x^p)(C, \lambda)$ [or $o(x^p)(C, \lambda)$] if $x^{-p-\lambda}f_\lambda(x) = 0(1)$ [or $o(1)$] as $x \to \infty$.

In (5), we found conditions necessary and sufficient in order that $f(x)g(x) = o(x^{p+q})(C, r)$ whenever $f(x) = o(x^p)(C, k)$, where r, k are non-negative integers and $r \geqslant k$. (See (5), Theorem 1). This is the integral analogue of a theorem given in (3). The following theorem is a direct consequence of the above Theorem 1.

THEOREM A : Let $r, k \in N_v$, $r \geqslant k$, $p > -1, p+q > -1$. Also let $f \in L_{loc}$ and $g \in L^\infty_{loc}$ if $k = 0$, $r \geqslant 1$, and $g^{k-1} \in AC_{loc}$ if $\equiv k \geqslant 1$.

Then, conditions necessary and sufficient in order that for some l', $f(x)g(x) \sim l'x^{p+q}(C, r)$ whenever $f(x) \sim lx^p(C, k)$ for some l are :

* (5), Theorem 1.

(a) (i)$_a$ $\int_1^x |\phi(t)|\,dt = 0(x)$ as $x \to \infty$,

(ii)$_a$ $\phi(x) \to l''$ as $x \to \infty$ (C, r) for some l'', where $\phi(x) = x^{-q}g(x)$, in the case $k = 0$, $r \geqslant 1$ and

(b) (i)$_b$ $\phi(x) = 0(1)$ as $x \to \infty$,

(ii)$_b$ $\int_1^x t^{k-q}|g^k(t)|\,dt = 0(x)$ as $x \to \infty$,

(iii)$_b$ $\phi(x) \to l''$ (C, r) as $x \to \infty$,

in the case $r \geqslant k \geqslant 1$.

In this paper, we generalise Theorem A. We replace the integers r, k by real numbers μ, λ respectively, where $\mu \geqslant \lambda \geqslant 1$. We also drop the restriction $g^{k-1} \in AC_{loc}$. We prove the following theorem.

THEOREM B : Let $\mu \geqslant \lambda \geqslant 1$, $p > -1$, $p + q > -1$ and $f \in L_{loc}$. Then conditions necessary and sufficient in order that, for some l', $f(x)g(x) \sim l'x^{p+q}(C, \mu)$ whenever $f(x) \sim lx^p(C, \lambda)$ for some l are that, for some a $(\geqslant 1)$,

(i) $g \in L^\infty(1, a)$,

(ii) $$\frac{1}{u}\int_a^u t^{-q}g(t)dt = l_o - \frac{1}{\Gamma(\lambda+1)}\int_u^\infty (v-u)^\lambda d\alpha(v) \text{ for all } u > a,$$

where l_o is a constant and $\int_a^\infty t^\lambda |d\alpha(t)| < \infty$.

See (1) and (4), where Cesaro summability problems of a similar nature have been considered.

Theorem B is deduced from some theorems stated and proved in section 3.

2. Auxiliary Results

We first define the following subspaces of L_{loc} :

(i) $(C, \lambda, p, l) = \{f/f(x) \sim lx^p\ (C, \lambda)\}$ with the norm defined by

$$\| f \| = \sup_{t \geqslant 1} t^{-p-\lambda}|f_\lambda(t)|.$$

(ii) $C_\lambda = \{f/f \in (C, \lambda, 0, 1) \text{ for some } l\}$.

(iii) $N_\lambda^a = \{f/f \in (C, \lambda, 0, 0), f(t) = 0 \text{ for } t < a, G \in L(a, \infty)\}$,

where $G(u) = uf(u) - \int_1^u f(t)dt$, with

$$\| f \| = \sup_{t \geqslant a} t^{-\lambda} |f_\lambda(t)| = \sup_{t \geqslant a} \left| \int_t^t u^{-\lambda-1} G_{\lambda-1}(u)du \right|$$

(iv) $(B, \lambda, p) = \{f/f(x) = 0(x^p)(C, \lambda)\}$

(v) $B_\lambda = (B, \lambda, 0)$

(vi) $C_o[a, \infty) = \{f/f \text{ is continuous for } t \geqslant a, f(t) \to 0 \text{ as } t \to \infty\}$ with $\| f \| = \sup_{t \geqslant a} |f(t)|$.

(vii) $BV[a, \infty) = \{f/f \text{ is of bounded variation in } [a, \infty)\}$.

The following lemmas will be used in the proofs of the theorems.

LEMMA 1 : If $(N_\lambda^a)^*$ denotes the dual space of N_λ^a, then every continuous linear functional $\Lambda \in (N_\lambda^a)^*$ is given by an equation of the form

$$\Lambda(f) = \frac{1}{\Gamma(\lambda)} \int_a^\infty f(u)du \int_u^\infty (t-u)^{\lambda-1} \, d\alpha(t), \text{ where}$$

$\int_a^\infty t^\lambda |d\alpha(t)| < \infty$, the norm of the functional Λ being given by

$$\| \Lambda \| = \frac{1}{\Gamma(\lambda)} \int_a^\infty t^\lambda |d\alpha(t)|.$$

Proof : Consider the equation $T_f(t) = y(t) = t^{-\lambda} \int_1^t (t-u)^{\lambda-1} f(u)du \quad \ldots \quad (2.1)$

Then, $T_f \in C_o[a, \infty)$ whenever $f \in N_\lambda^a$.

Also, $\| T_f \|_{C_o(a, \infty)} = \sup_{t \geqslant a} |T_f(t)| = \| f \|_{N_\lambda^a}$ and thus the linear operator

$T : N_\lambda^a \to C_o[a, \infty)$ defined by (2.1) is a continuous linear operator which maps N_λ^a isometrically onto a subspace of $C_o[a, \infty)$. By the Riesz representation theorem, every $\Lambda \in (C_o[a, \infty))^*$ is given by

$$\Lambda(y) = \int_a^\infty y(t)d\beta(t), \; y \in C_o[a, \infty), \text{ where } \beta \in BV(a, \infty) \text{ and } \| \Lambda \| = \int_a^\infty |d\beta(t)|.$$

* See (4), Lemma 2.

Hence, by extending the functional $\Lambda(y)$, we can write every $\Lambda \in (N_\lambda^a)^*$ in the form

$$\Lambda(f) = \int_a^\infty (t^{-\lambda} \int_1^t (t-u)^{\lambda-1} f(u)du)\, d\beta(t),\ \beta \in BV(a,\infty). \text{ ------ } *$$

$$\text{i.e. } \Lambda(f) = \int_a^\infty f(u)du \int_u^\infty (t-u)^{\lambda-1} t^{-\lambda} d\beta(t)$$

$$= \frac{1}{\Gamma(\lambda)} \int_a^\infty f(u)du \int_u^\infty (t-u)^{\lambda-1} d\alpha(t) \text{ where}$$

$$\alpha(t) = -\Gamma(\lambda) \int_t^\infty u^{-\lambda} d\beta(u) \text{ and}$$

$$\| \Lambda \| = \int_a^\infty |d\beta(t)| = \frac{1}{\Gamma(\lambda)} \int_a^\infty t^\lambda \, |d\alpha(t)| .$$

Since $f \in N_\lambda^a$, the inversion of the order of integration is justified.

LEMMA 2 : Suppose $f.g \in B_\mu$ for some μ whenever $f \in C_\lambda$.

Then, (i) $g \in L^\infty(1,\infty)$,

(ii) There exist a ($\geqslant 1$) and K such that if

$$\Lambda(f) = \lim_{u\to\infty} \frac{1}{u} \int_1^u f(t)g(t)dt, \text{ then } \Lambda \in (N_\lambda^a)^* \text{ and } \| \Lambda \| \leqslant K.$$

Proof : The necessity of (i) follows trivially since constant functions belong to C_λ.

Now assume that (ii) is false, i.e. It is false that ' for some a, K, $|\Lambda(f)| \leqslant K \| f \|$ whenever $f \in N_\lambda^a$. ..... (2.2)

Now, for $\mu \geqslant 1$, $\frac{d}{du}(u^{-\mu} I_\mu f(u)g(u)) = u^{-\mu} I_{\mu-1} f(u)g(u) - \mu u^{-\mu-1} I_\mu f(u)g(u)$

$$= u^{-\mu-1} G_{\mu-1(u)} \quad \ldots\ldots\ldots\ldots (2.3)$$

where $G(u) = uf(u)g(u) - f(t)g(t)dt$.

We now define by induction an increasing sequence $\{a_n\}$ tending to $+\infty$ and a sequence of functions $\{f_n\}$ as follows :

Let $a_0 = 1$ and suppose $a_1, \ldots a_{n-1}$ and $f_1, \ldots f_{n-1}$ have been defined such that $f_r \in N_\lambda^{r-1}$, $r = 1, \ldots n-1$.

Let $G_r(u) = uf_r(u)g(u) - \int_1^u f_r(t)g(t)dt$ for every r.

By (2.2) there exists $f_n \in N_\lambda^{a_{n-1}}$ such that

$$\| f_n \| < 2^{-n} \text{ and } \Lambda(f_n) > 1 \quad \ldots\ldots\ldots\ldots (2.4)$$

Let $a_n = 2a_{n-1} + \sum_{r=1}^{n} \int_1^\infty |G_r(u)|du$ ((2.5)

Note that $\int_1^\infty |G_r(u)|du < \infty$ since $g \in L^\infty(1, \infty)$ and $f_r \in N_\lambda^{a_{r-1}}$.

Now define $f(t) = \sum_{r=1}^{\infty} f_r(t)$. Then $f(t) = 0$ for $t < 1$,

$f \in L_{loc}$ and $f(t) = \sum_{r=1}^{n} f_r(t)$ for $1 \leqslant t \leqslant a_n$.

Also, $\overline{\lim}_{\substack{t_1\to\infty \\ t_2\to\infty}} |t_2^{-\lambda} f_\lambda(t_2) - t_1^{-\lambda} f_\lambda(t_1)| \leqslant \overline{\lim}_{\substack{t_1\to\infty \\ t_2\to\infty}} \sum_{r=1}^{s} |t_2^{-\lambda}(fr)_\lambda(t_2) - t_1^{-\lambda}(fr)_\lambda(t_1)|$

$$+ \overline{\lim}_{\substack{t_1\to\infty \\ t_2\to\infty}} \sum_{r=s+1}^{\infty} |t_2^{-\lambda}(fr)_\lambda(t_2) - t_1^{-\lambda}(fr)_\lambda(t_1)|$$

$$\leqslant \overline{\lim}_{\substack{t_1\to\infty \\ t_2\to\infty}} \sum_{r=s+1} \| f_r \| \leqslant 2 \sum_{r=s+1} 2^{-r} = 2^{1-s} \text{ for arbitary } s \in N.$$

Hence $t^{-\lambda} f_\lambda(t) \to$ a finite limit as $t \to \infty$, and thus the function f constructed belongs to C_λ.

Now, $\int_1^{a_n} t^{-\mu-1}dt \int_1^t (t-u)^{\mu-2} G(u)du = \sum_{r=1}^{n} \int_1^{a_n} t^{-\mu-1}dt \int_1^t (t-u)^{\mu-2} Gr(u)du$

$$= \sum_{r=1}^{n} \int_\infty^\infty t^{-\mu-1}dt \int_1^t (t-u)^{\mu-2} Gr(u)du - \sum_{r=1}^{n} \int_{a_n}^\infty t^{-\mu-1}dt \int_1^t (t-u)^{\mu-2} Gr(u)du$$

$$= \sum_{r=1}^{n} \int_1^1 Gr(u)du \int_u^\infty (t-u)^{\mu-2} t^{-\mu-1}dt - \sum_{r=1}^{n} \int_{a_n}^\infty t^{-\mu-1}dt \int_1^t (t-u)^{\mu-2} Gr(u)du$$

$$= \sum_{r=1}^{n} \frac{\Gamma(\mu-1)}{\Gamma(\mu+1)} \Lambda(fr) - \sum_{r=1}^{n} \int_{a_n}^\infty t^{-\mu-1}dt \int_1^t (t-u)^{\mu-2} Gr(u)du$$

But $\left| \sum_{r=1}^{n} \int_{a_n}^\infty t^{-\mu-1}dt \int_1^t (t-u)^{\mu-2} Gr(u)du \right| \leqslant \sum_{r=1}^{n} \int_{a_n}^\infty t^{-3}dt \int_1^\infty |Gr(u)|du$

$$< \frac{1}{a_n} \sum_{r=1}^{n} \int_1^\infty |Gr(u)|du < 1 \text{ by (2.5).}$$

Hence $\int_1^{a_n} t^{\mu-1}dt \int_1^t (t-u)^{\mu-2} G(u)du > \frac{\Gamma(\mu-1)}{\Gamma(\mu+1)} n - 1$ by (2.4)

and by (2.3) it follows that $\int_1^{a_n} \frac{(a_n - u)^{\mu-1}}{a_n^{\mu}} f(u)g(u)du \to +\infty$ when $\mu > 1$.

contradicting the fact that $f.g \in B_\mu$ for some μ. Hence the necessity of (ii).

LEMMA 3 : If $p > -1$, $\lambda' > \lambda$, then $(C, \lambda, p, l) \subset (C, \lambda', p, l)$ and $(B, \lambda, p) \subset (B, \lambda', p)$.

This result is well known. Cf (2), Lemma 3.

LEMMA 4 : If $p > -1$, $p+q > -1$ and $g \in (C, \lambda, p, l)$ [or (B, λ, p)], then $h \in (C, \lambda, p+q, l)$ [or $(B, \lambda, p+q)$], where $h(x) = x^q g(x)$.

Cf. (2).Lemma 4.

LEMMA 5 : If $f \in B_\lambda$, $\lambda \geqslant 1$, then there exist constants H, K such that

(i) $\left|\int_1^t (t-u)^{\lambda-1} (v-u)^{\alpha} f(u)du\right| \leqslant H\, t^{\lambda} v^{\alpha}$ for $v \geqslant t$, $\alpha \geqslant 0$.

(ii) $\left|\int_1^t (t-u)^{\beta} [(v-u)^{\lambda-1} - v^{\lambda-1}] f(u)\, du\right| \leqslant Kt^{\beta+1} (t^{\lambda-1} + v^{\lambda-1})$ for $v \geqslant t$, $\beta \geqslant 0$.

Proof : The results are trivial for $\lambda = 1$, and hence take $\lambda > 1$.

(i) Let $\lambda = n + p$ where $n \in IN_o$, $1 < p \leqslant 2$, and $M = \sup_{t \geqslant 1} t^{-\lambda} \left|f_\lambda (t)\right|$.

By partial integration we have

$$\int_1^t (t-u)^{\lambda-1} (v-u)^{\alpha} f(u)du = (-1)^{n+1} \int_1^t f_{n+1}(u) \left(\frac{\partial}{\partial u}\right)^{n+1} [(t-u)^{\lambda-1} (v-u)^{\alpha}]\, du$$

$$= \sum_{r=0}^{n+1} c_r J_r \text{ where } c_r \text{ is independent of } t \text{ and } v, \quad \ldots\ldots\ldots\ldots\ldots \quad (2.6)$$

and $J_r = \int_1^t (t-u)^{p+r-2} (v-u)^{\alpha-r} f_{n+1}(u)du$

$$= \frac{(t-1)^r (v-1)^{\alpha}}{(v-1)^r} \int_1^{b_r} (t-u)^{p-2} f_{n+1}(u)du, \text{ where } 1 \leqslant b_r \leqslant t,$$

by the Second Mean Value Theorem.

By Riesz's Mean Value theorem,

$$|J_r| \leqslant (t-1)^r (v-1)^{\alpha-r} \sup_{1 \leqslant b \leqslant b_r} \left|\int_1^b (b-u)^{p-2} f_{n+1}(u)du\right|$$

$$= (t-1)^r (v-1)^{\alpha-1} \sup_{1 \leqslant b \leqslant b_r} |\Gamma(p-1) f'_{n+p}(b)| \leqslant \Gamma(p-1) M t^{\lambda} v^{\alpha},$$

since $\left[\frac{(t-1)}{(v-1)}\right]^r < 1$, and λ, α are non-negative.

Hence, (2.6) gives (i)

(ii) Take $\beta = n+p$ where $n \in \mathbb{N}_0$, $0 < p \leqslant 1$. As before, we have

$$\int_1^t (t-u)^{\beta} \left[(v-u)^{\lambda-1} - v^{\lambda-1}\right] f(u)du$$

$$= (-1)^{n+1} \int_1^t f_{n+1}(u) \left(\frac{\partial}{\partial u}\right)^{n+1} \left\{(t-u)^{\beta} \left[(v-u)^{\lambda-1} - v^{\lambda-1}\right]\right\} du \quad \ldots\ldots (2.7)$$

But, $\left(\frac{\partial}{\partial u}\right)^{n+1} \left\{(t-u)^{\beta} \left[(v-u)^{\lambda-1} - v^{\lambda-1}\right]\right\} = C_0 (t-u)^{\beta-n-1} \left[(v-u)^{\lambda-1} - v^{\lambda-1}\right]$

$$+ \sum_{r=1} C_r (t-u)^{\beta-n-1+r} (v-u)^{\lambda-1-r} \quad \ldots\ldots (2.8)$$

As in (i), $\left| \int_1^t (t-u)^{\beta-n-1+r} (v-u)^{\lambda-1-r} f_{n+1}(u)du \right| \leqslant \Gamma(\beta-n) M t^{\beta+1} v^{\lambda-1}$

$\ldots\ldots (2.9)$

Also, $\left| \int_1^t (t-u)^{\beta-n-1} \left[(v-u)^{\lambda-1} - v^{\lambda-1}\right] f_{n+1}(u)du \right|$

$= \left[v^{\lambda-1} - (v-u)^{\lambda-1}\right] \left| \int_{\eta}^t (t-u)^{\beta-n-1} f_{n+1}(u)\, du \right|$ where $1 \leqslant \eta \leqslant t$

$\leqslant 2\Gamma(\beta-n) M t^{\beta+1} \left[t^{\lambda-1} + (\lambda-1) t v^{\lambda-1}\right]$

(2.7), (2.8), (2.9) and (2.10) give the required result.

3. Theorems and their Proofs

THEOREM 1: If $f.g \in B_{\mu}$ for some u whenever $f \in C_{\lambda}$, then there exists a $(\geqslant 1)$ such that

(i) $g \in L^{\infty}(1, a)$

(ii) $\frac{1}{u} \int_1^u g(t)dt = l_0 - \frac{1}{\Gamma(\lambda+1)} \int_u^{\infty} (v-u)^{\lambda} \, d\alpha(v)$ for all $u > a$,

where l_0 is a constant, and $\int_a^{\infty} v^{\lambda} |d\alpha(v)| < \infty$.

Proof : The necessity of (i) follows from Lemma 2 (i).

By Lemma 2, there exist a_o and K such that

$$\lim_{u \to \infty} \left| \frac{1}{u_1} \int_1^u f(t)g(t)dt \right| \leqslant K \|f\| \text{ whenever } f \in N_\lambda^{a_o} \quad \ldots\ldots\ldots\ldots (3.1)$$

Also, if $f \in N_\lambda^{a_o}$, then $\frac{1}{u_1} \int_1^u |f(t)|\,dt \in V(a_o, \infty)$ $\quad \ldots\ldots\ldots\ldots (3.2)$

Now, (3.1) implies that there exists $a \geqslant a_o$ such that if

$$\Lambda_u(f) = \frac{1}{u_1} \int_1^u f(t)g(t)dt, \text{ then, whenever } u > a, \ \Lambda_u \in (N_\lambda^a)^* \quad \ldots\ldots\ldots (3.3)$$

For, if (3.3) is false, by the method used in Lemma 2, we can construct

$$\{b_n\} \uparrow, b_n \to +\infty \text{ and } f \in N_\lambda^{a_o} \text{ such that } \frac{1}{b_n} \int_1^{b_n} f(t)g(t)dt > n,$$

contradicting the fact that $\frac{1}{u} \int_1^u f(t)g(t)dt$ is bounded whenever $f \in N_\lambda^{a_o}$, which is a consequence of (3.2) and $g \in L^\infty(1, \infty)$.

Hence, (3.3) and Lemma 1 give : Whenever $u > a$,

$$\frac{1}{u} \int_1^u f(t)g(t)dt = \frac{1}{\Gamma(\lambda)} \int_a^\infty f(u)du \int_u^\infty (t-u)^{\lambda-1}\, d\alpha(t), \text{ where}$$

$$\int_a^\infty t^\lambda |d\alpha(t)| < \infty, \text{ for } f \in N_\lambda^a. \quad \ldots\ldots\ldots\ldots (3.4)$$

Clearly, the function $\overset{*}{X}_{(a,u)}$ belongs to N_λ^a. Hence (3.4) gives

$$\frac{1}{u} \int_a^u g(t)dt = \frac{1}{\Gamma(\lambda)} \int_a^u dt \int_t^\infty (v-t)^{\lambda-1}\, d\alpha(v) \text{ for all } u > a.$$

Since $\int_a^\infty t^\lambda |d\alpha(t)| < \infty$, $\frac{1}{\Gamma(\lambda)} \int_a^u dt \int_t^\infty (v-t)^{\lambda-1}\, d\alpha(v)$

$$= \frac{1}{\Gamma(\lambda)} \int_a^\infty dt \int_t^\infty (v-t)^{\lambda-1}\, d\alpha(v) - \frac{1}{\Gamma(\lambda)} \int_u^\infty dt \int_t^\infty (v-t)^{\lambda-1}\, d\alpha(v)$$

$$= I_o - \frac{1}{\Gamma(\lambda+1)} \int_a^\infty (v-u)^\lambda\, d\alpha(v), \text{ where } I_o = \frac{1}{\Gamma(\lambda+1)} \int_a^\infty (v-a)^\lambda\, d\alpha(v).$$

Hence the result,

THEOREM 2 : If $f \in B_\lambda$ and (i) $h \in L^\infty(1,a)$

(ii) $\frac{1}{u}\int_a^u h(t)dt = \frac{1}{\Gamma(\lambda+1)}\int_u^\infty (v-u)^\lambda \, d\alpha(v)$, where $\int_a^\infty v^\lambda |d\alpha(v)| < \infty$, then

$$I: \lim_{t\to\infty} t^{-\lambda} I_\lambda f(t)h(t) = -\lim_{t\to\infty} \frac{t^{-1}}{\Gamma(\lambda)} \int_a^t I_\lambda (vf(v) - f_1(v))d\alpha(v).$$

Proof : Since $f \in B_\lambda$, by Lemma 4 we have

$I_\lambda (vf(v) - f_1(v)) = o(v^{\lambda+1})$, and hence the R.H.S. of I exists, since $\int_a^\infty v^\lambda |d\alpha(v)| < \infty$.

Now (ii) gives $h(u) = \frac{1}{\Gamma(\lambda+1)}\int_u^\infty (v-u)^\lambda \, d\alpha(v) - \frac{u}{\Gamma(\lambda)}\int_u^\infty (v-u)^{\lambda-1} \, d\alpha(v)$

for $u > a$.

Hence $t^{-\lambda} I_\lambda f(t)h(t) = t^{-\lambda}\int_1^a \frac{(t-u)^{\lambda-1}}{\Gamma(\lambda)} f(u)h(u)du + I_1 + I_2$ ..... (3.5)

where $I_1 = \frac{t^{-\lambda}}{\Gamma(\lambda)}\left\{\frac{1}{\Gamma(\lambda+1)}\int_a^t (t-u)^{\lambda-1} f(u)du \int_u^t (v-u)^\lambda d\alpha(v) - \frac{1}{\Gamma(\lambda)}\int_a^t (t-u)^{\lambda-1} uf(u)du \int_u^t (v-u)^{\lambda-1} d\alpha(v)\right\}$

$$= \frac{t^{-\lambda}}{\Gamma(\lambda)}\left\{\frac{1}{\Gamma(\lambda+1)}\int_a^t d\alpha(v)\int_a^v (v-u)^\lambda (t-u)^{\lambda-1} f(u)du\right.$$

$$\left. - \frac{1}{\Gamma(\lambda)}\int_a^t d\alpha(v)\int_a^v (v-u)^{\lambda-1}(t-u)^{\lambda-1} uf(u)du\right\} \quad \ldots\ldots (3.6)$$

and $I_2 = \frac{t^{-\lambda}}{\Gamma(\lambda)}\left\{\frac{1}{\Gamma(\lambda+1)}\int_a^t (t-u)^{\lambda-1} f(u)du \int_t^\infty (v-u)^\lambda d\alpha(v)\right.$

$$\left. - \frac{1}{\Gamma(\lambda)}\int_a^t (t-u)^{\lambda-1} f(u)du \int_t^\infty (v-u)^{\lambda-1} d\alpha(v)\right\}$$

$$= \frac{t^{-\lambda}}{\Gamma(\lambda)}\left\{\left(\frac{1}{\Gamma(\lambda+1)} + \frac{1}{\Gamma(\lambda)}\right)\int_t^\infty d\alpha(v)\int_a^t (t-u)^{\lambda-1}(v-u)^\lambda f(u)du.\right.$$

$$-\frac{1}{\Gamma(\lambda)}\int_t^\infty d\alpha(v)\int_a^t v(t-u)^{\lambda-1}\ (v-u)^{\lambda-1} f(u)du \Big\}$$

Hence, by Lemma 5(i) we get

$$|I_2| \leqslant K_1 t^{-\lambda}\int_t^\infty t^\lambda v^\lambda\ |d\alpha(v)| \to 0 \text{ as } t \to \infty \qquad \ldots\ldots\ldots\ldots\ldots\ldots (3.7)$$

Now, by (3.6) we get $I_1 - \frac{t^{-1}}{\Gamma(\lambda)}\int_a^t I_\lambda\ (f_1(v) - vf(v)d\alpha(v)$

$$= \frac{t^{-\lambda}}{\Gamma(\lambda)}\Big\{\frac{1}{\Gamma(\lambda+1)}\int_a^t d\alpha(v)\int_a^v (v-u)^\lambda\Big[\ (t-u)^{\lambda-1} - t^{\lambda-1}\ \Big] f(u)du$$

$$-\frac{1}{\Gamma(\lambda)}\int_a^t d\alpha(v)\int_a^v (v-u)^{\lambda-1}\ [(t-u)^{\lambda-1} - t^{\lambda-1}]\ uf(u)\ du\Big\}$$

Hence $\Big|\ I_1\ -\frac{t^{-1}}{\Gamma(\lambda)}\int_a^t I_\lambda\ (f_1(v) - vf(v))\ d\alpha(v)\Big|$

$$\leqslant K_2 t^{-\lambda}\int_a^t v^{\lambda+1}\ (v^{\lambda-1} + t^{\lambda-1})|d\alpha(v)| \qquad \text{by Lemma 5 (ii)}$$

$$\leqslant K_2 t^{-\lambda}\int_a^w v^{\lambda+1}\ (v^{\lambda-1} + t^{\lambda-1})\ |d\alpha(v)| + 2K_2\int_w^\infty v^\lambda\ |d\alpha(v)|\ ,\text{where } a<w<t, \text{ and}$$

Hence $\overline{\lim_{w\to\infty}}\ \overline{\lim_{t\to\infty}}\ |I_1 - \frac{t^{-1}}{\Gamma(\lambda)}\int_a^t I_\lambda\ (f_1(v) - vf(v)d\alpha(v)| = 0 \qquad \ldots\ldots\ldots\ldots (3.8)$

Now, (i) implies that $t^{-\lambda}\int_1^a \frac{(t-u)^{\lambda-1}}{\Gamma(\lambda)} f(u)h(u)du\ 0$ as $t \to \infty$.

Hence, (3.5), (3.7) and (3.8) give I.

THEOREM 3 : Conditions necessary and sufficient in order that $f.g \in C_\lambda$ whenever $f \in C_\lambda$ are that, for some $a\ (\geqslant 1)$

(i) $g \in L^\infty(1, a)$,

(ii) $\frac{1}{u}\int_a^u g(t)dt = l_o - \frac{1}{\Gamma(\lambda+1)}\int_u^\infty (v-u)^\lambda\ d\alpha(v)$ for all $u \geqslant a$

where l_o is a constant and $\int_a^\infty t^\lambda |d\alpha(t)| < \infty$.

Proof : If $f.g \in C_\lambda$ whenever $f \in C_\lambda$, then $f.g \in B_\lambda$ whenever $f \in C_\lambda$, and by Theorem 1, (i) and (ii) are necessary.

If (i) and (ii) hold, then $g(u) = l_0 + h(u)$, where $h(u)$ is as in Theorem 2.

Hence $t^{-\lambda}I_\lambda f(t)g(t) = l_0 t^{-\lambda} f_\lambda(t) + t^{-\lambda} I_\lambda f(t)h(t) \to$ a finite limit as $t \to \infty$ whenever $f \in C_\lambda$, by Theorem 2.

THEOREM 4 : If $\mu \geqslant \lambda \geqslant 1$, $p+q > -1$, $p > -1$ then conditions necessary and sufficient in order that, for some l',

$f.g \in (C, \mu, p+q, l')$ whenever $f \in (C, \lambda, p, 1)$ for some l are that for some $a(\geqslant 1)$,

(i) $g \in L^\infty(1, a)$

(ii) $$\frac{1}{u}\int_a^u t^q g(t)\,dt = l_0 - \frac{1}{\Gamma(\lambda+1)}\int_u^\infty (v-u)^\lambda \, d\alpha(v) \text{ for all } u > a,$$

where l_0 is constant, $\int_a^\infty t^\lambda |d\alpha(t)| < \infty$.

Proof : Since $p > -1$, $p+q > -1$ we can consider $x^{-p}f(x)$ and $x^{-q}g(x)$ instead of $f(x)$ and $g(x)$ in the previous theorem, and use Lemma 4.

Hence Theorem 1 gives the necessity of (i) and (ii).

Again by Theorem 3, (i), (ii) and $f \in (C, \lambda, p, 1)$ imply that $f.g \in (C, \lambda, p+q, l')$ for some l', and hence $f.g \in (C, \mu, p+q, l')$, by Lemma 3.

This completes the proof.

References:

1. BORWEIN, D. (1954) *J. Lond. Math. Soc.* **29** : 198 – 206.
2. BORWEIN, D. (1956) *J. Lond. Math. Soc.* **25** : 289 – 302.
3. BOSANQUET, L. S. (1954) *Mathematika*, **1**: 24 – 44.
4. SARGENT, W. L. C. (1952) *J. Lond. Math. Soc.* **27** : 401 – 413.
5. YOGACHANDRAN, C. (1981) *J. Natn. Sci. Coun. Sri Lanka* **9** : 17 – 23.

J. Natn. Sci. Coun. Sri Lanka 1987 **15**(*1*) : 83–86

ON SOME SEQUENCE TO SEQUENCE TRANSFORMATIONS

C. YOGACHANDRAN
Department of Mathematics and Statistics, University of Maiduguri, Nigeria.

(Date of receipt : 23 December 1985)
(Date of acceptance : 24 March 1987)

Abstract : In this paper we prove two theorems on sequence to sequence transformations given by $y_n = \sum_{k=1}^{\infty} a_{nk} x_k$, $n = 1, 2, \ldots$ The theorems give necessary and sufficient conditions in order that

(1) $y \in l$ whenever $x \in bv$, and

(2) $y \in bv$ whenever $x \in l^{\infty}$, where $x = \{x_n\}$ and $y = \{y_n\}$, and l = The space of all sequences x such that $\sum_{n=1}^{\infty} |x_n| < \infty$, l^{∞} = The space of al sequences x such that $x_n = 0(1)$, bv = The space of all x such that $\sum_{n=1}^{\infty} |x_n - x_{n-1}| < \infty$.

1. Introduction

We assume that the transformation is given by

$$y_n = \sum_{n=1}^{\infty} a_{nk} x_k, \quad n = 1,2,3,\ldots$$

We prove the following theorems:

1.1 THEOREM 1 : Necessary and sufficient conditions in order that $y \in l$ whenever $x \in bv$ are :

$(i)_1$ $\sum_{k=1}^{\infty} a_{nk}$ converges for every $n = 1,2 \ldots\ldots$

$(ii)_1$ There exists $M > 0$ such that $\sum_{n=1}^{\infty} |\sum_{k=1}^{m} a_{nk}| \leqslant M$ for all $m \geqslant 1$.

1.2 THEOREM 2 : Necessary and sufficient conditions in order that $y \in by$ whenever $x \in l^{\infty}$ are that

$(i)_2$ $\sum_{k=1}^{\infty} |a_{nk}| < \infty$ for every $n \geqslant 1$.

$(ii)_2$ There exists $M > 0$ such that $\sum_{k=1}^{\infty} |\sum_{n \in N} (a_{nk} - a_{n-1,k})| \leqslant M$

for all $N \in F$, where F is the space of all finite sets N of natural numbers.

There are many well known classical theorems on sequence to sequence transformations of the above type, some of which have been proved by Toeplitz, Hahn, Knopp and Lorentz, Mears, Sunouchi and others. Usually, the longest part of the proof is the proof of the necessity of conditions of

the type $(ii)_1$ and $(ii)_2$. In this paper, we give a technique which shortens the proof considerably. (See (1) for similar theorems and for the references given. See also (2) for the use of this technique for integral transformations.)

2. Results used in the Proofs of the Theorems

2.1 THEOREM A (Toeplitz's Theorem)

Necessary and sufficient conditions in order that $y \in l^\infty$ whenever $x \in l^\infty$ are :

$(i)_a \sum_{k=1}^{\infty} | a_{nk} | < \infty$ for every $n \geqslant 1$

$(ii)_a$ There exists $M > 0$ such that $\sum_{k=1}^{\infty} | a_{nk} | \leqslant M$ for all $n \geqslant 1$.

2.2 THEOREM B (Hahn's Theorem)

Necessary and sufficient conditions in order that $y \in l^\infty$ whenever $x \in bv$ are that

$(i)_b \sum_{k=1}^{\infty} a_{nk}$ converges for every $n \geqslant 1$

$(ii)_b$ There exists $M > 0$ such that $\left| \sum_{k=1}^{m} a_{nk} \right| \leqslant M$ for all $m \geqslant 1$ and all $n \geqslant 1$.

These two theorems are well known.

The following lemma is a simple consequence of the definition of absolute convergence. (See (1).

LEMMA 1: Let F be the space of all finite sets of natural numbers. Then, a necessary and sufficient condition that $x \in l$ is that :

I. There exists K independent of N such that $|B_N| \leqslant K$ for all $N \in F$,

where $B_N = \sum_{n \in N} x_n$.

When this condition is satisfied, we have $\sum_{n=1}^{\infty} | x_n | \leqslant 2K$.

LEMMA 2: Let $y_n = \sum_{k=1}^{\infty} a_{nk} x_k$, where $x \in X$, X being a sequence space. Then,

I. $y \in l$ for every $x \in X$ iff B_N is bounded for all $N \in F$ for every $x \in X$,

where $B_N = \sum_{k=1}^{\infty} b_{N,k} x_k$ and $b_{N,k} = \sum_{n \in N} a_{nk}$.

II. $y \in bv$ for every $x \in X$ if D_N is bounded for all $N \in F$ for every $x \in X$, where $D_N = \sum_{k=1}^{\infty} d_{N,k}\, x_k$ and $d_{N,k} = \sum_{n \in N} (a_{nk} - a_{n-1,k})$.

Proof I : By Lemma 1, $y \in l$ iff $|B_N| \leqslant K$ for all $N \in F$, where $B_N = \sum_{n \in N} y_n$.

But $B_N = \sum_{n \in N} \sum_{k=1}^{\infty} a_{nk} x_k = \sum_{k=1}^{\infty} (\sum_{n \in N} a_{nk}) x_k = \sum_{k=1}^{\infty} b_{N,k}\, x_k$.

Hence the result.

II. $y \in bv$ iff $\sum_{n=1}^{\infty} |y_n - y_{n-1}| < \infty$.

Since $y_n - y_{n-1} = \sum_{k=1}^{\infty} (a_{nk} - a_{n-1,k}) x_k$, the result follows.

3. Proofs of the Theorems

3.1 Proof of Theorem 1: Note that $(i)_1$ is necessary and sufficient for the existence of y_n whenever $x \in bv$. (Theorem B).

Sufficiency: If $(i)_1$ and $(ii)_1$ hold and $x \in bv$, then

$|\sum_{k=1}^{m} b_{N,k}| = |\sum_{k=1}^{m} \sum_{n \in N} a_{nk}| = |\sum_{n \in N} \sum_{k=1}^{m} a_{nk}| \leqslant \sum_{n=1}^{\infty} |\sum_{k=1}^{m} a_{nk}| \leqslant M$ for all $N \in F$, by $(ii)_1$.

By Theorem B, this implies that $\sum_{k=1}^{\infty} b_{N,k} x_k$ is bounded for all $N \in F$. Hence by Lemma 2, $y \in l$.

Necessity By Lemma 2, $y \in l$ implies that $B_N = 0(1)$ for all $N \in F$ for every $x \in bv$.

Hence, by Theorem B, there exists M such that

$|\sum_{k=1}^{m} b_{N,k}| \leqslant \frac{1}{2}M$ for all $N \in F$ and all m.

i.e. $|\sum_{n \in N} \sum_{k=1}^{m} a_{nk}| \leqslant \frac{1}{2}M$ for all $N \in F$ and all m, and Lemma 1 gives the required condition $(ii)_1$.

Hence the theorem.

3.2 Proof of Theorem 2: $(i)_2$ is necessary and sufficient for the existence of y_n whenever $x \in l^{\infty}$. (Theorem A).

Sufficiency: If $(i)_2$ and $(ii)_2$ hold, and $x \in l^{\infty}$, then

$|D_N| = |\sum_{k=1}^{\infty} \sum_{n \in N} (a_{nk} - a_{n-1,k}) x_k| \leqslant M \sum_{k=1}^{\infty} |x_k|$ and hence $y \in bv$ by Lemma 2 II.

Necessity: Again by Lemma 2 II, $y \in bv$ implies that

$D_N = \sum_{k=1}^{\infty} d_{N,k}\, x_k$ is bounded for all $N \in F$ whenever $x \in l^\infty$, and

Theorem A gives the necessary condition

$\sum_{k=1}^{\infty} |d_{N,k}| \leqslant M$ for all $N \in F$, which is $(ii)_2$.

Note: We see that condition $(ii)_2$ involves N. We can show that $(ii)_2$ cannot be replaced by the condition:

$(ii)' : \sum_{k=1}^{\infty} \sum_{n=1}^{\infty} |a_{nk} - a_{n-1,k}| < \infty$, which is independent of N. Clearly, (i) and (ii)' are sufficient for y to be in bv whenever $x \in l^\infty$, but (ii)' is not necessary.

In (1), Peyerimhoff has constructed $x \in l^\infty$ for which $y'_n = \sum_{k=1}^{\infty} a'_{nk}\, x_k$ satisfies $\sum_{n=1}^{\infty} |y'_n| < \infty$ but $\sum_{k=1}^{\infty} \sum_{n=1}^{\infty} |a'_{nk}| = L$.

By taking $a'_{nk} = a_{nk} - a_{n-1,k}$, $y_n = \sum_{k=1}^{\infty} a_{nk} x_k$, we see that for the same x in l^∞, $\sum_{n=1}^{\infty} |y_n - y_{n-1}| < \infty$, but

$$\sum_{k=1}^{\infty} \sum_{n=1}^{\infty} |a_{nk} - a_{n-1,k}| = \infty.$$

Thus (ii)' is not necessary in Theorem 2.

References:

1. PEYERIMHOFF, A. (1957) *Journal London Math. Soc.* **32** : 33 – 36.

2. YOGACHANDRAN, C. (1973) *Journal London Math. Soc.* **216** : 639 – 648.

J. Natn. Sci. Coun. Sri Lanka 1987 15(1): 87–99

STUDIES ON CHLORINE AND FLUORINE IN EPPAWELA APATITE

R. P. GUNAWARDANE
Department of Chemistry, University of Peradeniya, Peradeniya, Sri Lanka.

(Date of receipt : 05 December 1986)
(Date of acceptance : 02 April 1987)

Abstract : Dehalogenation of Eppawela apatite, which is mainly in the form of chlorfluorapatite, has been investigated in the temperature range 900 to 1300°C. The loss of fluorine is relatively small while much higher loss of chlorine has been observed. There is a linear correlation between the extent of dehalogenation and the available phosphorus content of the products. Presence of moisture enhances the dehalogenation process. Addition of silica facilitates the removal of fluorine much more than chlorine. In the presence of soda ash, retention of fluorine is greater while almost total chlorine content is removed even at 1100°C. It is evident that chlorfluorapatite first undergoes isomorphous replacement of halogen with hydroxyl groups to form hydroxyfluorapatite which then undergoes decomposition at higher temperatures to yield more soluble phosphates. Mostly chlorine is removed as HCl while fluorine is evolved as HF, SiF_4 and H_2SiF_6.

1. Introduction

The apatite group of minerals has the general formula, $Ca_5(PO_4)_3$ X, where X can be usually F, Cl, OH or a mixture of any of these ions. The end members of this family are referred to as fluorapatite, chlorapatite and hydroxyapatite. Fluorapatite[2] is found to be the most stable form and as such most natural apatites contain more F than Cl or OH.

An estimated reserve of about 25–30 million tons of apatite[6] occurs at Eppawela in the North Central Province of Sri Lanka. It has been reported[6] that the samples from the "leached zone" of the deposit at Eppawela contain more chlorine than fluorine. Eppawela apatite has an unusual chemical composition: its Cl^-/F^- ratio[5] is close to 1.3 and it contains negligible OH^-. In contrast, some workers [12] have reported the existence of hydroxyapatite in the same deposit.

Available phosphorus content of apatite is low,[4] making it unsuitable for direct application as a fertilizer to short term crops. It is believed that fluorine plays[9] an important role in the solubility of apatite minerals. It has been demonstrated[13] that defluorination of some rock phosphates at high temperature, yields products possessing higher contents of available phosphorus. Furthermore, haloapatites can be considered as a potential source of halogen although it may not be economical to exploit these minerals commercially for halogens.

In the present study, the loss of fluorine and chlorine components in Eppawela apatite at high temperature has been estimated. Furthermore, the

effect of water, silica and soda ash on dehalogenation has also been investigated in an attempt to postulate a mechanism for the dehalogenation process and to correlate the extent of halogen loss with available phosphorus content of the product.

2. Experimental

2.1 Thermal treatment

Rock phosphate No. 1 sample (100 mesh) from the "leached zone" at Eppawela, apatite – quartz (100 mesh) mixtures and apatite – soda ash mixtures were heated at temperatures of 700–1300°C in muffle furnaces using platinum crucibles. Selected samples were also heated at 1350–1400°C. After heat treatment the samples were quenched in water and the products were examined by powder X-ray diffraction. Differential thermal analysis (DTA) of the rock samples was carried out using a Mettler TA12 Thermoanalyzer at a heating rate of 10°C per minute in air, while thermogravimetric (TG) analysis was performed using a Perkin-Elmer TGS-2 Thermogravimetric Analyzer.

2.2 Chemical Analysis

Four different samples labelled 1,2,3 and 4 were collected from four different hillocks in the "leached zone" at Eppawela. Three determinations for each of the components F, Cl, total P_2O_5 and available P_2O_5 have been made for these samples and the average values are reported in Table 1.

Table 1. Some analytical data of Eppawela apatite

	Sample 1	Sample 2	Sample 3	Sample 4
Wt. % P_2O_5	38.10	39.60	34.20	37.70
Wt. % F	1.70	1.03	1.34	0.78
Wt. % Cl	2.20	2.41	2.33	2.11
2% Citric acid soluble P_2O_5	6.3	6.1	5.4	5.9

2.2.1 Halogen estimation:

About 50mg samples were dissolved in 5M HCl for F^- analysis. Analyses were made using an Orion Model 94–09 fluoride ion electrode[3] by employing an alkali buffer system. Chloride analyses were made on 25–50mg samples dissolved in 1:1 HNO_3. These were diluted with ethanol and titrated to a potentiometric end-point against standard 0.05M $AgNO_3$. Two per cent citric acid extracts of some fired samples were also subjected to F^- and Cl^- analyses by the same procedures.

2.2.2 Phosphorus estimation.

Total phosphorus contents of the samples were determined by extracting the samples with a mixture[7] of conc. HNO_3 followed by 65% $HClO_4$. Available phosphorus contents (in wt % P_2O_5) have been estimated[11] by the 2% citric acid method. Approximately 1.0g samples of finely powdered (100 mesh) samples were extracted with 100 ml of 2% citric acid using a mechanical shaker operating at about 250 oscillations per minute for a period of 30 minutes. All the extracts were analysed for phosphorus by the vanadomolybdate method[7] using a Unicam SP 600 colorimeter at a wave length of 460 nm.

3. Results and Discussion

3.1 Data on Eppawela apatite

Results of phosphorus and halogen analysis of four different samples collected from the 'leached zone' at Eppawela are shown in the Table 1. These values are compared with some of the known rock phosphates[9] from other countries in the Table 2.

Present chemical analysis confirms that Eppawela apatite contains more chlorine than fluorine and hence it is different from most of the known rock phosphates. Its total phosphorus content is high, when compared to other known deposits, which makes this deposit commercially very important. On the other hand, available phosphorus content of Eppawela apatite is found to be the lowest among the phosphate rocks listed in the Table 2.

Table 2. Comparison with foreign phosphate rock samples

Phosphate rock	Wt. % F	Wt. % P_2O_5	2% citric acid soluble P_2O_5 (% Wt.)
Florida hard rock	3.4 – 4.0	31 – 36	7.2
Florida land pebble	3.2 – 4.1	30 – 36	6.7
Tennessee brown rock	2.6 – 4.1	25 – 38	6.2
Tennessee blue rock	3.3 – 4.0	28 – 34	6.8
South Carolina rock	2.2 – 3.8	16 – 29	7.8
Curacao, West Indies	0.3 – 0.9	38 – 41	14.6
Morocco	4.1 – 4.3	33 – 35	10.4
Nauru and Ocean Islands	2.0 – 3.3	38 – 41	10.1
Christmas Island	1.0 – 1.5	39	13.2
Eppawela, Sri Lanka	0.8 – 1.7	34 – 40	5.9

Note: Wt. % Cl values for foreign rock samples are not available in the literature.

Synthetic experiments made using tricalcium phosphate, calcium chloride and calcium fluoride followed by the comparison of powder X-ray diffraction patterns of natural and synthetic samples confirmed that the Eppawela apatite is in fact a chlorfluorapatite. Its X-ray powder pattern could be indexed using a hexagonal unit cell with $\underline{a}$ = 9.470(10) Å and $\underline{c}$ = 6.863(5) Å. Differential thermal analysis of this sample did not show any thermal transition up to 1000°C while thermogravimetric analysis showed a weight loss of 0.6 – 1.0% in the temperature range 500 – 1000°C. This is mainly due to the loss of halogen as evidenced by the available experimental data. However, the confirmation of identity of the evolved gases by mass spectroscopy was not possible in this study.

3.2 Dehalogenation

Halogen loss observed in Eppawela apatite on heat treatment as well as 2% citric acid solubility of the products are shown in Table 3. Total loss of halogen (both chlorine and fluorine) after heat treatment in the temperature interval 700 – 1300°C was found to be in the range 6 – 15%. The loss of fluorine was nearly a constant (∿ 5 – 6.5%) while much higher loss of chlorine (∿ 7 – 22%) was observed in the same temperature range (Figure 1). When the heating time was increased to 25 hours at 1300°C, 70% of chlorine was lost while only about 12% of fluorine was evolved under the same conditions.

Table 3. Halogen loss in Eppawela apatite at high temperature

Temperature °C	Time hrs.	Fluorine		Chlorine		2% Citric acid soluble P_2O_5 (wt. %)
		% wt. F	% loss F	% wt. of Cl	% loss Cl	
700	2	1.62	4.7	2.04	7.3	6.5
900	2	1.61	5.3	1.99	9.5	7.2
1100	2	1.60	5.9	1.96	10.9	8.8
1300	2	1.59	6.5	1.72	21.8	10.1
1300	25	1.50	11.8	0.66	70.0	13.0

Correlation between the available P_2O_5 contents and the percentage dehalogenation in Eppawela apatite is shown in Figure 2. It is apparent that there is an increase in the available phosphorus contents with increase in the extent of dehalogenation. It has also been observed that the presence of water enhances dehalogenation. For example, about 50% increase in dehalogenation was observed when the experiment was repeated in the presence of added water at 1100°C.

During heat treatment the rock phosphate changed its colour from yellowish white (room temperature) through greenish pink (1100°C) to green (1300°C). X-ray powder pattern of the products clearly show that

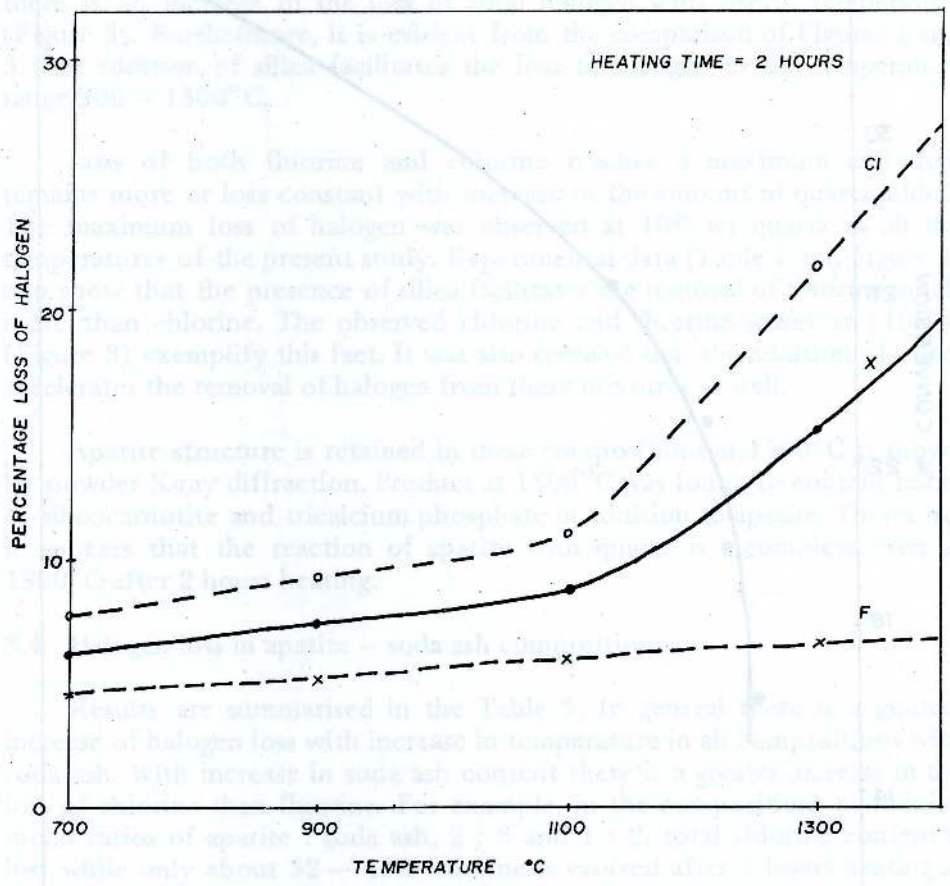

Figure 1. Effect of temperature on dehalogenation of Eppawela apatite.

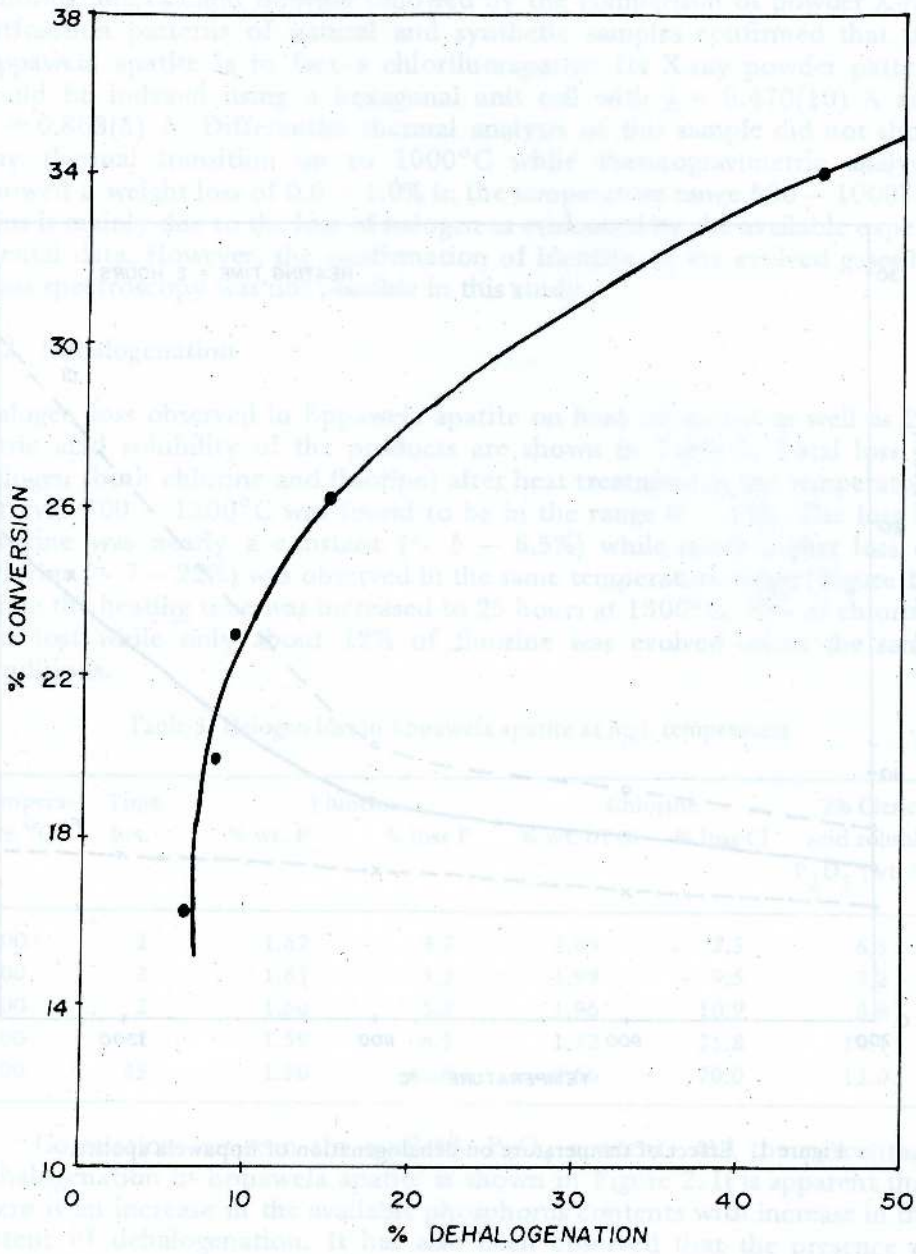

Figure 2. Relationship between dehalogenation and percentage conversion.

$$\left(\%\ \text{conversion} = \frac{\text{2\% citric acid soluble } P_2O_5}{\text{Total } P_2O_5} \times 100\right)$$

there is a pronounced shift in the powder lines of chlorfluorapatite towards hydroxyfluorapatite. Apatite structure is retained even after 2 hours heat treatment at 1450°C.

3.3 Halogen loss in apatite – quartz mixtures

Loss of chlorine and fluorine in some mixtures containing apatite and quartz at high temperature is presented in Table 4. It has been observed that there is an increase in the loss of total halogen with rise in temperature (Figure 3). Furthermore, it is evident from the comparison of Figures 1 and 3 that addition of silica facilitates the loss of halogen in the temperature range 900 – 1300°C.

Loss of both fluorine and chlorine reaches a maximum and then remains more or loss constant with increase in the amount of quartz added. The maximum loss of halogen was observed at 10% wt quartz in all the temperatures of the present study. Experimental data (Table 4 and Figure 3) also show that the presence of silica facilitates the removal of fluorine much more than chlorine. The observed chlorine and fluorine losses at 1100°C (Figure 3) exemplify this fact. It was also revealed that the addition of water accelerates the removal of halogen from these mixtures as well.

Apatite structure is retained in these compositions at 1100°C as shown by powder X-ray diffraction. Product at 1300°C was found to contain traces of silicocarnotite and tricalcium phosphate in addition to apatite. Therefore, it appears that the reaction of apatite with quartz is incomplete even at 1300°C after 2 hours heating.

3.4 Halogen loss in apatite – soda ash compositions

Results are summarised in the Table 5. In general there is a gradual increase of halogen loss with increase in temperature in all compositions with soda ash. With increase in soda ash content there is a greater increase in the loss of chlorine than fluorine. For example, in the compositions containing molar ratios of apatite : soda ash, 2 : 3 and 1 : 2, total chlorine content is lost while only about 32 – 48% fluorine is evolved after 2 hours heating at 1300°C. The major phase in the products was identified as rhenanite, $CaNaPO_4$.

Effect of soda ash on dehalogenation is shown in Figure 4. Loss of total chlorine and fluorine increases with increase in soda ash content up to about 1.5 mole of soda ash per mole of apatite and beyond this value the effect is negligible. This therefore indicates that the optimum soda ash requirement for the maximum removal of halogen is about 1.5 moles of soda ash per mole of apatite.

It is evident that chlorine removal is greatly facilitated by the presense

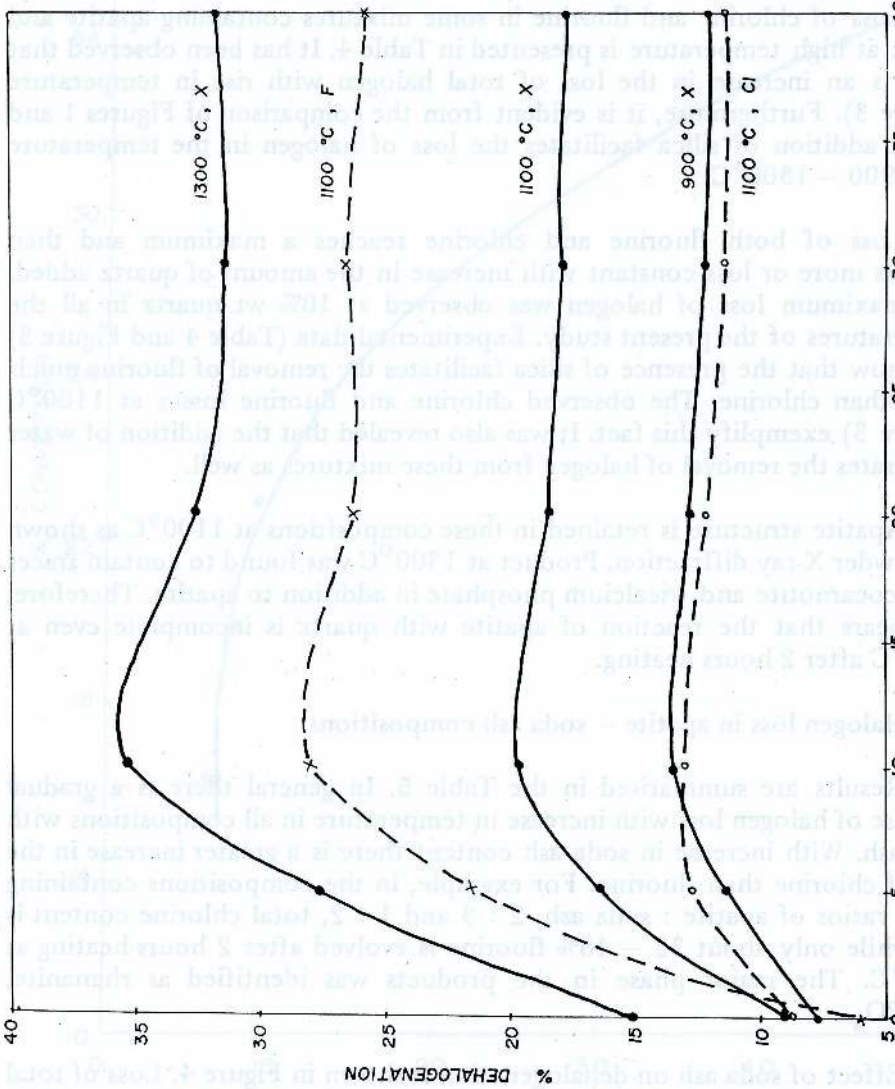

Figure 3. Effect of silica (quartz) on dehalogenation.

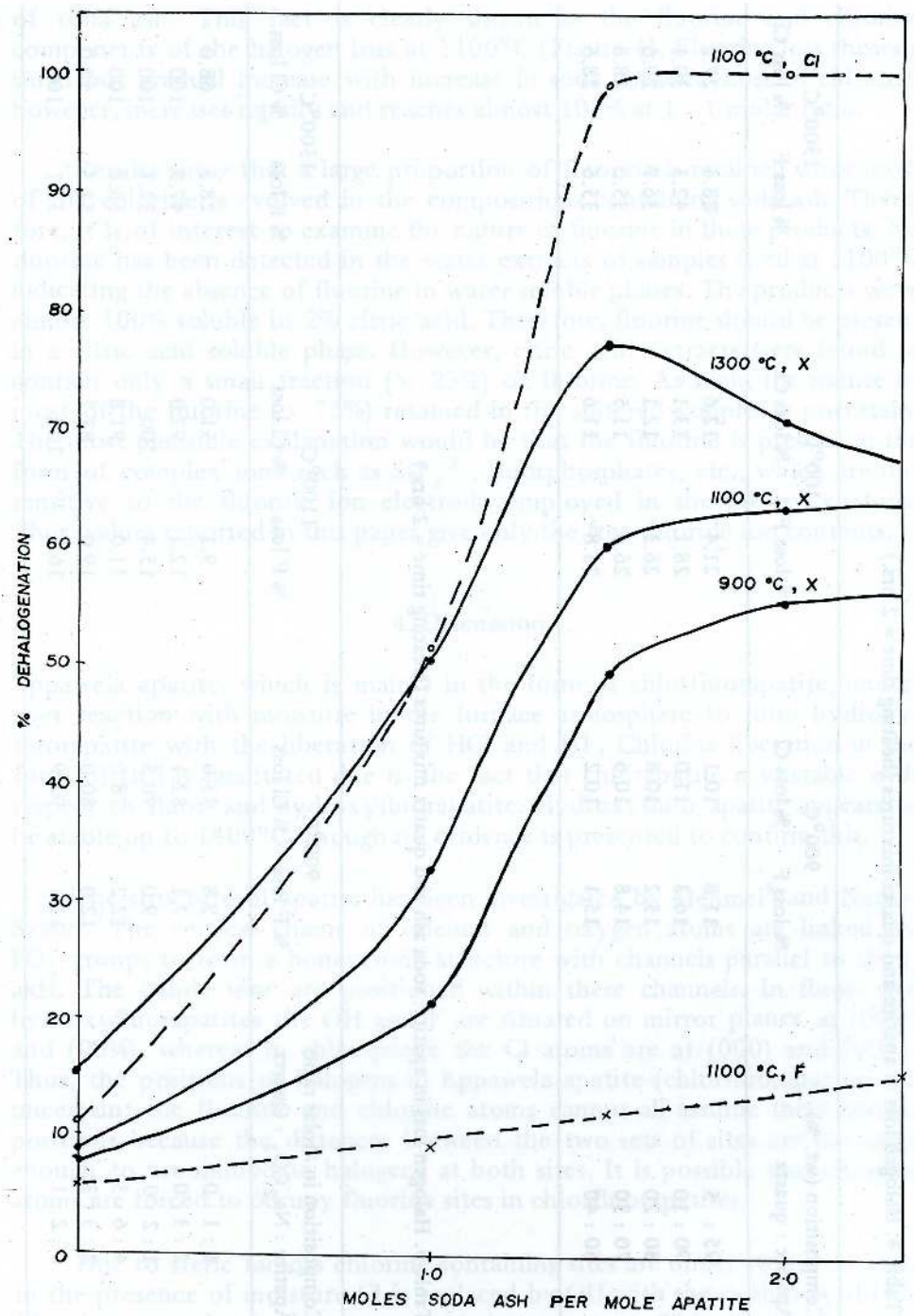

Figure 4. Effect of soda ash on dehalogenation.

Table 4. Halogen loss in apatite and quartz mixtures (heating time = 2 hrs.)

Composition (wt. %) Apatite : quartz	900°C		1100°C		1300°C	
	% loss F	% loss Cl	% loss F	% loss Cl	% loss F	% loss Cl
95 : 5	11.8	10.1	21.4	12.6	28.4	27.2
90 : 10	16.3	11.0	28.1	13.1	42.3	30.1
80 : 20	15.2	10.8	26.3	12.1	36.7	29.6
70 : 30	14.8	10.6	26.6	11.5	35.0	28.8
60 : 40	15.1	10.2	25.8	11.6	35.6	28.6

Table 5. Halogen loss in apatite, soda ash and quartz mixtures (Heating time = 2 hrs.)

Composition in Molar ratio Apatite : Na_2CO_3 : Quartz	900°C		1100°C		1300°C	
	% F loss	% Cl loss	% F loss	% Cl loss	% F loss	% Cl loss
1 : 1 : 0	5.8	33.0	9.1	51.0	28.5	68.0
2 : 3 : 0	7.1	82.1	12.1	97.0	47.9	100
1 : 2 : 0	9.0	90.8	15.4	100	32.1	100
4 : 6 : 3	12.2	78.0	21.0	91.8	58.2	100
2 : 3 : 3	12.0	80.0	19.0	87.7	51.3	92.0
1 : 2 : 1	11.1	92.9	16.8	100	35.1	100

of soda ash. This fact is clearly shown in the fluorine and chlorine components of the halogen loss at 1100°C (Figure 4). Fluorine loss shows a small but gradual increase with increase in soda content. Loss of chlorine, however, increases rapidly and reaches almost 100% at 1 : 1 molar ratio.

Results show that a large proportion of fluorine is retained while most of the chlorine is evolved in the compositions containing soda ash. Therefore, it is of interest to examine the nature of fluorine in these products. No fluorine has been detected in the water extracts of samples fired at 1100°C indicating the absence of fluorine in water soluble phases. The products were almost 100% soluble in 2% citric acid. Therefore, fluorine should be present in a citric acid soluble phase. However, citric acid extracts were found to contain only a small fraction ($\sim$ 25%) of fluorine. As such, the nature of most of the fluorine ($\sim$ 75%) retained in the sintered samples is uncertain. The most plausible explanation would be that the fluorine is present in the form of complex ions such as SiF_6^{2-}, fluorphosphates, etc., which are not sensitive to the fluoride ion electrode employed in the present analysis. Thus, values reported in this paper give only the free fluoride ion contents.

4. Discussion

Eppawela apatite, which is mainly in the form of chlorfluorapatite, undergoes reaction with moisture in the furnace atmosphere to form hydroxyfluorapatite with the liberation of HCl and HF. Chlorine liberation in the form of HCl is facilitated due to the fact that chlorapatite is unstable with respect to fluor- and hydroxyfluorapatite. Hydroxyfluor apatite appears to be stable up to 1400°C, though no evidence is presented to confirm this.

The structure of apatite has been investigated by Mehmel[8] and Naray-Szabo.[10] The vertical chains of calcium and oxygen atoms are linked by PO_4 groups to form a honeycomb structure with channels parallel to the $\underline{c}$ axis. The halide ions are positioned within these channels. In fluor- and hydroxyfluorapatites the OH and F are situated on mirror planes at (00¼) and (00¾), whereas in chlorapatite the Cl atoms are at (000) and (00½). Thus, the positions of halogens in Eppawela apatite (chlorfluorapatite) are uncertain: the fluorine and chlorine atoms cannot all assume their normal positions because the distances between the two sets of sites are not large enough to accommodate halogens at both sites. It is possible that chlorine atoms are forced to occupy fluorine sites in chlorfluorapatites.

Due to steric factors chlorine containing sites are under strain. As such, in the presence of moisture Cl is replaced by OH with the evolution of HCl. Fluorine may also be lost to a much lesser extent. This also explains the enhanced loss of halogen when extra water is introduced to the furnace. In the presence of silica highly volatile SiF_4 and H_2SiF_6 would also be formed which accelerates the loss of fluorine.

Table 6. Solubility data of some phases

Material	2% citric acid soluble P_2O_5 (wt. %)	Solubility as a % of total P_2O_5
$Ca_5(PO_4)_3(OH)$ (hydroxyapatite)	16.2	38
β-$Ca_3(PO_4)_2$	34.0	74
α-$Ca_3(PO_4)_2$	36.6	80
$Ca_4P_2O_9$	38.9	100
$Ca_5(SiO_4)(PO_4)_2$ (silicocarnotite)	30.1	100
$Ca_7(SiO_4)_2(PO_4)_2$ (Nagelschmidtite)	21.9	100
$CaNaPO_4$ (Rhenanite)	45.0	100

Available phosphorus content of hydroxyapatite is higher than that in haloapatites. Thus, increase in available phosphorus content with increase in dehalogenation is due to the increase in the extent of the replacement of halogen by OH in the structure. Table 6 gives the available phosphorus values of some phases that may be encountered in the fired products.

Decomposition of chlorfluorapatite on thermal treatment proceeds via two stages.

(a) Isomorphous replacement of chlorine and to a lesser extent fluorine with hydroxyl ions, and

(b) breakdown of the resulting hydroxyfluorapatite to give as the major phases, (i) α and β tricalcium phosphate, tetracalcium phosphate,[9] etc., at 1500 – 1600°C; (ii) silicocarnotite and nagelschmidtite in addition to (i), in the presence of silica at 1300 – 1400°C; (iii) rhenanite in the presence of soda ash at 900 – 1300°C.

Acknowledgement

The author is grateful to Dr. M. Masson of the University of Aberdeen, U.K. for her assistance in the fluorine analysis and the International Seminar in Chemistry of the Uppsala University in Sweden for financial assistance to perform thermal analysis at the Arrhenius Laboratory, University of Stockholm, Sweden.

References

1. BARRET, R. L. & McCAUGHEY, W. J. (1942) *Am. Minerologist,* **27** : 680.

2. CORBRIDGE, D. E. C. (1974) The structural chemistry of phosphorus, Elsevier Publishing Company, Amsterdam, London, New York.

3. EDMOND, C. R. (1969) *Anal. Chem.* **41** (10) : 1327 – 1328.

4. GUNAWARDANE, R. P. (1982) *J. Natn. Sci. Coun. Sri Lanka* **10** (2) : 181 – 194.

5. GUNAWARDANE, R. P. and GLASSER, F. P. (1979) *J. Mater. Sci.,* **14** : 2797 – 2816.

6. JAYAWARDANA, D. E. De S. (1976) The Eppawela carbonatite complex in North-west Sri Lanka, Economic Bulletin No. 3, Geological Survey Department, Colombo.

7. JEFFERY, P. G. (1971) Chemical method of rock analysis, Pergamon Press, Oxford.

8. MEHMEL, M. (1930) *Z.Krist.,* **75** : 323.

9. MELLOR, J. W. (1971) Comprehensive treatise on inorganic and theoretical chemistry, Volume 3 – supplement 3, Longmans, London.

10. NARAY – SZABO, S. (1930) *Z.Krist.,* **75** : 387.

11. PIERRE, W. H. & NORMAN, A. G. (1953) Soil and fertilizer phosphorus in crop nutrition, Academic Press, London, New York.

12. TAZAKI, K., FYRE, W. S. and DISSANAYAKE, C. B. (1986) *Applied Geochemistry,* **1** : 287 – 300.

13. WHITNEY, W. T. & HOLLIWGSWORTH, C. A. (1949) *Ind. Eng. Chem.,* **41** : 1325 – 1327.

References

1. BARRETT, R. L. & McCAUGHEY, W. J. (1942) Am. Mineralogist, 27 : 680.

2. CORBRIDGE, D. E. C. (1974) The structural chemistry of phosphorus, Elsevier Publishing Company, Amsterdam, London, New York.

3. EDMOND, C.R. (1969) Anal. Chem. 41(10) : 1327 – 1328.

4. GUNAWARDANE, R. P. (1982) J. Natn. Sci. Coun. Sri Lanka. 10(2) : 181 – 184.

5. GUNAWARDANE, R. P. and GLASSER, F. P. (1979) J. Mater. Sci. 14 : 2797 – 2816.

6. JAYAWARDANA, D. E. De S. (1976) The Eppawela carbonatite complex in North-west Sri Lanka. Economic Bulletin No. 3, Geological Survey Department, Colombo.

7. JEFFERY, P. G. (1971) Chemical method of rock analysis. Pergamon Press, Oxford.

8. MEHMEL, M. (1930) Z. Krist. 75 : 323.

9. MELLOR, J. W. (1971) Comprehensive treatise on inorganic and theoretical chemistry. Volume 8 supplement 3, Longmans, London.

10. NARAY – SZABO, S. (1930) Z. Krist. 75 : 387.

11. PIERRE, W. H. & NORMAN, A. G. (1953) Soil and fertilizer phosphorus in crop nutrition. Academic Press, London, New York.

12. TAZAKI, K., FYFE, W. S. and DISSANAYAKE, C. B. (1986) Applied Geochemistry, 1 : 287 – 300.

13. WHITNEY, W. T. & HOLLINGSWORTH, C. A. (1969) Anal. Chem. 41 : 1325 – 1327.

J. Natn. Sci. Coun. Sri Lanka 1987 **15**(1): 101–108

CHEMISTRY OF MARINE ORGANISMS OF SRI LANKA : LIPID AND TRITERPENOID CONSTITUENTS OF AN UNIDENTIFIED ALCYONACEAN AND AN UNIDENTIFIED HOLOTHURIAN

B. M. R. BANDARA, A. A. L. GUNATILAKA, S. D. G. S. SAMARANAYAKE
Department of Chemistry, University of Peradeniya, Peradeniya, Sri Lanka.

and

E. D. DE SILVA AND L. M. V. TILLEKERATNE
Department of Chemistry, University of Colombo, Colombo, Sri Lanka.

(Date of receipt : 23 December 1986)
(Date of acceptance : 08 April 1987)

Abstract : The major constituents of the lipid fraction of an unidentified alcyonacean is shown to be hexadecyl hexadecanoate and the sterols, gorgosterol, 23-demethylgorgosterol, brassicasterol, cholesterol and 24-methylcholesterol. The aglycone of the saponin from an unidentified holothurian species had been characterized as 22, 25-oxidoholothurinogenin.

1. Introduction

1.1 Alcyonaceae

The Order Alcyonaceae belongs to the subclass Octocorallia of the phylum Coelenterata. The animals belonging to this order are commonly known as soft corals. Soft corals are relatively abundant in Sri Lankan waters and have recently been the subject of extensive chemical investigations.[2,3] A large number of novel secondary metabolites which include sesquiterpenoids, diterpenoids and prostaglandins[11] have been isolated from soft corals. The sterols of the soft corals are particularly interesting because of the diversity of their side chains.[4] As the soft corals are known to contain unicellular algae, the zooanthellae, which are symbiotically associated with them, several studies to define the origin of the sterols have been reported.[6,12]

1.2 Holothroidea

The marine phylum Echinodermata can be divided into five classes: Crinoidea (sea lilies), Holothuroidea (sea cucumbers), Echinoidea (sea urchins), Ophiuroidea (brittle-stars) and Asteroidea (star fishes). The dried body wall of certain sea cucumber species (e.g. *Holothuria atra)* is a well known Chinese culinary delicacy traded under the name trepany or beche-de-mer. In contrast, the poisonous properties of sea cucumbers have also been known for many centuries in parts of the Pacific where mashed or chopped sea cucumbers have traditionally been used to poison fish. The

general toxicity of the sea cucumbers have been attributed to a group of compounds known as holothurins, a class of water soluble saponins. Although saponins have been isolated from several terrestrial plants, in the animal kingdom they have so far been found in Echinodermata with only sea cucumbers and star fishes having appreciable quantities. Curiously, holothurins have triterpenoid aglycones whereas star fish saponin (asterosaponin) have steroid aglycones.[4]

2. Results and Discussion

2.1 Analysis of the lipid part of the soft coral

The combined petroleum and chloroform extracts of the soft coral on flash chromatography on silica gel gave a waxy solid which on purification by repeated recrystallization afforded a t.l.c. homogeneous compound as colourless plates, m.p. 51 – 52°C. This compound had a molecular weight of 480 by mass spectrometry. The IR spectrum showed strong bands at 1730, 1240 and 1180 cm^{-1} indicating the presence of an ester carbonyl group. The ^1H N.M.R. spectrum confirmed the presence of the ester group by triplets at δ 4.00 (J = 6Hz) and 2.16 (J = 6Hz) which could be assigned to the protons of the methylene groups attached to the alkoxy oxygen and the carbonyl carbon of the ester group, respectively. The remaining broad band at δ 1.26 indicated the presence of a long alkyl chain and possible absence of other functional groups.

Treatment of this ester with lithium aluminium hydride ($LiAlH_4$) afforded a single alcohol indicating the 'symmetric' nature of the natural ester. The identity of the reduced product as l-hexadecanol (2) was established by comparing its mass spectrum with computer-recorded known mass spectra.[13] Mixed m.p. and Co-I.R. spectrum of this alcohol with an authentic sample prepared by $LiAlH_4$ reduction of hexadecanoic acid further confirmed its identity as hexadecanol. Saponification of the natural ester yielded hexadecanol. Further, the mass spectrum of the natural ester compared with that for hexadecylhexadecanoate (1).[14] The ester (1) was also synthesized from hexadecanoic acid.

Further elution of the above column afforded a sterol mixture constituting about 0.02% of dry weight of the concentrate from soxhlet extraction. The sterol mixture was silylated and subjected to gas chromatographic analysis. The sterols present were identified as brassicasterol (3a). 24-methylcholesterol (3b), gorgosterol (3c), cholesterol (3d), and 23-demethylgorgosterol (3e)(Fig. 1).Subsequent gas chromatographic-mass spectral (GC-MS) analysis confirmed the above findings (see Table 2). Relative concentrations of the sterols in the column fraction calculated from gas chromatographic trace were: gorgosterol (40%); 24-methylcholesterol (45%); brassicasterol (10%); cholesterol (5%), 23-demethylgorgosterol (trace).

Table 1. ^{1}H N.M.R. spectral data[a] (δ in $CDCl_3$ at 60 MHz) of 22, 25-oxidoholothurinogenin (**4**) and its 3-acetate (**5**)

Compound	3–H	7–H 11–H	22–H	C–4 $(Me)_2$	C–14 Me	C–10 Me	C–20 $(Me)_2$	C–25 Me
(4)	3.26 m	5.51 m 5.20 m	4.25 m	0.85 s 1.00 s	1.17 s	1.20 s	1.38 s	1.26 s
(5)	4.56 bt	5.40 m	4.20 m	0.91 s 0.99 s	1.13 s	1.23 s	1.26 s 1.28 s	1.33 s

[a]abbreviations: s, singlet; bt, broad triplet; m, multiplet

Cholesterol (3d) is the most common steroid found in marine organisms. Brassicasterol (3a) and 24-methylcholesterol (3b) have been reported to be present in some sponges, coelentrates, molluscs, crustaceans and echinoderms.[8] Gorgosterol (3c) first isolated from the gorgonian *Plexaura flexuosa* occurs in many coelentrates. The uncommon steroid 23-demethylgorgosterol (3e) which was initially obtained from the gorgonian *Gorgonia flabellum*[9] has been found in some alcyonacean species.[10]

Table 2. G.C.-M.S. data[a] of sterols isolated from the soft coral

Sterol	R.R.T./min[b]	Mass fragmentation (m/z)
Brassicasterol (**3a**)	1.17	398(M^+), 380($M^+ - H_2O$), 355, 300, 273(M^+ –side chain), 271, 255($M^+ - H_2O$- side chain).
24-methylcholesterol (3b)[c]	1.35	400(M^+), 367, 273(M^+-side chain), 301
Gorgosterol (**3c**)	2.43	426(M^+), 314, 300, 299, 271
Cholesterol (**3d**)	1.00	386(M^+), 372, 301, 273, 255
23-demethylgorgosterol (**3e**)	1.79	M.S. not recorded.

[a]Using Varian MAT–44(3% OV–17 column, 260°C)

[b]Relative Retention Time (R.R.T.) for cholesterol = 1.00

[c] Stereochemistry of C 24–Me was not determined.

2.2 22,25-Oxidoholothurinogenin

Hot methanolic extract of the dried holothurian was hydrolysed with HCl in methanol-water under reflux conditions. The reaction mixture was filtered and the precipitate was chromatographed over silica gel to yield a white solid which when recrystallised from chloroform-methanol yielded colourless needles. The ^{1}H N.M.R. spectrum (60 MHz) of this compound showed seven tertiary methyl singlets in the region δ 0.85 – 1.38. This along with the molecular ion peak observed at m/z 484 in its mass spectrum suggested that the compound could be a triterpenoid. The presence of a lactone carbonyl absorption band at 1750 cm^{-1} in the I.R. spectrum, and two olefinic hydrogens at δ 5.51 and 5.20 in its ^{1}H N.M.R. spectrum suggested it to be a holothurinogenin. Comparison of physical data of 4 and its acetylated product (5) with those reported from *Actinophyta agrossert*[5] confirmed the triterpenoid to be 22,25-oxidoholothurinogenin (4).

3. Experimental

3.1 Investigation of the soft coral

The unidentified soft coral collected at Nilaveli, on the East coast of Sri Lanka was stored in methanol. Methanol was decanted and the residue (dry wt. 1 kg) was extracted successively and exhaustively with hot light petroleum, hot chloroform and hot methanol. The light petroleum (29 g, 3%) and the chloroform (3.5 g, 0.35%) extracts were combined as there was no significant difference in their behaviour on T.L.C.

Flash chromatography of the above combined extract (10 g) over silica gel (T.L.C. grade 250 g) with chloroform containing increasing amounts of methanol furnished three fractions; hexadecyl hexadecanoate (1), a mixture of sterols and a fraction which mainly consisted of a diterpenoid (by mass spectroscopy). Further characterization of the last fraction was not possible due to lack of sufficient material.

3.1.1 *Hexadecyl hexadecanoate* (1)

The crude fraction containing (1) was recrystallised from light petroleum to obtain colourless plates (0.519 g; 0.17% from dry weight) m.p. 51 – 52°C (lit.[15] 51°C); I.R. ν_{max} (KBr) 2820, 2900, 1725, 1460, 1180, 725 cm^{-1}; ^{1}H N.M.R. δ (CCl_4, 60MHz) 4.00 (2H,t, J =6.0Hz), 2.16 (2H, t, J = 7.8Hz), 1.26 (methylene envelope); M.S. m/z (rel. int.) 480 (M^+, 18%) and 257 (1.0%).

3.1.2 *Lithium Aluminium Hydride Reduction of* (1) *to obtain hexadecanol* (2)

To an ice-cold solution of hexadecyl hexadecanoate (25 mg) in dry THF

(5ml), $LiAlH_4$ (5 mg) was added portion-wise. Usual work-up afforded the reduced product which was purified by preparative T.L.C. and recrystallised from acetone to yield hexadecanol (2) (21 mg; 34%) m.p. 53 – 54° (lit.[7] m.p. 49°C); IR ν_{max} (KBr) 3340, 2830, 2900, 1480 cm^{-1}; ^1H N.M.R. δ (CCl_4, 60MHz) 3.23(2H,t, J = 6Hz), 1.26 (methylene envelope).

3.3.3 Saponification of hexadecyl hexadecanoate (1) *to obtain hexadecanol* (2)

A mixture of the ester (62 mg) and methanolic KOH (7%, 1 ml) was refluxed for 3h. The reaction mixture was concentrated under *vacuo* and the residue was partitioned between ether and water. The ether layer was washed with water (3 x 10 ml). Evaporation of ether yielded a crude solid which was purified by preparative T.L.C. Recrystallisation from acetone yielded hexadecanol (35 mg, 58%) m.p. 53 – 54°C (lit.[7] 49°C); I.R. ν_{max} (KBr) 3340, 2830, 2900, 1480 cm^{-1}; ^1H N.M.R. δ (CCl_4, 60 MHz) 3.23 (2H,t, J = 6Hz), 1.26 (methylene envelope); M.S. m/z (rel. int.) 224 ($M^+ - H_2O$; 0.9%), 196, 182, 168, 154, 111, 97, 83, 69, 55, 43.

3.1.4 Synthesis of hexadecyl hexadecanoate (1)

Hexadecanoic acid (960 mg) was dissolved in dry ether (10 ml). $LiAlH_4$ (15 mg) was added portion-wise. The mixture was heated under reflux for 2h. The reaction mixture was cooled, acidified with dilute hydrochloric acid and extracted into chloroform (50 ml x 2). Evaporation of chloroform yielded a white solid (225 mg). The crude product (225 mg) and hexadecanoic acid (220 mg) were dissolved in acetone (20 ml), and conc. H_2SO_4 (1 ml) in acetone (5 ml) was slowly run down to the acetone solution along the wall of the flask. After heating under reflux for 4h the reaction mixture was worked-up in usual manner. Subsequent purification by preparative TLC and recrystallization from acetone afforded pure compound (1) (200 mg, 50%) m.p. 51–52°C; IR ν_{max} (KBr) (cm^{-1}) 2900, 2820, 1730, 1180, 760–720.

3.1.5 Gas Chromatographic-Mass Spectral analysis of the Sterol mixture

The above sterol mixture obtained as a T.L.C. homogeneous colourless crystalline solid was subjected to G.C.–M.S. analysis. The results of this analysis are depicted in Table 2.

3.2 Investigation of the Holothurian

The holothurian collected at Negombo, on the West coast of Sri Lanka was sun-dried and the dried material (397 g) was extracted exhaustively with hot light petroleum and then with hot methanol to yield 4.5 g (1.0%) and 20 g (5%) of extracts, respectively.

3.2.1 Isolation of 22,25-oxidoholothurinogenin (4)

Total methanol extract (20 g) in aqueous methanol (50%, 200 ml) was heated under reflux while a solution of dil. HCl (60%, 200 ml) was run down to the reaction mixture during 0.5 hours. Heating was continued for further 8 hours. The resulting precipitate (1.73 g) was filtered and chromatographed over T. L. C. grade silica gel to obtain pure 22, 25- oxidoholothurinogenin (4). Recrystallization from chloroform-methanol yielded needles (103 mg, 0.05%), m.p. 310 – 312°C (lit.[5] 315 – 316°C); $(\alpha)_D$ –22.5° (lit.[5] – 22.2°); I.R. ν_{max} (KBr) 3500 and 1750 cm^{-1}; see Table 2 for ^1H N.M.R. data.

3.2.2 22,25-Oxidoholothurinogenin-3-acetate (5)

22,25-Oxidoholothurinogenin (25 mg) was dissolved in dry pyridine (5 ml), acetic anhydride (2 ml) was added dropwise to the solution, and the reaction mixture was heated under reflux for 3 hours. Usual work-up of this mixture, yielded a white solid which on crystallization from chloroform-methanol yielded colourless needles of 22, 25-oxidoholothurinogenin-3-acetete (5); m.p. 288 – 289°C (lit.[5] 289 – 290°C); $(\alpha)_D$ + 6.7° (lit[5]+ 6.5°); I.R. ν_{max} (CCl_4) 3565 and 1770 cm^{-1}.

Acknowledgements

We thank the Natural Resources, Energy and Science Authority of Sri Lanka for financial assistance; Prof. Carl Djerassi (Stanford University, U.S.A.) for G.C. – M.S. data of the sterol mixture; Dr. J. K. MacLeod (Australian National University, Canberra) for MS Computer matching of l-hexadecanol; Ms. P. Liyanage, P. Rajanathan and D. V. Ariyapala for technical assistance and Mrs. S. C. Weerasekera for typing the manuscript.

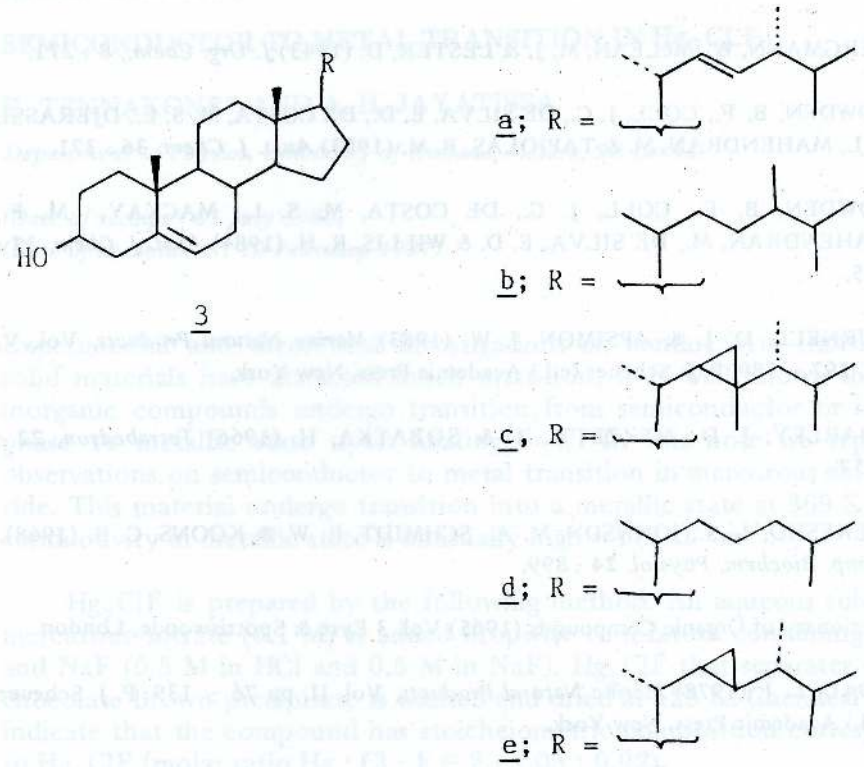

Fig. 1 Structures of sterols from the soft coral

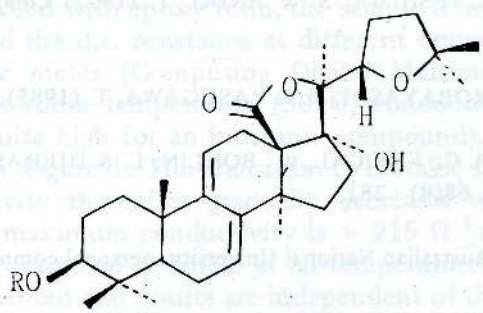

(4); R = H

(5); R = Ac

References

1. BERGMANN, W., McLEAN, M. J. & LESTER, D. (1943) *J. Org. Chem.*, **8** : 271.
2. BOWDEN, B. F., COLL, J. C., DE SILVA, E. D., DE COSTA, M. S. L., DJERASSI, P. J., MAHENDRAN, M. & TAPIOLAS, B. M. (1983) *Aust. J. Chem.* **36** : 371.
3. BOWDEN, B. F., COLL, J. C., DE COSTA, M. S. L., MACKAY, M. F., MAHENDRAN, M., DE SILVA, E. D. & WILLIS, R. H. (1984) *Aust. J. Chem.* **37** : 545.
4. BURNELL, D. J. & APSIMON, J. W. (1983) *Marine Natural Products,* Vol. V, pp. 297 – 389. P. J. Scheuer (ed.) Academic Press, New York.
5. CHARLEY, J. D., MEZZETTI, T. & SOBATKA, H. (1966) *Tetrahedron,* **22** : 1857.
6. CIERESKO, L. S., JOHNSON, M. A., SCHMIDT, R. W. & KOONS, C. B. (1968). *Comp. Biochem. Physiol.* **24** : 899.
7. Dictionary of Organic Compounds (1965) Vol. 3 Eyre & Spottiswoode, London.
8. GOAD, L. J. (1978) *Marine Natural Products,* Vol. II, pp 76 – 139; P. J. Scheuer (ed.) Academic Press, New York.
9. HALE, R. L., LECLERCQ, J., TURSCH, B., DJERASSI, C., GROSS, R. A., WEINHEIMER, A. J., GUPTA, K. & SCHEUER, P. J. (1970) *J. Amer. Chem. Soc.,* **92** : 2179.
10. KANAZAWA, A., TESHIMA, S. & ANDO. T. (1977) *Comp. Biochem. Physiol.* **57(B)** : 317.
11. KITAGAWA, I., KOBAYASHI, M. & YASUGAWA, T. (1985) *Tetrahedron,* **41** : 955.
12. KOKKE, W. C. M. C., FENICAL, W., BOHLIN, L. & DJERASSI, C. (1981) *Comp. Biochem. Physiol.* **68(B)** : 281.
13. McLEOD, J. K., Australian National University, personal communication.
14. VADJI, M. & NAWAR, W. W. (1981) *J. Amer. Oil Chem. Soc.,* 106.
15. WHITBY, G. S. (1926) *J. Chem. Soc.,* 1463.

J. Natn. Sci. Coun. Sri Lanka 1987 **15(1)** *109–111*

SHORT COMMUNICATION

SEMICONDUCTOR TO METAL TRANSITION IN Hg_2ClF

K. TENNAKONE* AND A. H. JAYATISSA

Department of Physics, University of Ruhuna, Matara, Sri Lanka.

(Date of receipt : 01 July 1986)
(Date of acceptance : 10 February 1987)

Experimental and theoretical investigations on conductivity transitions in solid materials have attracted much attention. It is well known that some inorganic compounds undergo transition from semiconductor or insulator phase to metallic state upon heating/1–4/. In this note we report our observations on semiconductor to metal transition in mercurous chlorofluoride. This material undergo transition into a metallic state at 369 K and the conductivity in metallic state is unusually high $\simeq 177\ \Omega^{-1}m^{-1}$.

Hg_2ClF is prepared by the following method. An aqueous solution of mercurous nitrate (0.1 M) is added dropwise to mixture containing dil HCl and NaF (0.5 M in HCl and 0.5 M in NaF). Hg_2ClF that separates out as a chocolate brown precipitate is washed and dried at 423 K. Chemical analysis indicate that the compound has stoicheiometric composition corresponding to Hg_2ClF (molar ratio Hg : Cl : F $\in$ 2 : 1.05 : 0.92).

To measure the conductivity, the powder is compacted into a glass tube (diameter $\sim$ 0.8 cm) and pressed between stainless steel electrodes to a pressure of 2×10^6 pa, when a pellet (length $\sim$ 0.6 cm) is formed. The ends of the tube are sealed with epoxy resin, the sample is immersed in a thermostatic oil bath and the d.c. resistance at different temperatures is measured using a resistance meter (Computing Digital Multimeter, Takeda Riken Model 6877). The room temperature (30°C) conductivity of the material is $177\ \Omega^{-1}m^{-1}$ (quite high for an inorganic compound). The plot of ln δ vs T^{-1} is indicated in Figure 1. The transition to metallic state occurs at 369 K and the conductivity thereafter gradually decreases with the increase of temperature, the maximum conductivity is $\sim 215\ \Omega^{-1}m^{-1}$. Current-voltage characteristics are found to be linear at all temperatures. Again polarization effects are not detected and results are independent of the electrode material and a.c. measurements show the same behaviour. Above observations indicate that the conductivity is electronic and ionic conduction is negligible or absent.

Attempts were made to prepare single crystals of Hg_2ClF by diffusion and gel methods, sizeable crystals could not be obtained. Again authors had no facilities to elucidate the crystal structure of Hg_2ClF.

* *Institute of Fundamental Studies, Sri Lanka.*

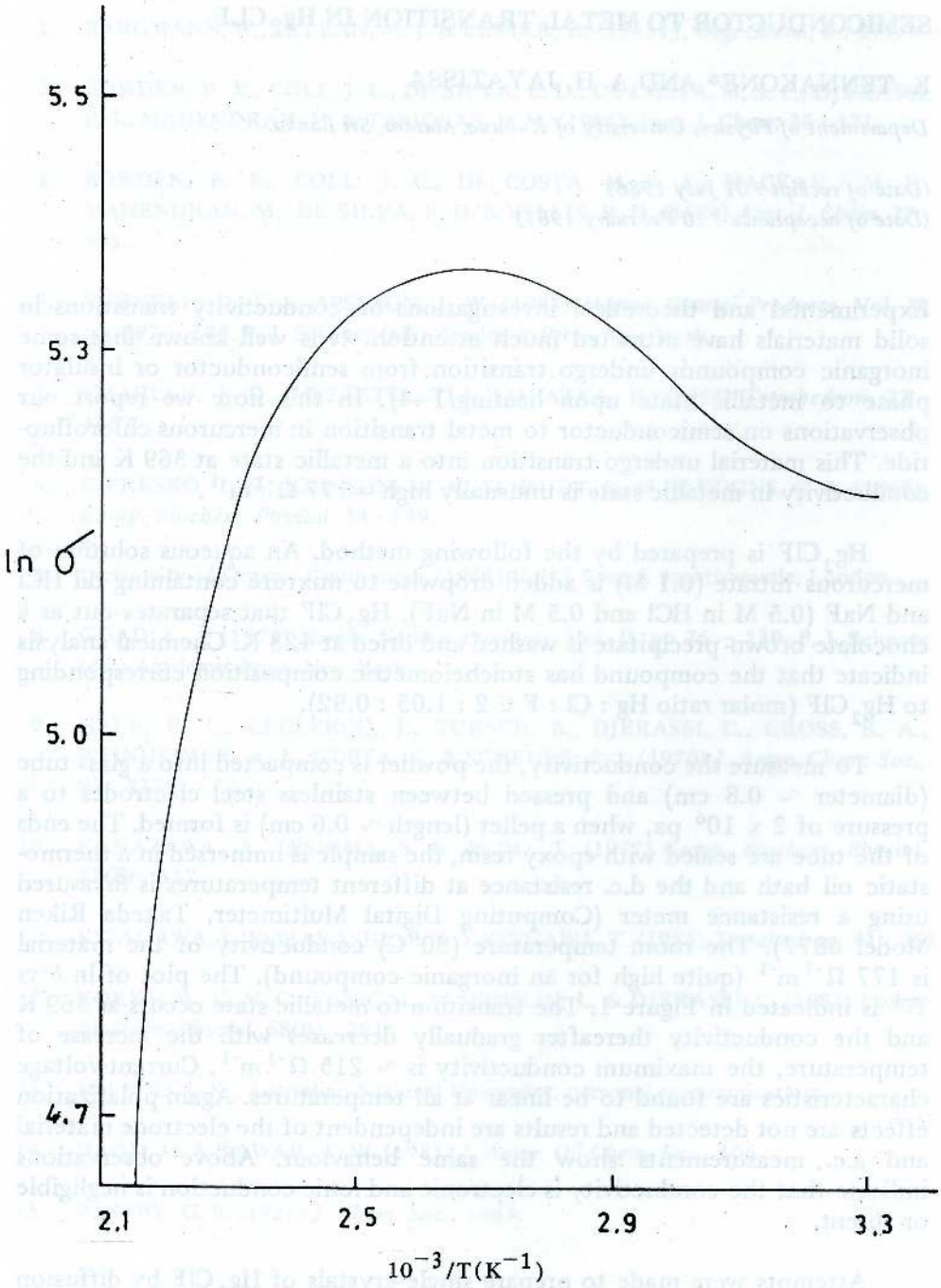

Figure 1 : Plot of ln σ (σ in $\Omega^{-1}m^{-1}$) vs T^{-1}

References

1. AUSTIN, I. G. & MOTT, N. F. (1970). *Science*, **168** : 71.

2. MOTT, N. F. (1956). *Can. J. Phys.* **34** : 1356.

3. MOTT. N. F. & DAVIS, E. A. (1971) *Electronic Processes in Non-Crystalline Solids, Oxford University Press, London.*

4. SWENUMSON, R. D. & EVEN, U. (1981). *Phys. Rev. B.*, **24** : 5743.

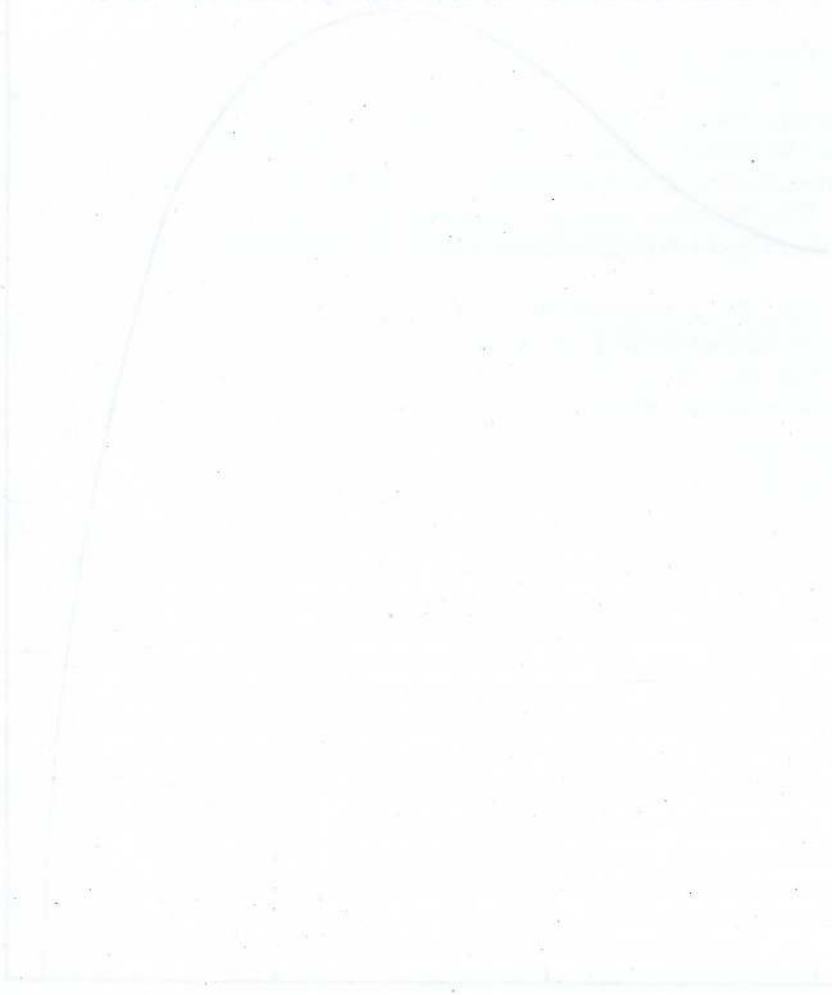

Journal
of the
National
Science
Council of
Sri Lanka

Instructions to Contributors

Aims and Scope

The purpose of this Journal is to provide a medium for the quick dissemination of the results of research in all fields of Science and Technology. Published material will range from original contributions to review articles describing the state of the art in specific areas, together with short communications.

Manuscripts and all correspondence relating to them should be sent to : The Editor, Editorial Board, Journal of the National Science Council of Sri Lanka, 47/5 Maitland Place, Colombo 7, Sri Lanka.

JOURNAL OF THE NATIONAL SCIENCE COUNCIL OF SRI LANKA

INSTRUCTIONS TO CONTRIBUTORS

Manuscripts and all correspondence relating to them should be sent to :
The Secretary, Editorial Board,
Journal of the National Science Council of Sri Lanka,
47/5 Maitland Place, Colombo 7,
SRI LANKA.

EDITORIAL POLICIES

Submission of Papers : Papers are accepted for editorial consideration with the understanding that they have not been published, submitted or accepted for publication elsewhere. Papers accepted for publication may not be published elsewhere in the same form, either in the language of the paper or any other language, without the consent of the Editorial Board.

Research papers, Papers read at Symposia and Reviews may be submitted to the Editorial Board. Research papers should describe original investigations or technological achievements. Reviews should be critical evaluations of existing knowledge in a specialised field. The Journal also accepts Short Communications. They should be submitted if the results are of sufficient importance to merit publication in advance of a full paper.

Languages of Publication : Sinhala, Tamil and English.

Refereeing and Editing : All material submitted is examined by two or more referees prior to publication. Papers are edited to increase clarity and ease of communication. In preparation for the press, particular attention is paid to grammar and the conventions of the Journal with regard to symbols, illustrations, tables, references and nomenclature.

Manuscripts submitted for editorial consideration can be processed expeditiously if they conform from the outset to the style of the Journal. Authors are therefore advised to follow closely the form described in these instructions.

PRESENTATION OF MANUSCRIPTS

No maximum length of contributions is prescribed but papers should be written clearly and concisely. All unnecessary textual matter, figures and tables must be eliminated. In general, the impersonal form should be used.

Supplementary material of a detailed nature, which is not essential in the printed paper, but may be useful to other workers, may be deposited with the Secretary. Such material will be made available to other scientists on request and a note to this effect should be included in the paper.

The paper should be reasonably subdivided into sections, and if necessary, sub-sections. The following pattern is suggested for Research Papers : (a) Introduction (b) Experimental (c) Results (d) Discussion (e) Conclusions (f) Acknowledgements (g) References. In many cases, two of sections (b), (c) and (d) can be combined. When a separate Discussion is used, it should not recapitulate the results but discuss their significance and relation to the object of the work and to the work of other people. Conclusions should not merely repeat preceding sections.

Special care must be taken in citing references correctly. Responsibility for the accuracy of these rests entirely with the authors. It is the authors' responsibility to obtain written permission to reproduce material which has appeared in another publication.

FORM OF MANUSCRIPTS

Manuscripts should be submitted in **triplicate** — including the original typewritten copy — typed throughout in double spacing on one side of the paper only. Adequate margins should be left (4 cm) with liberal spacing at the top and bottom of each page. The typescript should be free of corrections.

Headings of major sections should be centred and sub-section headings should be placed on the left of the page. The complete set of headings and sub-headings in an article should be numbered following the style adopted in this Journal and the set should reflect the logical development of ideas.

Paging : Each page of the manuscript should be numbered and the name of the first author and page number indicated in the upper right-hand corner of the page.

The *first* page should contain the article title, the name(s) of the author(s) and name and address of the establishment where the work was carried out. In the case of co-authors, respective addresses should be clearly indicated. Female authors should include one of their given names. The title should be concise but informative. The first word of the title should preferably be one useful in indexing and information retrieval. Where a series of related papers is submitted, each individual paper should have the same general heading, followed by a series number and title of the part. Any footnote to the title should be given at the bottom of this page.

The *second* page should contain an abstract (of not more than 250 words) which should be a summary of the entire paper, not of the conclusions alone and intelligible without reference to the paper itself. The text should begin on page three and each subsequent major section—references, figure legends and table legends should begin on a new sheet.

The *last* page should contain (a) a note as to the number of manuscript pages, figures and tables, (b) proposed running title of less than 42 characters (letters and spaces) and (c) the name and mailing address of the person to whom the proofs should be sent.

Illustrations : All illustrations are considered as figures and each graph, drawing or photograph should be numbered in sequence with Arabic numerals. Authors must submit the original and two duplicates of each figure. Figures should be planned to fit the proportions of the printed page (12 x 17 cm).

Figures must be drawn in Indian ink on plain white paper or board or tracing paper, not larger than 20 x 30 cm. Drawings should be lettered with a lettering set; lettering should be kept large enough to be legible after a reduction of 50 to 60%. If this is not possible, all letters and numerals must be inserted clearly and lightly in blue pencil and not in ink.

Each figure should carry a legend so written that the general meaning of each illustration can be understood without reference to the text. The amount of lettering on a drawing should be reduced as far as possible by transferring it to the legend. Figure legends should be typed on a separate sheet and placed at the end of the manuscript.

Graphs should be plotted on white or blue-lined graph paper or tracing cloth; grid lines that are to be shown in the engraving should be inked in black. The caption of each axis should be lettered parallel to its axis. Each figure should be identified in the margin with author's name and figure number. The preferred position of all illustrations should be ndicated in pencil in the manuscript.

Photographs : Half-tone illustrations should be included only when essential. Good glossy prints with sharp contrasts between black and white areas should accompany the manuscripts; they should not be attached to manuscript pages. The size should be such that when the print is reduced to the normal size for reproduction (12 x 17 cm maximum), the detail is still clear. Magnification should be indicated with a scale line on the photograph. The author's name and figure number should be given on the back of each photograph.

Tables should not repeat data which are available elsewhere in the paper. Each table should be typed on a separate sheet with due regard for the proportions of the printed page. They should be numbered consecutively with Arabic numerals. Tabulated matter should be clearly set out and the number of columns in each table should be kept as low as possible. Tables should have legends which make their general meaning clear without reference to the text and all table columns should have explanatory headings. Units of measure should be indicated in parentheses in the heading of each column. Vertical lines should not be used and horizontal rules used only in the heading and at the bottom. A one-column table may be up to 42 characters (letters and spaces) wide. A two-column table may be 90 characters wide. Footnotes to the tables are to be

placed directly below the table and should be indicated by superscript lower-case italic letters (*a*, *b*, *c*, etc.). Each table should carry on the back of the sheet the author's name and figure number. The preferred position of tables should be indicated in pencil in the manuscript.

References to the literature must be indicated in the text by a small superior number referring to the list of references which must be inserted on a separate sheet at the end of the paper. The list should be arranged in alphabetical order by author and numbered in Arabic numerals. All authors' initials must be given after surnames. The year of publication should follow in parentheses. When journal articles are listed, the journal name should be abbreviated in accordance with the *World List of Scientific Periodicals* 1900—1960, 1972, 4th edn, London : Butterworths Scientific Publications. If the journal is not in this list, the name should be given in full. The abbreviated journal title should be underlined to indicate italic type and followed by the volume number underlined with a wavy line to indicate bold type, the issue number in parentheses and then the inclusive pages. When books are listed, the order should be : author(s), year, book title, volume number, edition, pagination/inclusive pages, place of publication and publisher. When sections of a book are listed the order should be : author (s) of section, year, the word *In* followed by author of book, book title, volume number, edition, inclusive pages, place of publication and publisher. The series title of a book should be given in parentheses after the publisher.

Examples :

Journal — ANGMOR, J.E., DICKS, D. M., EVANS, W. C. & SANTRA, D.K. (1972) *Planta Med.* **21**(4) : 46-420.

Book — SCHOKMAN, D. (1966) *Vegetable growing : local and exotic varieties*, 29p. Colombo: Agriculture Department.

Section of Book — ZITNAK, A. (1973) *In Chronic cassava toxicity : proceedings of an interdisciplinary workshop, London, England,* 29-30 *January* 1973, pp. 89-95. Ottawa: International Development Research Centre. (IDRC-00e).

Footnotes which are *indispensable* should be indicated in the text by small superior figures and listed on a separate page in the manuscript.

Abbreviations and Symbols recommended in the various parts of British Standard 1991 : *Letter symbols, signs and abbreviations* should be used. Authors are encouraged to use the S.I. System of units (see description in British Standard PD 5686 : *The use of S. I. Units*).

Authors whose papers contain mathematical expressions should submit a list of the symbol used carefully and clearly indicated for the guidance of the printer. This list will not appear in print.

Formulae and Equations : Equations should be typewritten and *quadruple* spaced. They should be started on the left margin and the number placed in parentheses to the right of the equation.

Nomenclature : Scientific names of plants and animals will be printed in italics, and should be underlined in the manuscript. In the first citation, genus, species and authority must be given. e. g. *Tylenchorhynchus claytoni* Steiner. In later citations, the generic name may be abbreviated to its initial letter. e.g. *T. claytoni*.

Special instructions in the fields of Physical, Chemical and Medical Sciences are available on application to the Secretary.

Short Communications : The Journal may include a limited number of short communications. Authors should submit short communications only when they believe that rapid publication of their results is of the utmost importance. A short communication must not exceed 1,200 words, i.e. 4 pages of copy inclusive of illustrations and tables. Short communications should be complete in their own right and suitable for citation. The title should indicate the content clearly as these papers do not carry abstracts.

Proofs : Corrected galley proofs must be returned to the Secretary without delay as directed. Failure to do so will result in delay in publication. Correction of proofs by authors must be restricted to printer's and similar errors. They should be marked in pencil. Any modification of the original text is to be avoided. Responsibility for correcting proofs rests entirely on the authors though editorial assistance will be provided.

Reprints : 50 reprints will be supplied free of charge for each article. Additional reprints can be ordered on the reprint order form which will accompany the proofs.

CONTENTS OF PREVIOUS VOLUME

Vol. 14 No. 1 June 1986

Vol. 14 No. 2. December 1986

Journal of the
National Science Council
of Sri Lanka
Vol. 15 No. 1 June 1987

Contents

Published by
The Natural Resources, Energy and Science Authority of Sri Lanka (NARESA) and
Printed at NARESA Printing Unit, 47/5, Maitland Place, Colombo 7.